EVALUATION OF MECHANICAL AND CORROSION PROPERTIES OF MMFX REINFORCING STEEL FOR CONCRETE

By

Lien Gong

David Darwin

JoAnn P. Browning

Carl E. Locke, Jr.

A Report on Research Sponsored by

KANSAS DEPARTMENT OF TRANSPORTATION
Contract Nos. C1131 and C1281

SOUTH DAKOTA DEPARTMENT OF TRANSPORTATION
Project No. SD 2001-05

THE NATIONAL SCIENCE FOUNDATION
Research Grant No. CMS - 9812716

Structural Engineering and Engineering Materials
SM Report No. 70

THE UNIVERSITY OF KANSAS CENTER FOR RESEARCH, INC.

December 2002

ABSTRACT

The corrosion performance of MMFX and conventional reinforcing steels is compared based on macrocell and bench-scale tests. The conventional steel includes epoxy-coated and uncoated bars. Macrocell tests are conducted on bare bars and bars symmetrically embedded in a mortar cylinder. Specimens are exposed to a simulated concrete pore solution with 1.6 or 6.4 molal ion concentration of sodium chloride. Bench-scale tests include the Southern Exposure and cracked beam tests. A 15 percent (6.04 m ion) NaCl solution is ponded on the top of both Southern Exposure and cracked beam specimens. Mechanical properties are compared with the requirements of ASTM A-615. The uniformity and consistency in chemical composition is evaluated using a scanning electron microscope and an energy dispersive spectrometer. The microstructure of corrosion products is analyzed using a scanning electron microscope.

The results indicate MMFX steel exhibits better corrosion resistance compared to conventional reinforcing steel, but less than epoxy-coated bars. In rapid and bench-scale tests, MMFX steel exhibits a macrocell corrosion rate between 33 percent and 67 percent that of conventional reinforcing bars, while epoxy-coated reinforcement with the coating penetrated corrodes at a rate between 5 percent and 25 percent that of conventional steel. It is not recommended to use MMFX reinforcing steel instead of epoxy-coated reinforcement unless it is used with a supplementary corrosion protection system

Key Words: chlorides; concrete; corrosion; corrosion testing; reinforcing bars; MMFX steel

ACKNOWLEDGEMENTS

The report is based on a thesis prepared by Lien Gong in partial fulfillment of the requirements of the MSCE degree from the University of Kansas. The research was supported by the Kansas Department of Transportation under Contracts C1131 and C1281, with technical oversight by Dan Scherschligt, the South Dakota Department of Transportation under project SD 2001-05, with supervision by the SD2001-05 Technical Panel, Dan Johnson (chair), Mark Clausen, Tom Gilsrud, Todd Hertel, Darin Hodges, David Huft, Darin Larson, and Paul Nelson, the National Science Foundation under Research Grant No. CMS-9812716, and the United States Department of Transportation Federal Highway Administration.

TABLE OF CONTENTS

Page

LIST OF FIGURES

LIST OF TABLES

CHAPTER 1
INTRODUCTION

1.1 GENERAL

Deicing salts can cause the deterioration of bridges as the deicers diffuse through bridge decks and cause corrosion of the reinforcing steel. In 1992, it was estimated that in the United States the cost of bridge repairs in the federal-aid system due to corrosion damage was 51 billion dollars (Fliz et al. 1992). Thus, cost-effective methods to prevent the corrosion of reinforcing steel are of great importance.

Methods that are used to reduce the corrosion of reinforcing steel include the use of corrosion-inhibiting concrete admixtures, low permeability concrete, greater concrete cover over the reinforcing steel, cathodic protection and epoxy-coated reinforcing bars. The research presented in this report addresses another solution: developing corrosion-resistant reinforcing steel. A new iron-alloy, containing 9% chromium with the trade name MMFX II, was developed to be corrosion resistant.

The goal of this study is to determine if the new steel provides significantly better corrosion resistance than conventional reinforcing steel. The research compares the corrosion performance of the new reinforcing steel with conventional reinforcement in the presence of sodium chloride and determines the mechanical properties and compositional uniformity of MMFX steel.

1.2 BACKGROUND

Reinforcing steel embedded in concrete is normally protected from corrosion due to the high pH of the concrete pore solution. This high level of alkalinity passivates the steel by causing the formation of a γ−ferric oxide coating on the steel surface that is self-maintaining and prevents rapid corrosion. As long as the passive film on the reinforcing steel remains intact, corrosion will not occur. The pH of the

concrete pore solution must be between 11.5 and 13.8 to maintain the passivity of the steel. If the pH is lowered, the film becomes unstable and oxygen is able to react with the steel, causing corrosion.

The passive film can be disrupted by two ways: by carbonation, due to the penetration of CO_2 into the concrete, or by the presence of aggressive ions, like Cl^-, found in deicing salts.

1.2.1 Carbonation

Carbonation is associated with low concrete cover, poor concrete quality, poor consolidation, and age. If atmospheric carbon dioxide diffuses into concrete continuously, the pH of the pore solution will be lowered because dissolution of CO_2 in water produces a weak acid. Carbonation can reduce the pH of the pore solution in concrete to as low as 8.0, causing the passive film to break down and the steel to corrode. The following reactions occur in carbonation:

$$CO_2 + H_2O \_ H_2CO_3 \quad (1.1)$$

$$H_2CO_3 + Ca(OH)_2 \_ CaCO_3 + 2H_2O \quad (1.2)$$

1.2.2 Chloride

The presence of aggressive ions is a serious problem in concrete. Chloride ions react with available iron ions from the passive film on the bar surface to form an iron-chloride complex. The complex is subsequently converted to iron oxide and chloride ions, which are again available to combine with the iron in the reinforcement.

$$Fe^{2+} + 4Cl^- \_ (FeCl_4)^{2-} \quad (1.3)$$

$$(FeCl_4)^{2-} + 2H_2O \_ Fe(OH)_2 + 2H^+ + 4Cl^- \quad (1.4)$$

To initiate corrosion, a “threshold” level of chlorides needs to be present. According to ACI 318, the ratio of chloride ions to the weight of cement needs to be

greater than 0.15%, which means that the concentration of chloride ions in concrete needs to exceed 0.6 kg/m^3 in a typical bridge deck with a cement content of 390 kg/m^3. Due to the importance of hydroxyl ions in protecting steel from corrosion, the threshold can also be expressed as a ratio of chloride to hydroxyl ions, $[Cl^-]/[OH^-]$. Passivity is lost when $[Cl^-]/[OH^-]$ exceeds 0.6 (Hausmann 1967).

When reinforcing steel corrodes, the corrosion products occupy a much larger volume than the original steel. The change in volume induces tensile stresses in the surrounding concrete, causing it to crack, and providing greater access for the chlorides.

1.2.3 Electrochemistry

The corrosion of reinforcing steel is an electrochemical process that includes a flow of electric current and several chemical reactions. For corrosion to occur, an electrochemical cell is necessary. There are four components of a cell: an anode, a cathode, an electron path and an electrolyte. The anode is the region where oxidation occurs, or where iron releases electrons. The cathode is the region where reduction occurs, or where electrons combine with other molecules. The electrons released at the anode move to the cathode along the electronic path. The electrolyte is an ionic solution, such as pore solution in concrete.

In a corrosion cell, iron is oxidized at the anode, releasing electrons and ferrous ions:

$$Fe \rightarrow Fe^{2+} + 2e^- \tag{1.5}$$

Electrons released at the anode flow to the cathode and combine with water and oxygen to form hydroxyl ions:

$$O_2 + H_2O + 2e^- \rightarrow 2OH^- \tag{1.6}$$

The ferrous ions, which dissolve in the solution surrounding the steel, combine with the hydroxyl ions to form ferrous hydroxide:

$$Fe^{2+} + 2OH^- \_ Fe(OH)_2 \quad (1.7)$$

This compound is unstable in oxygenated solutions and is further oxidized to the ferric hydroxide:

$$2Fe(OH)_2 + H_2O + 1/2\ O_2 \_ 2Fe(OH)_3 \quad (1.8)$$

$$2Fe(OH)_3 \_ Fe_2O_3 \cdot nH_2O \quad (1.9)$$

The final product is the familiar rust.

1.2.4 Corrosion Potential and Corrosion Rate

From a thermodynamics point of view, the electrochemical reactions of corrosion are driven by the potential difference between the anode and the cathode. The potential of the anode and cathode can be used to determine the tendency for corrosion to occur. These potentials are used in the Gibbs and Nernst equations (Uhlig and Revie 1985) to determine if the coupled reactions are spontaneous.

If the Gibbs and Nernst equations show that energy is released, corrosion will occur. However, a spontaneous reaction does not necessarily mean a rapid reaction. Thermodynamic analysis of corrosion only provides information concerning tendencies of reactions and does not tell anything about rates at which the reaction will occur.

Chemical kinetics can be used to determine the rates of electrochemical reactions. According to chemical kinetics, there is a rate corresponding to the potential of a reaction at which that reaction will occur. The relationship between the potential and the rate of a reaction is logarithmic and given by the Tafel Equation:

$$\eta = \pm\beta log(i/i_0) \quad (1.10)$$

where: $\eta = \phi_{meas.} - \phi_{equil.}$: polarization or overvoltage

$\phi_{meas.}$: the measured potential

$\phi_{equil.}$: the equilibrium potential

β: Tafel slope

i: current flowing

$i_{0:}$ exchange current density

Chemical kinetics also describes the behavior of an electrochemical cell. The potentials and rates of the anodic and cathodic reactions in an electrochemical cell will shift to common intermediate values, so both the cathodic and anodic reactions will have the same potential and rate, known as the corrosion potential and corrosion rate.

1.3 TESTING TECHNIQUES

Two testing techniques are used to obtain the corrosion properties of MMFX steel in this research: rapid tests and bench-scale tests. Rapid tests usually give results in 15 weeks; whereas, bench-scale tests have a testing period of 2 years. These tests are briefly described in this section and in greater detail in Chapter 2.

1.3.1 Rapid Macrocell Tests

The rapid macrocell tests used in this study were first developed by Martinez, Darwin, McCabe, and Locke (1990) under the SHRP program and updated by Smith, Darwin, Senecal (1995) under the NCHRP-IDEA program and in the current study. The goal of this technique is to evaluate the effects of deicing chemicals on steel reinforcing bars in a relatively short period of time. Both mortar-wrapped specimens and bare bars are used as test specimens to obtain corrosion-resistant properties of the steel.

The macrocell test measures the macrocell corrosion rate and corrosion potentials of reinforcing bars. One specimen is placed in simulated concrete pore solution with a specific concentration of salt. This specimen corrodes and acts as the anode in the macrocell. Two specimens are placed in simulated concrete pore solution. These specimens are passive and act as the cathode in the macrocell. Air is

supplied to the pore solution at the cathode. Crushed mortar fill is added to the containers with mortar-wrapped specimens to simulate the concrete environment. The specimens are immersed to a depth of 75 mm (3 in.) in the liquid. The solutions in the containers are connected by a salt bridge. The specimens at the anode and cathode are connected electrically across a 10-ohm resistor. The corrosion current is determined by measuring the voltage drop across the resistor. The corrosion rate is determined by using Faraday's law.

$$r = ia/(nFD) \tag{1.11}$$

where: r macrocell corrosion rate (thickness loss per unit time)

a atomic weight (55.84 g for iron)

i current density (amperes/cm^2 or coulombs/cm^2.sec)

n number of ion equivalents exchanged (For Fe^{2+} = 2)

F Faraday's constant (96500 amp-sec/equivalent)

D density of metal (7.87g/cm^3 for steel)

For current density (i) in μA/cm^2,

$$r = 11.59i \text{ (μm/yr)} \tag{1.12}$$

The corrosion potentials of the anode and the cathode are measured with respect to a saturated calomel electrode after the electrical connection is disconnected for at least two hours.

1.3.2 Bench Scale Tests

Bench-scale tests include Southern Exposure tests (SE) and cracked beam tests (CB). SE tests were developed by Pfeifer and Scali (1981). CB tests were used by McDonald, Pfeifer, Krauss, and Sherman (1994). The difference between these two tests is that the SE test simulates an uncracked bridge deck, whereas the CB test simulates a bridge deck with cracks parallel to and above the reinforcing steel. Bench-scale tests provide a very severe corrosion environment and are generally believed to

simulate 15 to 20 years of exposure for marine structures and 30 to 40 years of exposure for bridges within a 48-week period (Perenchio 1992).

In the SE and CB tests, rapid chloride ion transport is achieved by using a thin concrete cover over the reinforcing bars, a water-cement ratio of 0.35, 0.45 or 0.5 and an unusual "weathering" scheme. The weathering scheme involves ponding salt water on the SE and CB specimens for a period of time and then drying the specimen. The ponding and drying cycles are repeated, creating high concentrations of chloride ions in the concrete over a short period of time.

Both SE and CB specimens have two mats of steel cast in the concrete. The top layer of steel acts as the anode, and the bottom layer of steel acts as the cathode. The cathode layer has twice as many bars as the anode so that corrosion is not limited by the cathodic reaction. The top and bottom layers of steel are connected across an external resistor. Measurements are taken every week to determine the macrocell corrosion rate and corrosion potential.

1.4 OBJECTIVE AND SCOPE

The principle goal of this study is to evaluate a concrete reinforcing steel that is supposed to have superior corrosion–resistant properties in the presence of chloride ions. Rapid tests are used to determine the corrosion potential and macrocell corrosion rate of MMFX reinforcing steel when exposed to 1.6 and 6.04 molal ion concentrations of NaCl. These tests give an early comparison of the relative corrosion resistance of the reinforcement. Southern Exposure and cracked beam tests are used to provide a measure of the long-term corrosion resistance of the steel. The nature of the corrosion products on the steels is also evaluated using a scanning electron microscope.

Another goal of this study is to determine the mechanical properties of MMFX steel. Mechanical testing is done according to ASTM E 8 on conventional

and MMFX steel to obtain yield and tensile strength, elongation, and bendability. X-ray microanalysis is used to evaluate the bars for consistency and uniformity in composition.

Finally, the results of the corrosion evaluation are combined with construction and maintenance experience in South Dakota to evaluate the cost effectiveness of the new reinforcing steel when it is used in concrete bridge decks.

CHAPTER 2
EXPERIMENTAL WORK

This chapter describes the experimental work performed in this study. Both MMFX and conventional reinforcing steels are evaluated. The conventional steel includes epoxy-coated and uncoated bars. The test methods include updated versions of the macrocell tests developed by Martinez, Darwin, McCabe, and Locke (1990) and the Southern Exposure and cracked beam tests used by Pfeifer, Landgren, and Zoob (1987) and McDonald, Pfeifer, Krauss, and Sherman (1994). The tests are not standardized, so a full description of the test specimens, specimen fabrication, and test procedures is presented for each of the test methods. Mechanical tests and microanalysis methods are also presented.

2.1 RAPID CORROSION TESTS

The rapid tests are used to measure the macrocell corrosion rates and corrosion potentials of bare bars and mortar-wrapped specimens. The tests are designed so that the chloride ions can reach the steel surface quickly, resulting in early initiation of corrosion.

2.1.1 Materials

a) **Mortar –** The mortar is made with Type I portland cement, ASTM C 778 graded Ottawa sand, and distilled water. The mortar has a water-cement ratio of 0.5 and a sand-cement ratio of 2.0 by weight.
b) **Epoxy Coating –** Herbert's O′Brien™ 7-1870 Nap-Guard Rebar Patch Kit; Ceilcote 615 Ceilgard, manufactured by Ceilcote Co.

2.1.2 Test specimens

The corrosion resistance of MMFX and conventional steel are evaluated using bare bars and mortar-wrapped specimens. Three kinds of bare bar specimens are used in the rapid tests: straight bars, sandblasted bars, and bent bars. The bare bar specimen preparation is described as following:

a) Straight bar - The reinforcing bar is cut to a length of 127 mm (5 in.), and one end of the bar is drilled and tapped for a No. 10-24 machine screw to a depth of 13 mm (0.5 in.). The threaded hole is needed to make an electrical connection. The bar is then cleaned with acetone to remove oil, grease and dirt. Mill scale is left on the bar surface.

b) Sandblasted bare bar - The bar is prepared as described for the straight bar. The bar is then put into a sandblasting machine where the surface is sandblasted for 2 to 3 minutes using high-pressure sand directed though the nozzle and cleaned for a second time.

c) Bent bare bar – The reinforcing bar is cut to a length of 508 mm (20 in.), and bent cold through 180^{o} around a cylindrical mandrel with a diameter of 50 mm (2 in.). One end of the bar is drilled and tapped for a 10-24 threaded bolt to a depth of 13 mm (0.5 in.). The bar is then cleaned with acetone. The mill scale is left on the bar surface.

The wrapped specimen consists of a 127 mm (5 in.) long No. 16 [No. 5] reinforcing bar, symmetrically embedded in a 30 mm (1.18 in.) diameter mortar cylinder (Fig. 2.1). The cylinder is 152 mm (6 in.) long and provides a mortar cover of 7 mm over the reinforcing bar. The specimen configuration is based on research done by Matinez, Darwin, McCabe, and Locke (1990) and is modified in this study by completely, rather than partially, embedding the bar within mortar.

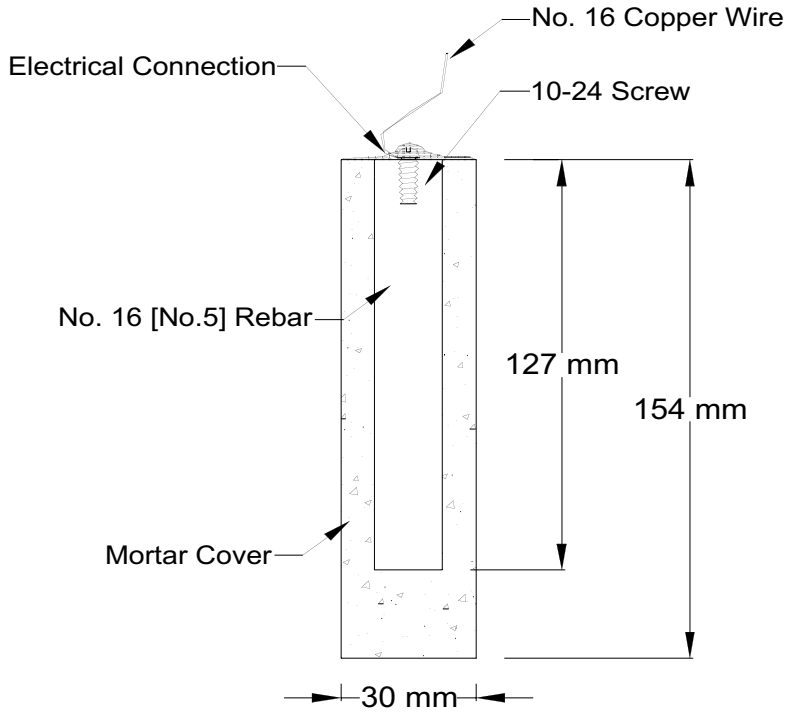

Figure 2.1 - Cross-Section of Mortar-wrapped Test Specimen Used for Rapid Corrosion Macrocell Test

Specimen fabrication proceeds in the following order:

a) **Reinforcing Bar Preparation** – A reinforcing bar is cut to a length of 127 mm (5 in.), and one end of the bar is drilled and tapped for a 10-24 threaded bolt to a depth of 13 mm (0.5 in.). The bar is then cleaned with acetone to remove oil, grease, and dirt. The mill scale is left on the bar surface. For epoxy-coated bars, the coating is breeched by four 3.2 mm ($^1/_8$-in.) diameter holes to simulate defects in the epoxy coating. The ends of epoxy-coated bars to be submerged in simulated pore solution are protected using a plastic cap filled with Herberts O'Brien Rebar Patch Kit epoxy.

b) Mold Assembly – The mold for the specimen is made of PVC pipe and fittings that are available at the local hardware store. The specimen mold and mold container are shown in Fig. 2.2.

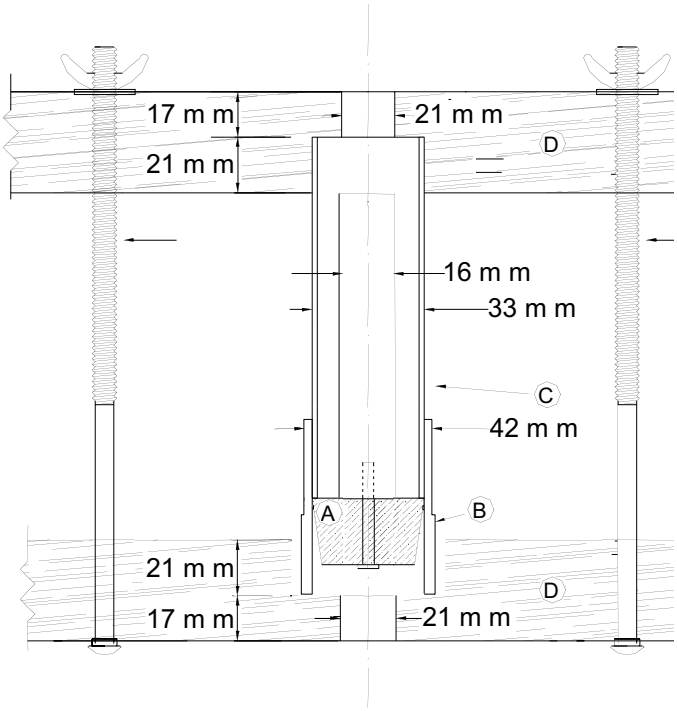

Fig 2.2 - Cross Section of the Mold for Mortar-wrapped Specimen

Assembly is explained in the following steps:

1. A rubber stopper, A, is inserted in the machined end of the connector, B. The widest end of the small rubber stopper is placed in contact with the shoulder (an integral ring) on the internal surface of the connector.
2. A bolt is inserted from the hole centered in the rubber stopper. The tapped end of the reinforcing bar is attached to the bolt.
3. The longitudinal slice along the side of the PVC pipe, C, is taped with masking tape. The pipe is then inserted in the free end of the connector.
4. The assembled mold is placed between the wooden boards, D, in the holes provided. The threaded rods, E, are then inserted between the wooden boards.

The rods are used to hold the molds together and center the reinforcing bar by tightening or loosening the nuts on the rods.

c) **Mortar –** The batch quantities given in Table 2.1 provide enough mortar to make fifteen specimens. First, the cement and water are put in the mixer and mixed at a slow speed (140 ± 5 r/min) for 30 seconds. Then the entire quantity of sand is added slowly over a 30 second period, while mixing at slow speed. The mixer is changed to medium speed (285 ± 10 r/min) to mix for 30 seconds. Then the mixer is stopped and the mortar is allowed to stand for 1.5 minutes. Finally the mortar is mixed for 1 min. at medium speed (285 ± 10 r/min) (ASTM C 305).

Table 2.1 Mortar Mix Design

Type of Mortar	Water (g)	Cement (g)	Sand (g)
Regular	500	1000	2000

d) **Casting –** The specimens are cast in three layers. Each layer is rodded 25 times with a 3.2 mm (0.125 in.) diameter rod that is 305 mm (12 in.) long. Each layer is consolidated on a vibrating table with amplitude of 0.15 mm (0.006 in.) and a frequency of 60 Hz.

e) **Curing –** After the specimens are cast, the specimens are cured in the molds for 24 hours at room temperature. The specimens are then removed from the molds and placed in lime-saturated water for 13 days.

After 14 days of curing, the specimens are vacuum dried for one day. For both bare and mortar-wrapped specimens, a 16-gauge copper wire is attached to the tapped end of each specimen with a 10-24 steel screw. The top of the screw, wire, and mortar are then coated with two layers of Herberts O'Brien epoxy for bare bars and two layers of Ceilgard 615 epoxy for mortar-wrapped bars to prevent crevice corrosion. Each coat is dried for 4 hours at room temperature after application.

2.1.3 Macrocell test procedure

The macrocell test (Figs. 2.3 and 2.4) measures the macrocell corrosion rates and corrosion potentials of reinforcing steels when they are exposed to specific concentrations of NaCl.

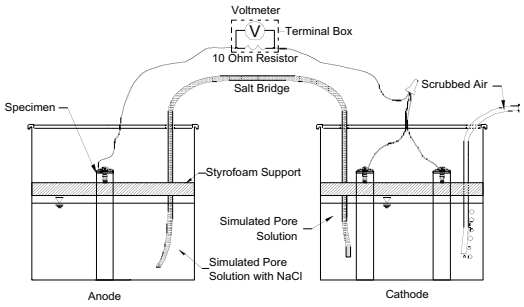

(a)

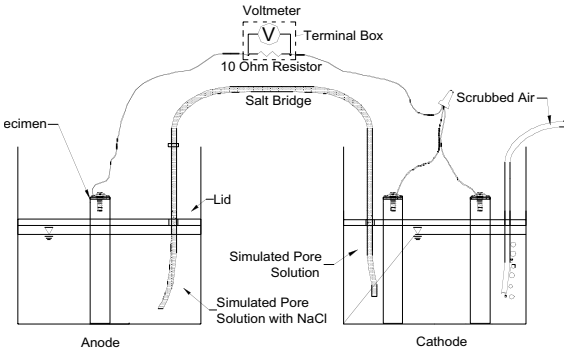

(b)

Fig 2.3 - Schematics of the Macrocell Test (Bare Bar) (a) Original Test Configuration and (b) New Test Configuration

Two specimens are placed in simulated concrete pore solution and act as the cathode, while a third specimen is placed in pore solution with NaCl and acts as the anode. The anode and cathode are ionically connected by a salt bridge between the two solutions and are electrically connected by a wire across a 10-ohm resistor. Air, scrubbed to remove CO_2, is supplied to the cathode.

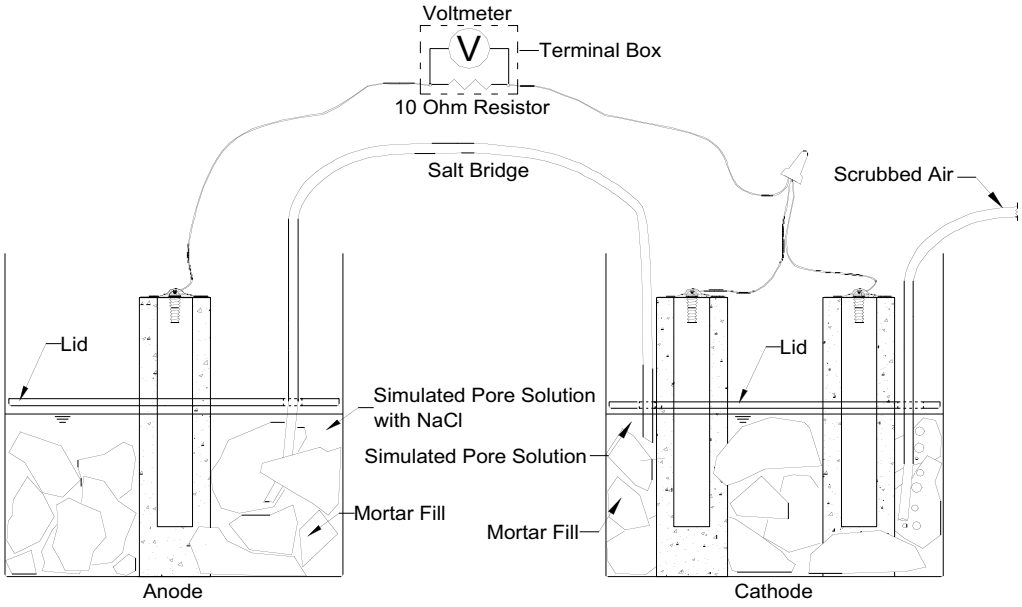

Figure 2.4 - Schematic of the Macrocell Test (Mortar-wrapped Specimen)

Details of the bare bar test follow:

a) Specimen – The specimen is prepared according to the procedures described in Section 2.1.2.

b) Concrete Pore Solution – Based on an analysis by Fazammehr (1985), one liter of simulated pore solution contains 974.8 g of distilled water, 18.81 g of KOH, 17.87 g of NaOH. In the current study, the simulated concrete pore solution used somewhat less KOH and NaOH, consisting of 974.8 g of distilled water, 16.5 g of KOH, and 17.55 g of NaOH.

c) NaCl Solution – Two molal ion concentrations of NaCl were used for this study: 1.6 m and 6.04 m (15%). To obtain these concentrations, 45.6 g and 172.1 g of NaCl are used per liter of pore solution.

d) Container – The specimen and solution are held in a 4.5-liter container with a lid. The container is 178 mm (7 in.) in diameter and 191 mm (7 1/2 in.) in height.

e) Salt Bridge – The salt bridge consists of a conductive gel in a flexible tube. It is prepared following procedures described by Steinbach and King (1950): 4.5 grams of agar, 30 grams of potassium chloride (KCl), and 100 grams of distilled water are combined and heated over a burner at 200°C (400°F) for three minutes; the mixture is poured into three flexible Tygon tubes, each 1 m (3.3 feet) long; finally, the salt bridges are placed in boiling water for one hour to finish the gel process.

f) Terminal Box – A terminal box is used to take electrical measurements of test specimens. The box is 178 mm (7 in.) x 102 mm (4 in.) x 51 mm (2 in.). Six binding posts are attached to the top of the box.

g) Wire – The 16 gauge copper wire is used to connect the test specimen to the terminal box.

h) Resistor – A 10 ± 0.5 ohm resistor is used to electronically connect the specimens at the anode and cathode. The resistance of each 10-ohm resistor is measured separately and used to calculate the corrosion rate.

i) Air Scrubber – Compressed air is used to supply oxygen for the cathode solution. An air scrubber is used to remove the carbon dioxide in the compressed air, because CO_2 lowers the pH of the pore solution. The air scrubber is a 19-liter plastic container filled with 1M NaOH solution. NaOH is added as needed to maintain the pH of the solution at 12.5.

j) Saturated Calomel Electrode (SCE) – The potential of the specimens is measured with respect to a SCE.

k) Voltmeter – A Hewlett-Packard 3456A digital voltmeter is used to measure the voltage drop and corrosion potential.

Two test configurations are used in this study. In one (Fig. 2.3a), the lid is placed on the top of the container and the specimens are held in place by a styrofoam support; in the other (Fig. 2.3b), the lid is lowered to a position just above the surface of solution and is used to hold the specimens in place.

The voltage drop across the resistor and the potentials of anode and cathode are measured once a day for the first week and once a week after that. The voltage drop is measured by connecting the voltmeter to binding posts on the terminal box to which the resistor is connected. The potentials are measured by immersing a SCE, which is connected to the voltmeter, into the solution after disconnecting the wires from the binding posts for at least 2 hours.

Macrocell tests with wrapped specimens (Fig. 2.4) are similar to the second of the two bare bar configurations, with the exception that mortar fill is added to the container. The fill material consists of the same mortar used to make the test specimen. The fill is cast in metal baking sheets, 25 mm (1 in.) deep, at the same time that the test specimens are fabricated. The mortar is broken into pieces after 24 hours.

2.1.4 Tests performed

Nine groups with bare specimens and five groups with mortar-wrapped specimens were tested. The test program is summarized in Table 2.2.

Table 2.2 Rapid Tests Performed

Steel Designation[1]	Heat No.	NaCl concentration	No. of tests	Notes
Bare specimens				
N3	S44407	1.6 m	6	
MMFX(1)	810737	1.6 m	6	Lid above bars
MMFX(2)	810737	1.6 m	6	
MMFXs	810737	1.6 m	6	Sandblasted bars
MMFXb	810737	1.6 m	3	Bent bars at anode
MMFX#6(1)	810737	1.6 m	3	
MMFX#6(2)	710788	1.6 m	3	
N2h	K0-C696	6.04 m	5	
MMFXsh	810737	6.04 m	6	Sandblasted bars
Mortar-wrapped specimens				
N3m	S44407	1.6 m	6	
MMFXm	810737	1.6 m	6	
ECRm	S44407	1.6 m	6	Epoxy-coated bars at anode
MMFX/N3	810737/S44407	1.6 m	3	
N3/MMFX	S44407/810737	1.6 m	3	

[1] N2 and N3: Conventional, normalized A 615 reinforcing steel
MMFX: MMFX Microcomposite steel
ECR: Epoxy-coated N3 steel
s: Sandblasted bars
b: Bent bars at anode
h: 6.04 m NaCl concentration
m: Mortar-wrapped specimens
Steel size: No.16 (No.5) except #6 which is No.19 (No.6)

2.2 BENCH-SCALE TESTS

The Southern Exposure (SE) and the cracked beam (CB) tests are accelerated tests to study macrocell corrosion of reinforcing bars in concrete. Both are used to evaluate the corrosion resistance of the MMFX steel in concrete when exposed to

NaCl. The macrocell corrosion rate, corrosion potential, and mat-to-mat resistance are measured. The tests are underway and will last 96 weeks.

2.2.1 Materials

a) Concrete – The concrete is air entrained, with 6% air (±1%), and a 3 in. slump (±0.5 in.). It has a water-cement ratio of 0.45. The concrete materials are:

1) Cement - Type I portland cement.
2) Coarse aggregate - 19 mm (3/4 in.) Crushed limestone, from Flogel Quarry, KS (bulk specific gravity ssd = 2.58, absorption dry = 2.33%)
3) Fine aggregate – Kansas River sand, KS (bulk specific gravity ssd = 2.62, absorption dry = 0.52%).
4) Air Entraining Agent - Vinsol Rison, from Master Builders, Inc.

b) Epoxy coatings – Ceilcote 615 Ceilgard, manufactured by Ceilcote Co.

c) Silicone Caulk – The caulk, 100 percent silicone manufactured by Macklenburg-Duncan.

2.2.2 Test Specimens

The Southern Exposure test specimen is shown is Fig. 2.5. It consists of six reinforcing bars embedded in a concrete block that is 305 mm (12 in.) wide, 305 mm (12 in.) long, and 178 mm (7 in.) high. Two reinforcing bars are placed 25 mm (1 in.) from the top of the specimen and four reinforcing bars are placed 25 mm (1 in.) from the bottom. Each bar is 305 mm (12 in.) long. The bars are drilled and tapped at both ends to provide connections for bolts so that they can be fixed in molds and to provide an electrical connection to the bars during tests. A dam is cast around the top surface of the specimen to facilitate ponding during the test.

The cracked beam test specimen is shown in Fig. 2.6. The specimen is similar to the SE specimen except it is half the width of the SE specimen, with one bar on top and two bars on the bottom. A simulated crack is placed in the concrete parallel to the top bars, as described in Section 2.2.3.

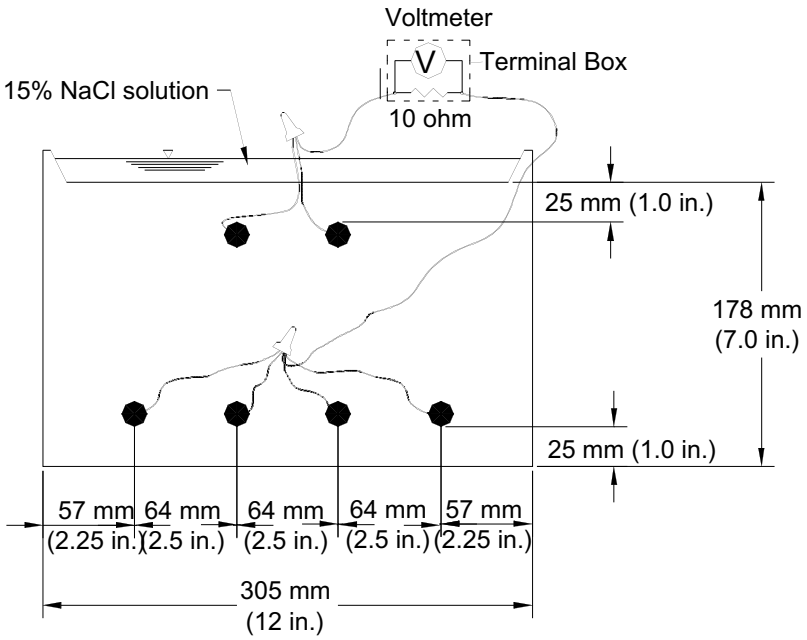

Figure 2.5 - Test Specimen for Southern Exposure Test

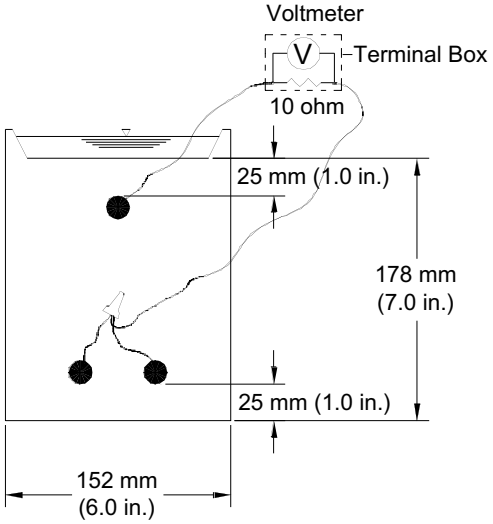

Figure 2.6 - Test Specimen for Cracked Beam Test

2.2.3 Test Specimen Fabrication

The SE and CB specimens are fabricated as follows:

a) Reinforcing Bar Preparation – Each reinforcing bar is cut to a length of 305 mm (12 in.). Both ends of the bar are drilled and tapped for a 10-24 threaded bolt to a depth of 13 mm (0.5 in.). The bar is then cleaned with acetone. The mill scale is left on the bar.

b) Form Assembly – The forms are made of 19 mm (3/4 in.) thick plywood and consist of four sides and a bottom. A rectangular piece of wood that is slightly smaller than the bottom is bolted to the bottom to create a dam in the edge of the specimen. The five pieces are fastened with clamps and the inside corners are sealed with caulk. Small holes, drilled in two side molds, are used to support the reinforcing bars using bolts.

c) Concrete Mixing – Concrete is mixed following the requirements of ASTM C 192. The mix design is given in Table 2.5.

Table 2.3 Concrete Mix design

Type	Water (kg/m^3)	Cement (kg/m^3)	Coarse Aggregate (kg/m^3)	Fine Aggregate (kg/m^3)	Vinsol Resin (mL/m^3)
Regular	160	355	874	852	90

d) Specimen Casting – The specimens are cast in two layers. Each layer is vibrated according to ASTM C 192. The final layer is finished with a wooden float.

e) Specimen Curing – After the specimens are cast, the molds are covered with plastic, and the specimens are cured for 24 hours at room temperature. The specimens are removed from the forms and cured in a plastic bag containing water for 48 hours at room temperature. Finally the specimens are removed from the bag and cured in air for 25 days.

f) Cracked Beam Specimen – A slot is cut in the bottom of the form and a 0.3 mm thick stainless steel shim is inserted to form a simulated crack to the steel surface. After 24 hours, the shim is removed, and a uniform crack is created in the beam.

g) Concrete Epoxy – Before testing begins, two coats of Ceilcote 615 epoxy are applied to the vertical sides of the specimen. The epoxy is mixed and applied according to the recommendations of the manufacturer.

h) Wiring – One day before testing begins, copper wires are used to connect the top and bottom steel to the exterior binding post on the terminal box. The exposed connections are also coated with two layers of Ceilcote 615 epoxy.

2.2.4 Bench-Scale Test Procedures

The test procedures are the same for the Southern Exposure and cracked beam tests. Ponding-drying cycles and ponding cycles are designed to accelerate the diffusion of chloride ions into the concrete.

a) Ponding-drying cycle _ A 15% (6.04 m ion) NaCl solution is ponded on the top of the specimen for four days at room temperature. The specimens are covered with a plastic sheet to reduce evaporation. After four days, the voltage drop and the mat-to-mat resistance of the specimen are measured. The salt solution is removed and the corrosion potentials of the anode and the cathode are measured. The specimens are heated to 38 ± 1.5CY (100 ± 3 FY) for three days under a portable heating tent to complete one cycle of testing. The specimens undergo 12 cycles (weeks) of testing.

The heating tent is movable and can hold 6 SE and 6 CB specimens. The tent is 1.2 m (3.5 ft) high, 1.33 m (4 ft) wide, and 2.67 m (8 ft) long. The roof and ends are made of 19 mm (3/4 in.) thick plywood and are connected by six 2.67 m (8 ft) studs. The sides of the tent are covered with two layers of plastic sheeting, separated by 25

mm (1 in.). Three 250-watt heating lamps are evenly spaced along the roof of the tent. When the tent is placed over the specimens, the lamps are 450 mm (18 in.) above the specimens. A thermostat is used to maintain the required temperature.

b) Ponding Cycle _ The 15% NaCl solution is ponded continuously on the top of the specimen for 12 weeks at room temperature. The specimens are covered with plastic paper to reduce evaporation. On the fourth day of each week, the voltage drop, the mat-to-mat resistance and corrosion potential of the specimen are measured.

The continued 12 weeks of ponding and 12 weeks of ponding-drying cycles are alternated for a total test period of 96 weeks.

The voltage drop across the 10-ohm resistor at the terminal box is measured with the use of a voltmeter. The mat-to-mat resistance, which is the total resistance between the two layers of reinforcing steel, is measured using a AC ohm meter after measuring the macrocell corrosion rate. To measure the mat-to-mat resistance and corrosion potential, the macrocell circuit must be broken. The corrosion potentials of both mats of steel are measured after the macrocell has been disconnected for two hours. For specimens in the ponding cycle, the corrosion potential is obtained by immersing a standard calomel electrode (SCE) into the solution. For specimens in the ponding-drying cycle, the corrosion potential is obtained using a copper-copper sulfate electrode (CSE), as described in ASTM C 876. The CSE gives corrosion potentials that are approximately 75 mV more negative than measured with a SCE.

2.2.5 Bench-scale Tests performed

Eight groups of Southern Exposure tests and five groups of cracked beam tests are underway in this study. The tests are summarized in Table 2.4.

Table 2.4 Bench-scale tests performed

Steel Designation[1]	Heat No.	No. of tests	Notes
Southern Exposure (SE) Tests			
N3(1)	S44407	4	
N3(2)	S44420	2	
MMFX	810737	6	
MMFXb	810737	3	Bent bars at anode
MMFX/N3	810737/S44420	3	MMFX top bars
N3/MMFX	S44420/810737	3	N3 top bars
ECR(1)	S44407	4	
ECR(2)	S44420	2	
Cracked Beam (CB) Tests			
N3(1)	S44407	4	
N3(2)	S44420	2	
MMFX	810737	6	
ECR(1)	S44407	4	
ECR(2)	S44420	2	

[1] N2 and N3: Conventional, normalized A 615 reinforcing steel
MMFX: MMFX Microcomposite steel
ECR: Epoxy-coated N3 steel

2.3 MECHANICAL TESTS

Conventional and MMFX steel are tested in tension to compare yield strength, tensile strength, and elongation. The steel is also tested in bending to determine compliance with the requirements of ASTM A 615.

The tensile tests were completed using an Instron hydraulic testing machine under stroke control. Dual loading speeds are used to meet the requirement of ASTM E 8 that requires a loading speed between 10 ksi/min and 100 ksi/min before the steel yields.

2.4 X-RAY MICROANALYSIS

The chemical compositions of conventional and MMFX steel are obtained using a scanning electron microscope (SEM) and energy dispersive spectrometer (EDS). Three points on each of two samples from each heat of MMFX steel and one heat of No. 5 conventional steel are analyzed to determine uniformity and consistency in chemical composition.

The conventional and MMFX bars are cut using a band saw and cleaned with acetone to remove grease, dirt, and oils. The specimens are then polished by hand using progressively finer grades of silicon carbide (SiC) paper, starting with 150 grade SiC paper and proceeding to 300, 600, 1000 and 2000 grades. The specimens are cleaned in soap and water before moving to the next polishing step. Finally, the specimens are mounted on aluminum stubs using carbon-coated tape.

The analysis is performed using an EDAX PV 9900 EDS mounted on a Philips 515 SEM. An accelerating voltage of 20 kV, a working distance between 0.906 and 1.102 in. (23 and 28 mm), a tilt angle of 40Y, and a take-off angle between 55 and 60Y are used. Specimens are analyzed for chemical compositions using standardless quantitative analysis (Superquant program 1989).

2.5 MICROSTRUCTURE ANALYSIS FOR CORROSION PRODUCTS

Corrosion products on both bare and mortar-wrapped bars are observed using a Phillips 515 scanning electron microscope (SEM) after completion of the macrocell tests. The technique used follows that developed by Axelsson, Darwin, and Locke (1999).

When the macrocell tests are finished, the specimens are visually inspected . For wrapped specimens, the mortar is removed for an evaluation of the bar surface. The surface damage and corrosion products are evaluated. The bar surface is examined with a light microscope to select areas on the specimen to be observed

using the SEM. The reinforcing bar is then sliced into pieces using a hacksaw to obtain specimens that are small enough for SEM imaging.

The sliced pieces of steel are mounted on aluminum stubs with conductive double-sided sticky carbon tabs. Conductive carbon paint is used to provide a good conductive path from the top of the specimen to the stub. An Anatech Hummer X sputter coater is used to coat the specimens with a 20 nm thick layer of gold palladium to prevent charging.

Specimens are observed using secondary electron imaging to record surface morphology. Images are recorded using an ELMDAS digital image acquisition system at an accelerating voltage of 20 kV with a spot size of 50 nm at a pixel density of 512 in both the vertical and horizontal directions.

CHAPTER 3
RESULTS AND EVALUATION

This chapter presents the test results from this study and the evaluation of those results. The chapter is divided in six sections, covering (1) the rapid corrosion tests for bare bars and mortar-wrapped specimens, (2) the bench-scale tests, (3) the mechanical tests, (4) the X-ray microanalysis of the reinforcing bars, (5) the microstructure analysis of the corrosion products, and (6) cost effectiveness.

3.1 RAPID CORROSION TESTS

The experimental work focuses on comparing the corrosion resistance of the MMFX and conventional steel. The test results are presented in terms of average values followed by a general discussion of the performance of the steel. The average corrosion rates for the specimens are summarized in Table 3.1. Results for individual specimens are presented in Appendix A.

3.1.1 Macrocell tests for bare bar specimens

The average corrosion rates for bare bar specimens in 1.6 m ion concentration NaCl solution shown in Fig 3.1 give a good indication of the corrosion resistance to be expected from MMFX steel. This figure includes the average corrosion rates for conventional steel and six batches of MMFX steel. MMFX(1) represents tests carried with the test configuration shown in Fig 2.3a. All other tests were carried out using the configuration shown in Fig. 2.3b. MMFX(1) and MMFX(2) No. 16 [No. 5] bars were tested in the "as delivered" condition. MMFXs and MMFXb tests evaluated No. 16 [No. 5] sand-blasted and bent bars, respectively. MMFX#6(1) and MMFX #6(2) tests included two heats of No. 19 [No. 6] bars in the "as delivered" condition.

Table 3.1 – Average corrosion rates and corrosion losses as measured in the macrocell tests

CORROSION RATE AT WEEK 15 (μm/yr)

Steel Designation	Heat No.	Specimen						Average	Std. Deviation
		1	2	3	4	5	6		
Bare specimens									
N3[1]	S44407	52.23	0.26	67.30	39.89	32.20	21.93	35.64	23.44
MMFX(1)[2]	810737	10.76	3.27	13.98	4.76	11.82	27.41	12.00	8.62
MMFX(2)	810737	12.25	7.98	22.90	18.08	32.03	24.85	19.68	8.77
MMFXs	810737	11.85	20.09	15.21	31.57	11.48	3.47	15.61	9.52
MMFXb	810737	7.58	17.84	6.70	6.73	7.08	6.63	8.76	4.46
MMFX#6(1)	810737	28.35	26.06	23.23	-	-	-	25.88	2.56
MMFX#6(2)	710788	23.21	25.89	28.39	-	-	-	25.83	2.59
N2h[1]	K0-C696	46.45	51.84	16.68	33.61	26.00	-	25.46	14.43
MMFXsh	810737	46.75	31.05	48.59	33.38	51.83	33.55	41.14	9.17
Mortar-wrapped specimens									
N3m	S44407	11.14	9.10	25.89	19.17	21.01	19.17	17.58	6.31
MMFXm	810737	8.81	17.25	10.05	9.47	11.59	5.94	10.52	3.79
ECRm[+]	S44407	3.65	1841.62	76.73	646.76	621.18	0.00	531.7	707.91
ECRm*	S44407	0.03	14.46	0.60	5.08	4.88	0.00	4.2	5.56
N3/MMFX	S44407/810737	14.92	10.50	10.48	-	-	-	12.0	2.56
MMFX/N3	810737/S44407	15.10	11.37	12.20	-	-	-	12.9	1.96

TOTAL CORROSION LOSS AFTER 15 WEEKS

Steel Designation	Heat No.	Specimen						Average	Std. Deviation
		1	2	3	4	5	6		
Bare specimens									
N3	S44407	12.98	4.81	13.12	11.02	6.92	5.27	9.02	3.81
MMFX(1)	810737	7.21	4.74	6.16	4.86	3.62	6.61	5.53	1.35
MMFX(2)	810737	3.08	2.09	3.23	1.12	1.62	3.81	2.49	1.04
MMFXs	810737	1.95	2.61	3.21	3.27	2.84	2.13	2.67	0.55
MMFXb	810737	1.51	2.76	1.20	1.46	1.51	1.99	1.74	0.56
MMFX#6(1)	810737	9.85	5.83	5.19	-	-	-	6.96	2.53
MMFX#6(2)	710788	3.60	6.17	5.36	-	-	-	5.04	1.32
N2h	K0-C696	16.67	14.73	8.38	11.51	11.75	-	10.41	3.19
MMFXsh	810737	15.32	8.39	12.66	6.20	9.84	13.16	10.93	3.38
Mortar-wrapped specimens									
N3m	S44407	5.13	4.74	6.69	5.17	4.75	5.08	5.26	0.72
MMFXm	810737	2.17	0.55	1.87	0.98	1.67	0.92	1.36	0.63
ECRm[+]	S44407	1.26	130.00	9.06	63.10	28.18	1.26	38.8	50.44
ECRm*	S44407	0.01	1.02	0.07	0.50	0.22	0.01	0.3	0.40
N3/MMFX	S44407/810737	3.30	2.19	2.33	-	-	-	2.6	0.60
MMFX/N3	810737/S44407	1.59	1.74	2.10	-	-	-	1.8	0.26

[1] N2 and N3: Conventional, normalized A 615 reinforcing steel
[2] MMFX: MMFX Microcomposite steel
[3] ECR: Epoxy-coated N3 steel
[+] Based on exposed area, four 3.2 mm (1/8 in.) diameter holes in epoxy
* Based on total area of bar exposed to solution

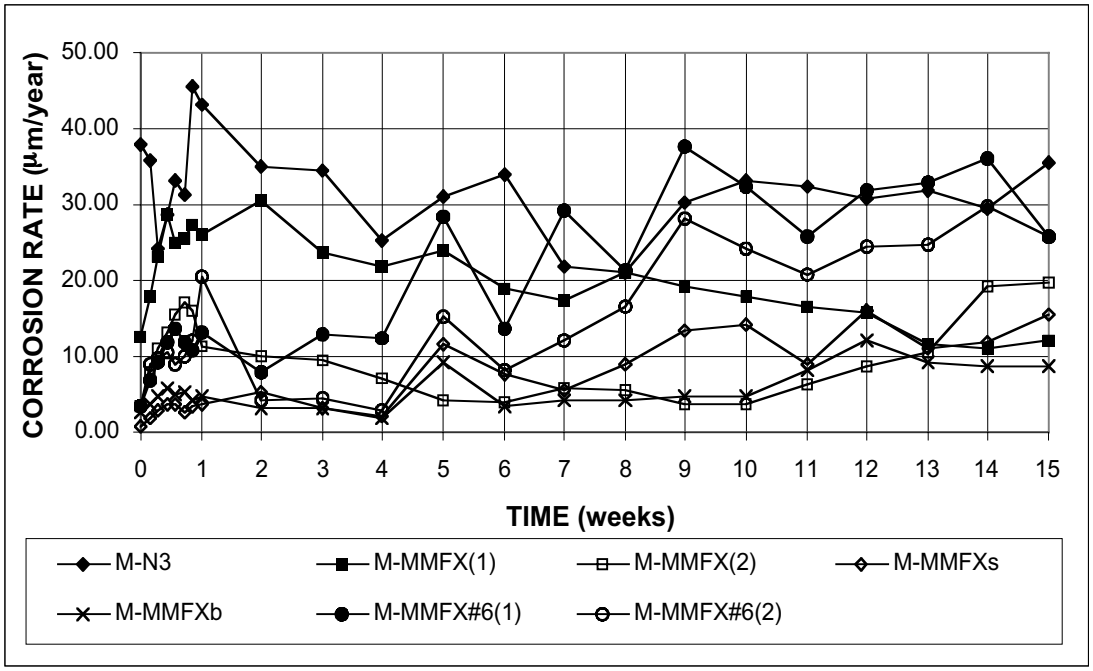

Figure 3.1 - Macrocell Test. Average corrosion rate. Bare specimens in 1.6 m ion NaCl and simulated concrete pore solution.

As shown in Fig 3.1, the N3 bars were corroding at 35.6 μm/yr at 15 weeks, which is higher than all of the MMFX bars. The average macrocell corrosion rates were 12 μm/yr for the MMFX(1) and 19.2 μm/yr for the MMFX(2). The total corrosion loss of N3 steel (9 μm) is also higher than that of MMFX(1) (5.5 μm) and MMFX(2) (2.5 μm). For the MMFX(1) specimens, corrosion always occurred on the surface of the bar between the solution surface and the lid, a region of high humidity, which may be a reason that the corrosion rate is different from that of the specimens with the newer test configuration. For MMFXs, the average corrosion rate is 16 μm/yr and the average total corrosion loss is 2.7 μm.

At 15 weeks, the average corrosion rate of the MMFXb specimens is 9 μm/yr. During the first few weeks, the corrosion rate was only 2 μm/yr, which is low compared to the other MMFX bare bars. Early in the test, the cathode reaction was thought to be limiting the corrosion rate, since the bent bar at the anode was four

times as long as the straight bare bar, while the bars at the cathode were the same as those used for straight bar anodes. The cathode bars for three tests were increased at the fifth week and the corrosion rate increased to 9.6 μm/yr immediately. However, the average corrosion rate for the other three tests increased to 8.9 μm/yr. Finally, the corrosion rate stabilized at about 10.7 μm/yr for the three with the greater number of bars at the cathode and 6.8 μm/yr for the other three. Since it was hypothesized that the bent bars might have microcracks on their surface, the average corrosion rate was expected to be higher than that of the straight bars or at least the same. In fact, the bent bar batch had the lowest corrosion rate of the MMFX bare bar macrocells, providing a good indication that bending did not increase the corrosion rate. The average total corrosion loss of MMFXb, which is 1.7 μm after 15 weeks, is also the lowest one of all the MMFX bare bar macrocells.

The average corrosion rate of all MMFX No. 16 [No.5] specimens is about 14 μm/yr, which equal to 39.3% of the corrosion rate of conventional reinforcement. The average total corrosion loss for the 24 No. 16 [No. 5] MMFX specimens is 3.1 μm, equal to 34% of the average loss for the N3 bars (9.0 μm). In contrast to the No. 16 [No. 5] bars, the No. 19 [No. 6] MMFX bars have a much higher corrosion rate, about 26 μm/yr, which is equal to 73% of that shown for the conventional bars, and a total corrosion loss of 6.0 μm on 67% of that for conventional steel.

The average corrosion potentials of the anodes and cathodes are shown in Figs. 3.2 and 3.3, respectively. The corrosion potentials are measured with respect to a saturated calomel electrode (SCE), and values more negative than –0.275 V indicate active corrosion. At 15 weeks, all anode bars were undergoing active corrosion. Conventional steel has the most negative corrosion potential at the anode, with a value of –0.56 V. For MMFX steel, the anode potentials are between –0.40 V and –0.50 V. The average corrosion potentials for the cathode bars are between –0.15 V and –0.25 V, indicating the bars are passive.

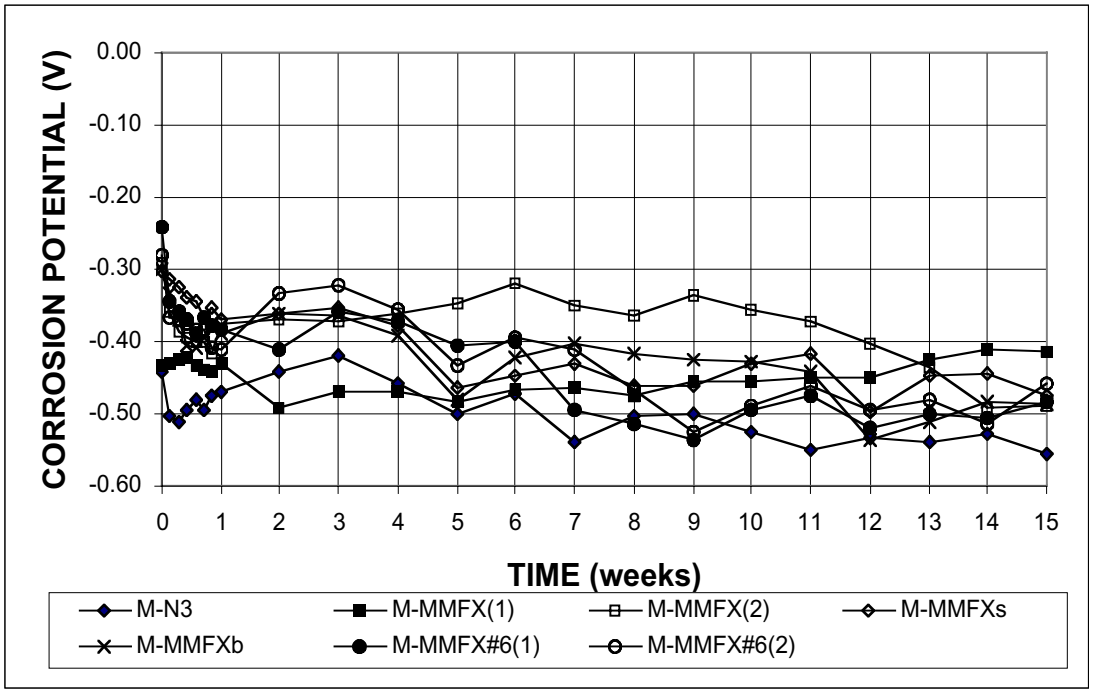

Figure 3.2 - Macrocell Test. Average corrosion potential vs. SCE, anode.
Bare specimens in 1.6 m ion NaCl and simulated concrete pore solution

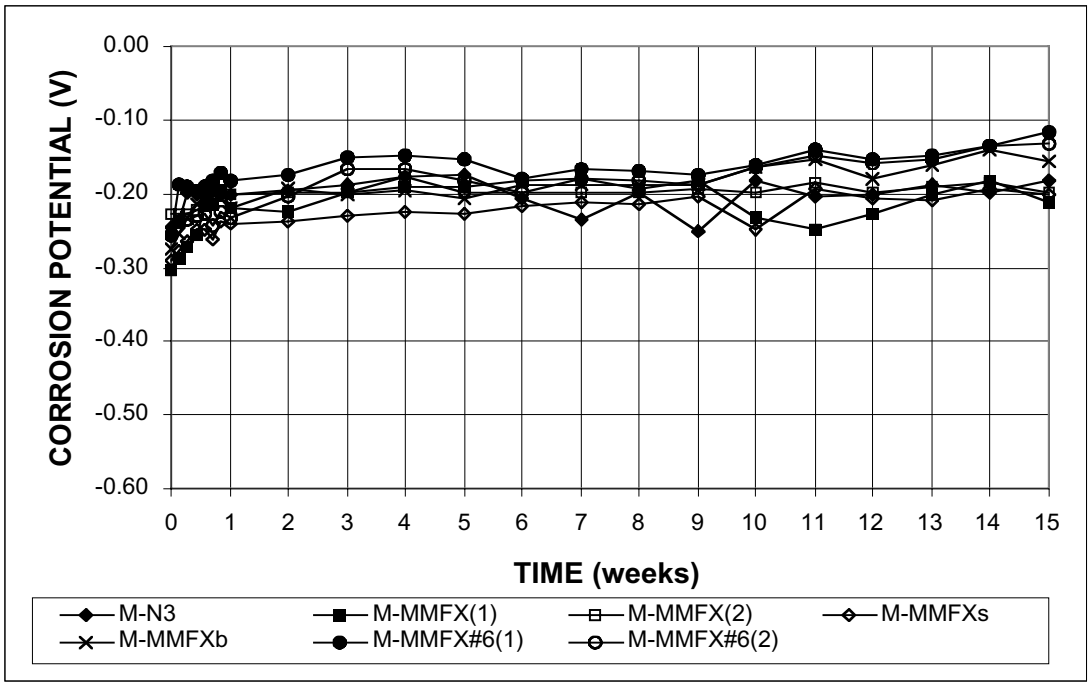

Figure 3.3 - Macrocell Test. Average corrosion potential vs. SCE, cathode.
Bare specimens in 1.6 m ion NaCl and simulated concrete pore solution

The corrosion rates of conventional and sandblasted MMFX bars in 6.04 m ion concentration solution are shown in Fig. 3.4. Initially, MMFX steel had a corrosion rate that was only half of the rate exhibited by conventional steel. However, the two steels corroded at a similar rate, about 30 um/yr, after seven weeks. At 15 weeks, the MMFX steel has a corrosion rate of about 41 um/yr, while the conventional steel corrodes at 26 um/yr. The average total corrosion losses are 10.4 μm and 10.9 μm for N3 and MMFX steel, respectively. The average anode corrosion potentials for both are more negative than –0.50 V (Fig. 3.5), while the cathodes remain passive, with corrosion potentials of about –0.20 V (Fig. 3.6).

Overall, MMFX steel corrodes at about one-third the rate of conventional steel in low chloride concentrations, but at a similar rate in high chloride concentrations.

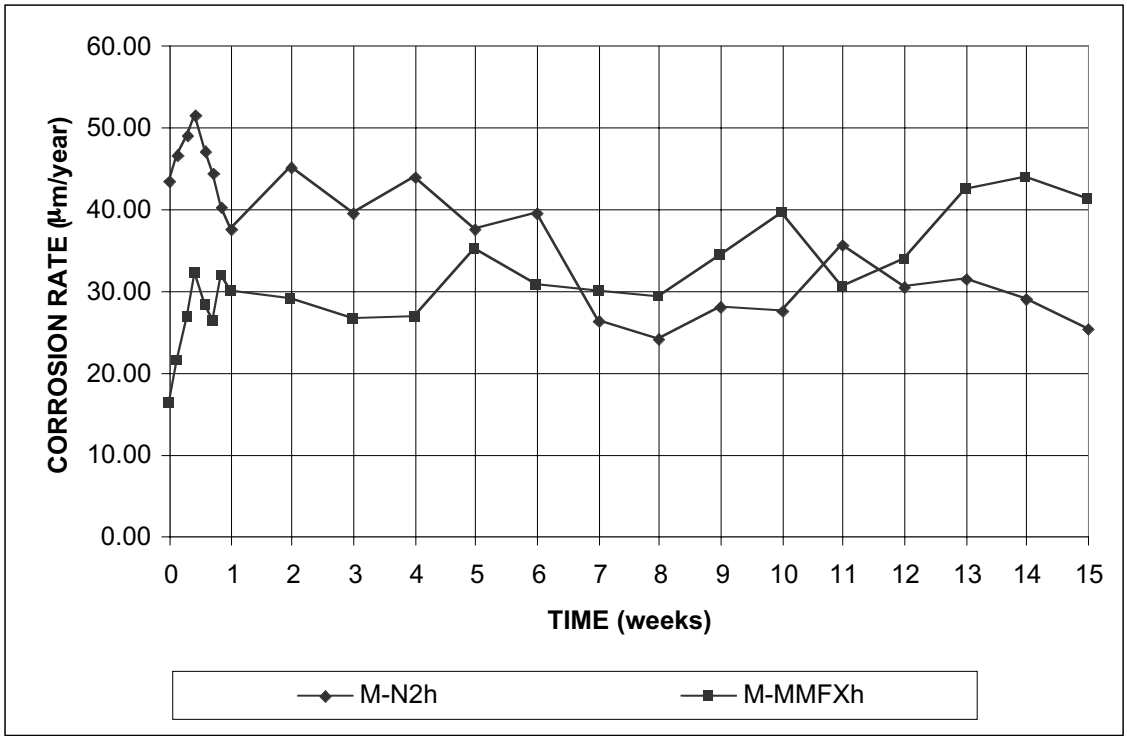

Figure 3.4 - Macrocell Test. Average corrosion rate. Bare specimens in 6.04 m ion (15%) NaCl and simulated concrete pore solution.

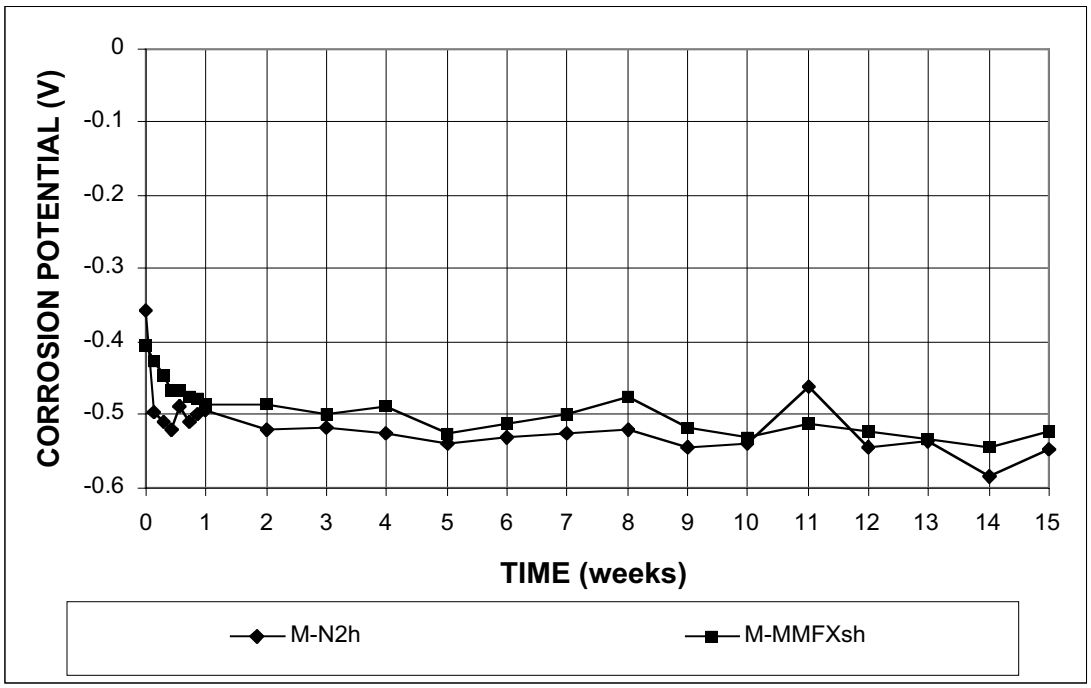

Figure 3.5 - Macrocell Test. Average corrosion potential vs. SCE, anode.
Bare specimens in 6.04 m ion (15%) NaCl and simulated concrete pore solution

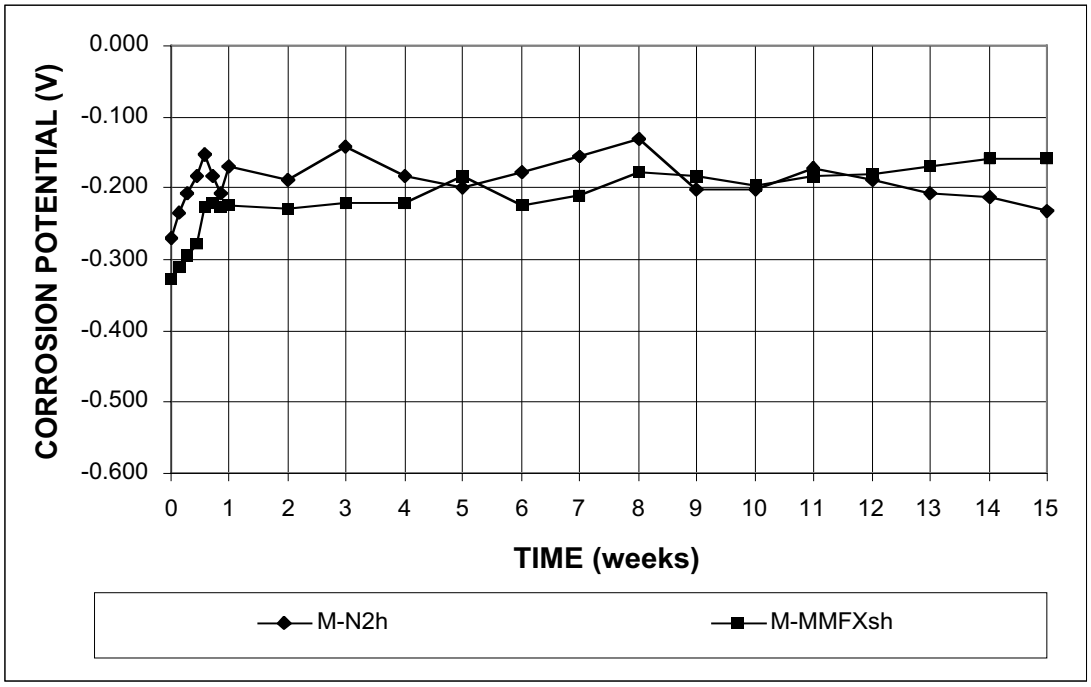

Figure 3.6 - Macrocell Test. Average corrosion potential vs. SCE, cathode.
Bare specimens in 6.04 m ion (15%) NaCl and simulated concrete pore solution

3.1.2 Macrocell tests for mortar-wrapped specimens

The rapid tests of mortar-wrapped specimens included six tests each of conventional, MMFX, and epoxy-coated (ECR) reinforcement, and three tests each of two combinations of MMFX and N3 steel, all in 1.6 m ion concentration solution. The average corrosion rates are shown in Figs. 3.7a and 3.7b. The difference between the two figures is the scale of the vertical axis. The results for the ECR are shown in terms of both the exposed area (area of the four holes), $ECRm^{+}$, and the total bar area exposed to the solution, ECRm*. Uncoated bars were used as the cathode bars in the ECR tests.

At 15 weeks, the corrosion rate reached a value of 532 μm/yr based on the exposed area for the ECR. The results demonstrate that very high corrosion rates can occur in localized areas, especially when the cathode is unprotected as it is in these tests.

However, the ECR specimens exhibit the lowest total corrosion rate based on the total bar area, which is 4.2 μm/yr. This value approximates the expected corrosion rate on the exposed surface, if the tests had used epoxy-coated bars at the cathode in which the coating was penetrated by four 3.2 mm (1/8 in.) diameter holes. The MMFX steel and conventional N3 steel were corroding at 10.5 μm/yr and 17.8 μm/yr, respectively. Again, the MMFX steel has a lower corrosion rate than conventional steel but the improvement is by less than a factor of 2. The total loss for MMFX steel is 1.4 μm, equal to 26% of the total loss for the N3 bars (5.3 μm).

The test results for the macrocells, consisting of mixed MMFX and conventional steel, show a higher average corrosion rate compared to the same tests with all MMFX steel independent of whether conventional steel is the anode (N3/MMFX) or the cathode (MMFX/N3). After 15 weeks, the N3/MMFX and MMFX/N3 steel combinations have average corrosion rates of 12 and 18 μm/yr,

respectively. Thus, combining steels appears to reduce the corrosion performance below that exhibited by MMFX alone.

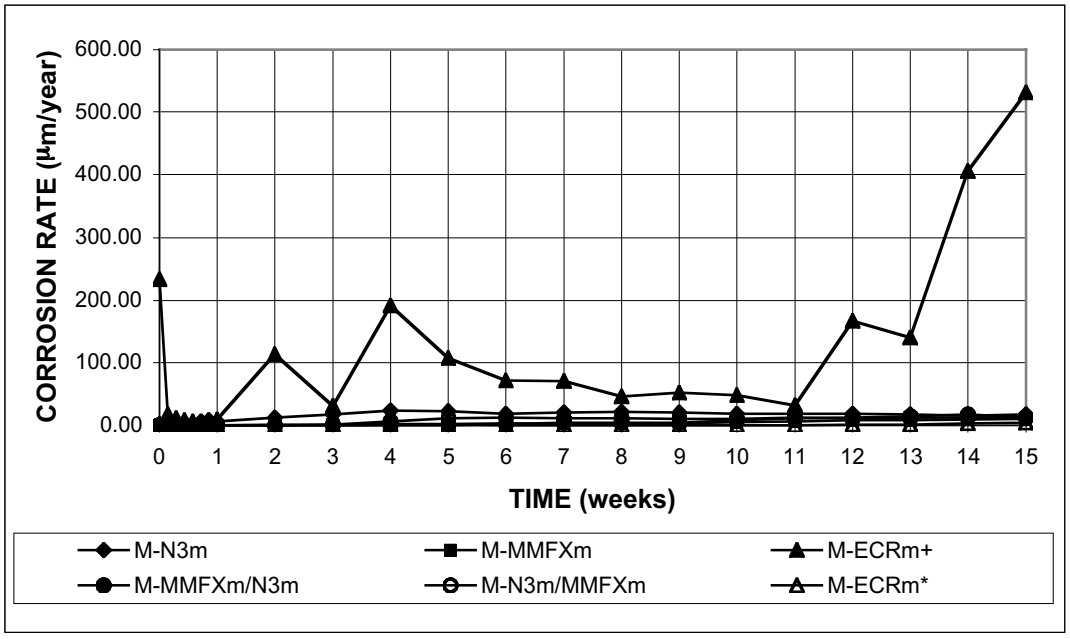

Figure 3.7 a - Macrocell Tests. Average corrosion rate. Mortar-wrapped specimens in 1.6 m ion NaCl and simulated concrete pore solution.

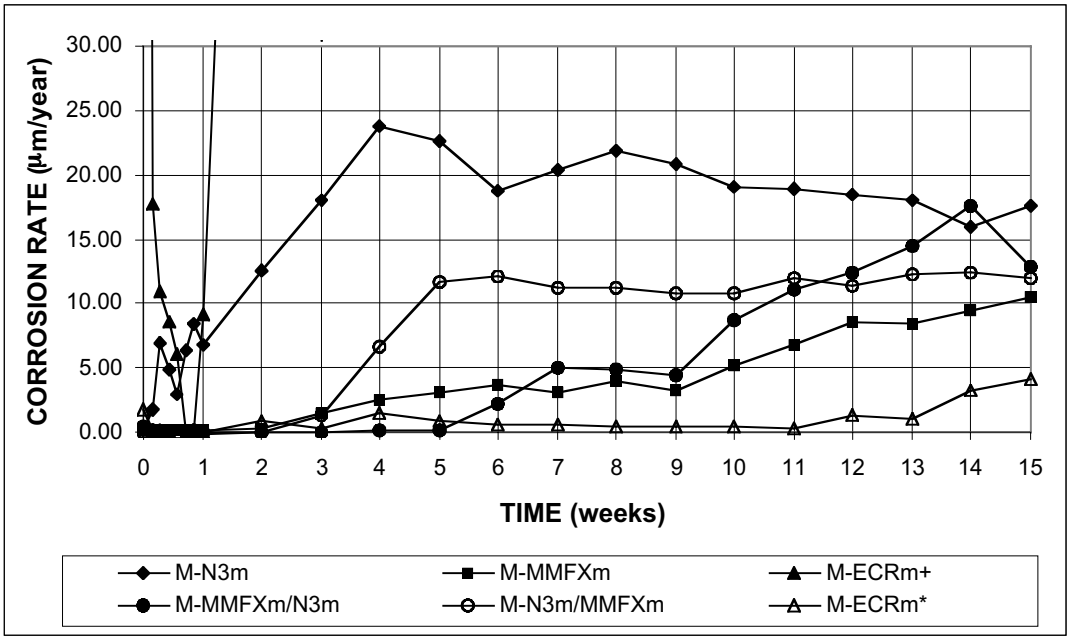

Figure 3.7 b - Macrocell Tests. Average corrosion rate. Mortar-wrapped specimens in 1.6 m ion NaCl and simulated concrete pore solution.

For the conventional steel specimens, the average corrosion potential at the anode dropped below –0.275 V on the second day and ended with a value of –0.61 V at 15 weeks. The ECR bars had a low corrosion potential, –0.47 V at the beginning of the tests, but this increased rapidly and remained near –0.3 V until week 13, finally ending with a value of –0.48 V at week 15. The anodes of the N3/MMFX and all-MMFX macrocells became active starting with week 4, although the corrosion potential in the latter tests remained relatively high until week 11. The average corrosion potentials at the anode in both the all-MMFX macrocells and the MMFX/N3 macrocells are –0.515 V at 15 weeks. The cathodes in the all-MMFX macrocells remained passive after 15 weeks. The cathode potentials are –0.23 V in ECR steel, –0.26 V in both N3/MMFX and N3 tests, and –0.28 V in MMFX/N3 macrocells, indicating a slight tendency to corrode in these specimens. The corrosion potentials are shown in Fig. 3.8 and 3.9.

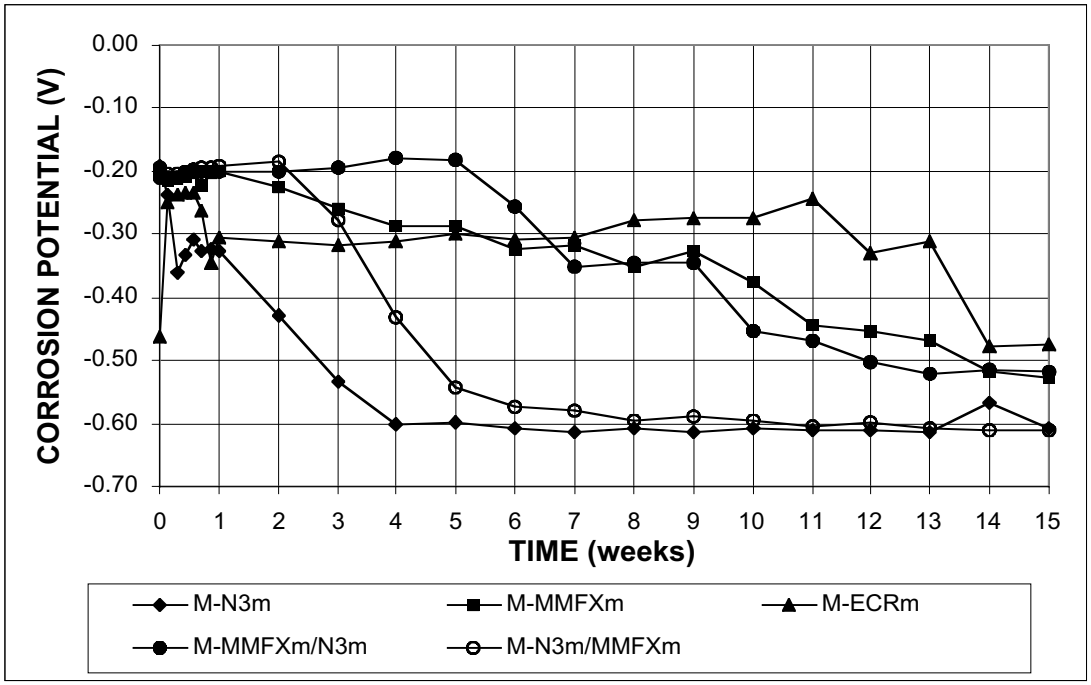

Figure 3.8 - Macrocell Test. Average corrosion potential vs. calomel electrode, anode. Mortar-wrapped specimens in 1.6m ion NaCl and simulated concrete pore solution.

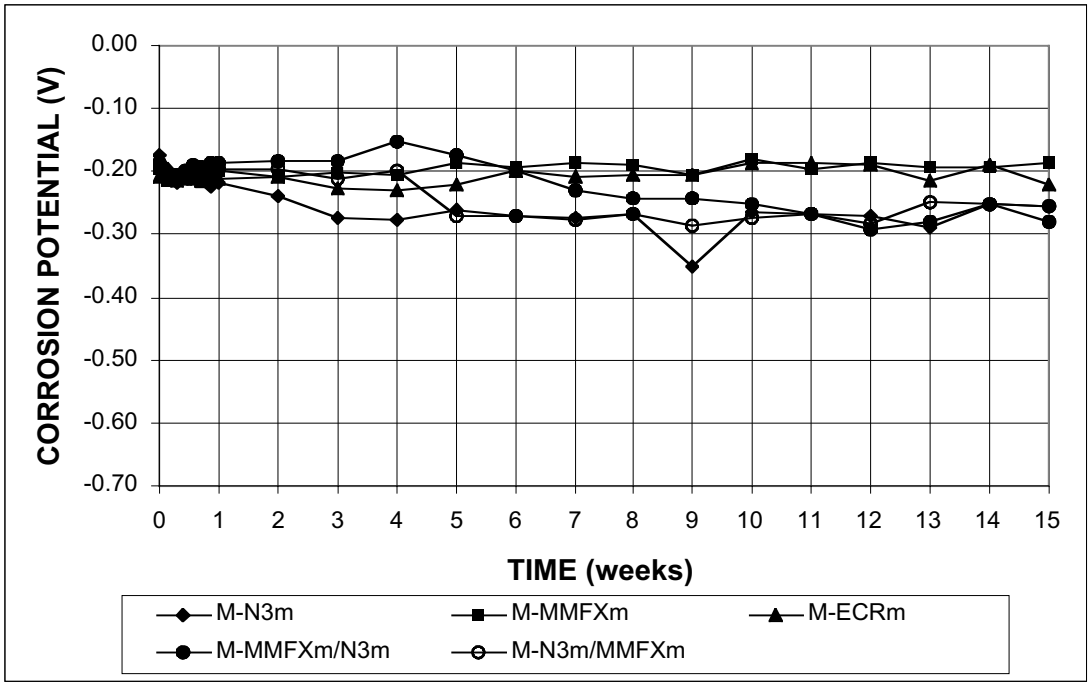

Figure 3.9 - Macrocell Test. Average corrosion potential vs. calomel electrode, cathode. Mortar-wrapped specimens with in 1.6m ion NaCl and simulated concrete pore solution.

3.1.3 Visual Inspection

As the tests were discontinued, the specimens were visually inspected. For bare bar specimens of MMFX(1), most of the corrosion product was found on the bar surface above the solution; for the other bare bar specimens, the corrosion product was observed on the bar surface within the solution. In some cases, corrosion product appeared on the bar at contact points with the plastic lid, presumably due to crevice corrosion. Fig. 3.10 shows a conventional steel anode bar at 15 weeks, with corrosion products that have formed on the bar both above and below the surface of the solution. Figs. 3.11 and 3.12 show bars from MMFX(1) and MMFX(2), respectively, with corrosion products that have formed above and below the surface of the solution.

For mortar-wrapped specimens, the specimens were broken and some corrosion product was found under the mortar. Figs 3.13 and 3.14 show conventional

and MMFX bars, respectively, with corrosion products that have formed on the bar surface.

Figure 3.10 - Bare conventional N3 anode bar, at 15 weeks

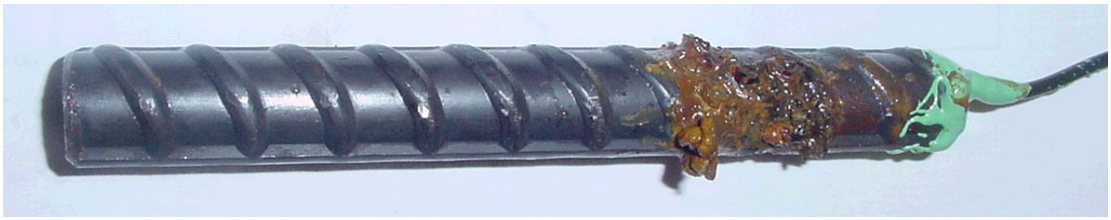

Figure 3.11 – Bare MMFX anode bar from group MMFX(1), at 15 weeks, showing corrosion products that formed above the surface of the solution.

Figure 3.12 – Bare MMFX anode bar from group MMFX(2), at 15 weeks, showing corrosion products that formed below the surface of the solution.

Figure 3.13 - Conventional N3 anode bar after removal of mortar, at 15 weeks.

Figure 3.14 - MMFX anode bar after removal of mortar, at 15 weeks.

3.2 BENCH-SCALE TESTS

The average corrosion rates and total corrosion losses at 40 weeks for the Southern Exposure and cracked beam tests are summarized in Table 3.2. Results for individual specimens are presented in Appendix A.

3.2.1 Southern Exposure Tests

The Southern Exposure tests included six tests each of conventional (N3), MMFX, and epoxy-coated (ECR) reinforcement, and three tests each of two combinations of MMFX and N3 steel. Three SE specimens with bent MMFX steel that started at a later date are also under test. Average corrosion rates, average total corrosion losses and average mat-to-mat resistances for N3, MMFX, ECR, MMFX/N3, N3/MMFX and MMFX bent bars are shown in Figs. 3.15, 3.16, and 3.17, respectively. The results (summarized in Table 3.2) show that, after 40 weeks of testing, the ECR specimens exhibit the lowest average macrocell corrosion rates (0.3 μm/yr for ECR(1) and 0.2 μm/yr for ECR(2)). At the same point in time, the specimens with N3 steel show the highest average corrosion rate (5.6 μm/yr for N3(1)

and 7.0 μm/yr for N3(2)). MMFX steel is corroding at a rate of 1.6 μm/yr, equal to 29% of that exhibited by conventional steel. The corrosion rates of MMFX/N3 combination (MMFX steel as the top layer) and the N3/MMFX combination (N3 steel as the top layer) are 2.2 μm/yr and 5.1 μm/yr, respectively, both higher than that exhibited by MMFX alone. The corrosion rate for MMFX bent bars is 4.3 μm/yr at the 27th week.

At this point, the average total corrosion loss of MMFX (0.56 μm) is 22% of that of conventional steel (2.6 μm), while ECR steel has a corrosion loss based on total bar surface (0.1 μm) equal to 4% of that exhibited by conventional steel.

The very low corrosion rate and total corrosion loss of the ECR bars based on total bar area can be compared with the very high corrosion rate (207 μm/yr) and total corrosion loss (63 μm) based on the exposed area [four 3.2 mm ($^1/_8$ in.) diameter holes in the coating] shown in Figs. 3.18 and 3.19, respectively. These specimens demonstrate again that very high corrosion rates can occur in localized areas.

Table 3.2 – Average corrosion rates and corrosion losses as measured in the bench-scale tests

CORROSION RATE AT WEEK 40 (µm/year)

Steel Designation	Heat No.	Specimen						Average	Std. Deviation
		1	2	3	4	5	6		
Southern Exposure Tests									
N3(1)	S44407	6.20	9.87	0.00	6.32	-	-	5.60	4.10
N3(2)	S44420	8.22	5.67	-	-	-	-	6.95	1.80
ECR(1)[+]	S44407	184.33	456.88	187.98	0.00	-	-	207.29	188.12
ECR(2)[+]	S44420	3.65	186.15	-	-	-	-	94.90	129.05
ECR(1)[*]	S44407	0.38	0.47	0.39	0.00	-	-	0.31	0.21
ECR(2)[*]	S44420	0.01	0.38	-	-	-	-	0.20	0.27
MMFX	810737	2.30	1.20	2.41	1.51	1.96	0.01	1.56	0.89
N3/MMFX	S44420/810737	3.64	4.99	6.77	-	-	-	5.13	1.57
MMFX/N3	810737/S44420	2.35	4.16	0.02	-	-	-	2.18	2.08
MMFXb	810737	4.16	3.60	5.02	-	-	-	4.26	0.72
Cracked Beam Tests									
N3(1)	S44407	5.53	6.63	4.74	2.45	-	-	4.84	1.77
N3(2)	S44420	1.88	4.83	-	-	-	-	3.36	2.09
ECR(1)[+]	S44407	1027.06	36.55	1260.98	1235.39	-	-	889.99	578.53
ECR(2)[+]	S44420	0.00	7.31	-	-	-	-	3.66	5.17
ECR(1)[*]	S44407	1.06	0.04	1.30	1.27	-	-	0.92	0.60
ECR(2)[*]	S44420	0.00	0.01	-	-	-	-	0.00	0.01
MMFX	810737	2.41	1.92	2.28	4.15	3.77	1.67	2.70	1.02

TOTAL CORROSION LOSS AFTER WEEK 40 (µm)

Steel Designation	Heat No.	Specimen						Average	Std. Deviation
		1	2	3	4	5	6		
Southern Exposure Tests									
N3(1)1	S44407	2.23	5.52	0.34	2.31	-	-	2.60	2.15
N3(2)	S44420	2.34	1.09	-	-	-	-	1.71	0.88
ECR(1)[+]	S44407	38.71	141.52	45.34	27.55	-	-	63.28	52.67
ECR(2)[+]	S44420	6.49	27.97	-	-	-	-	17.23	15.19
ECR(1)[*]	S44407	0.08	0.15	0.09	0.06	-	-	0.09	0.04
ECR(2)[*]	S44420	0.01	0.06	-	-	-	-	0.04	0.03
MMFX	810737	1.29	0.41	0.91	0.35	0.39	0.02	0.56	0.45
N3/MMFX	S44420/810737	1.35	3.27	3.30	-	-	-	2.64	1.12
MMFX/N3	810737/S44420	0.29	0.58	0.03	-	-	-	0.30	0.28
MMFXb	810737	2.63	1.48	2.83	-	-	-	2.31	0.73
Cracked Beam Tests									
N3(1)	S44407	6.85	7.39	5.97	4.49	-	-	6.17	1.27
N3(2)	S44420	4.87	6.03	-	-	-	-	5.45	0.82
ECR(1)[+]	S44407	1208.89	323.89	695.72	1042.87	-	-	817.84	392.62
ECR(2)[+]	S44420	134.74	143.95	-	-	-	-	139.35	6.51
ECR(1)[*]	S44407	1.01	0.97	0.23	0.41	-	-	0.65	0.40
ECR(2)[*]	S44420	0.14	0.15	-	-	-	-	0.14	0.01
MMFX	810737	2.80	1.80	2.31	3.12	2.79	2.17	2.50	0.49

[1] N3: Conventional, normalized A 615 reinforcing steel

[2] MMFX: MMFX Microcomposite steel

[3] ECR: Epoxy-coated N3 steel

[+] Based on exposed area, four 3.2 mm (1/8 in.) diameter holes in epoxy

* Based on total area of bar exposed to solution

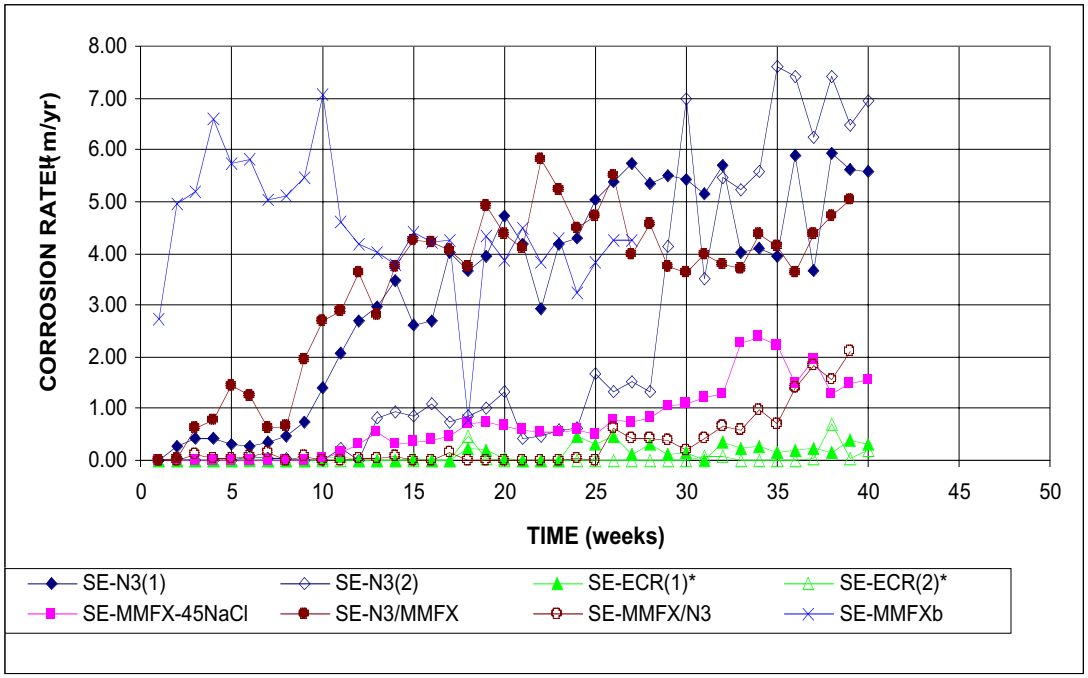

Figure 3.15 - Southern Exposure Test. Average corrosion rate, specimens with w/c = 0.45 and ponded with 15% NaCl solution. (ECR*: Based on total area of bar exposed to solution)

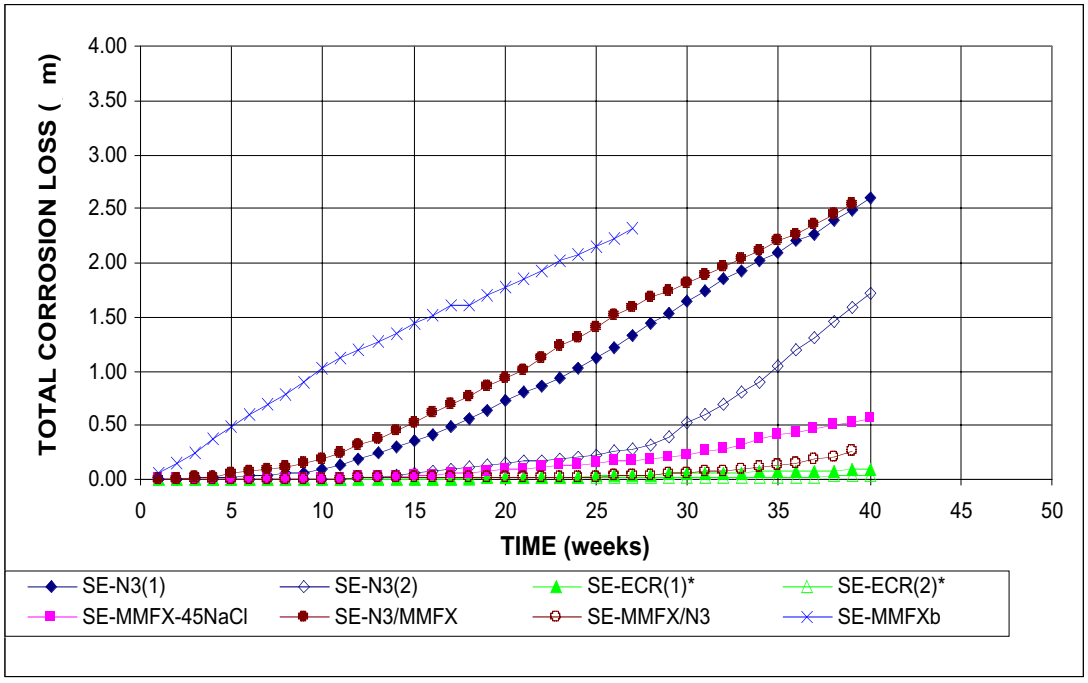

Figure 3.16 - Southern Exposure Test. Total corrosion loss, specimens with w/c=0.45 and ponded with a 15% NaCl solution. ((ECR*: Based on total area of bar exposed to solution)

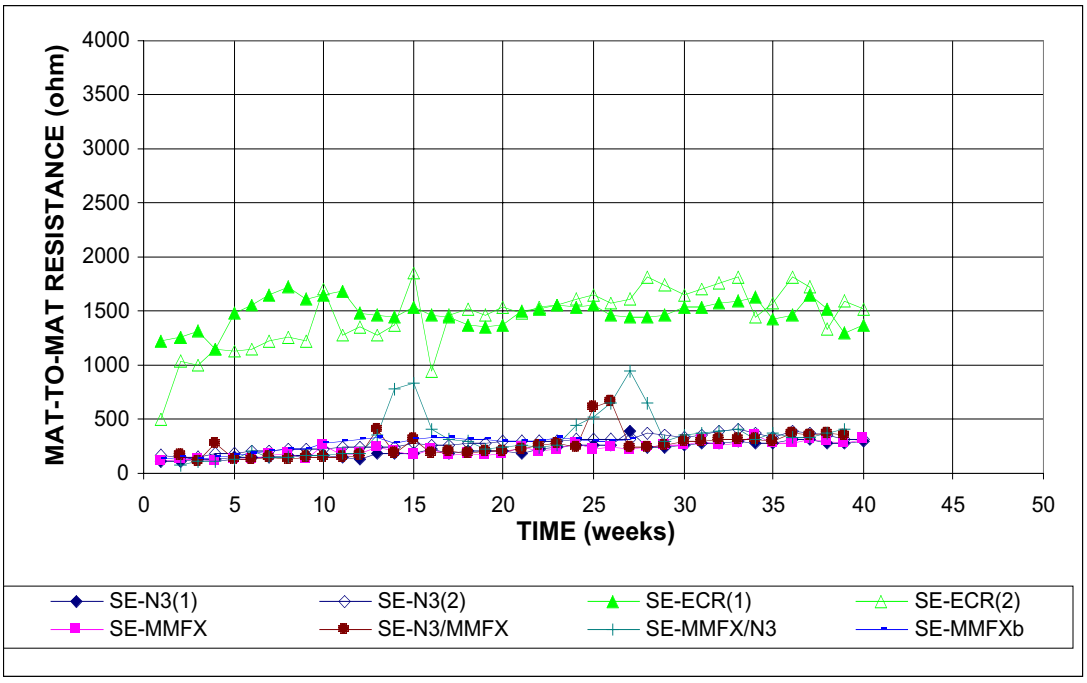

Figure 3.17 - Southern Exposure Test. Average mat-to-mat resistance. Specimens with w/c=0.45 and ponded with NaCl.

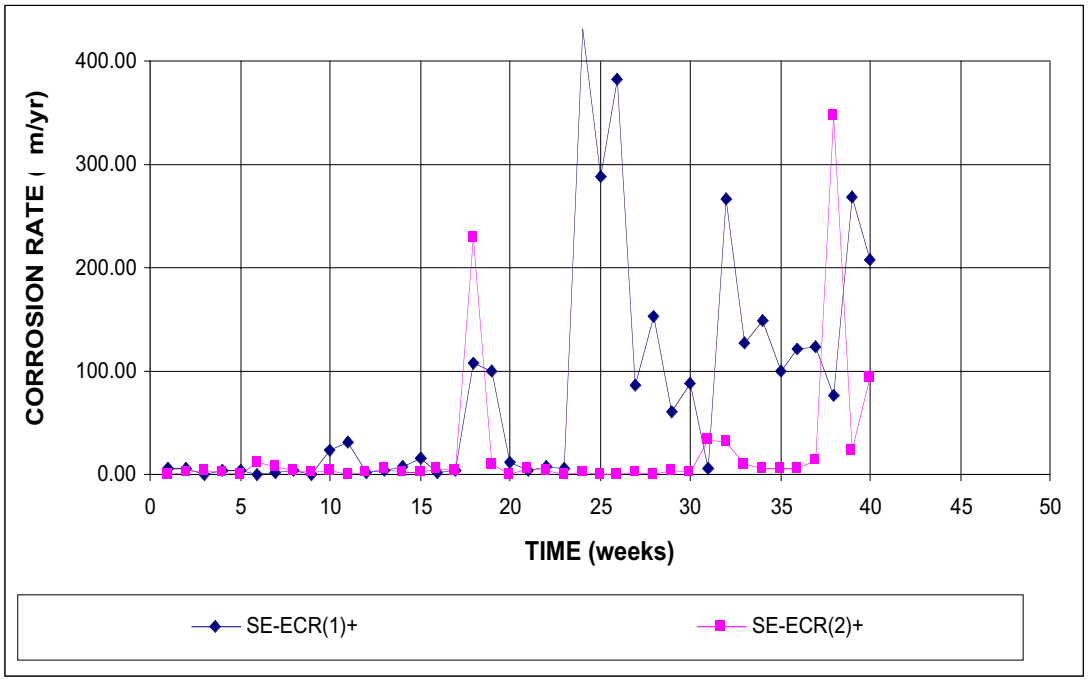

Figure 3.18 - Southern Exposure Test. Average corrosion rate, epoxy-coated bars, specimens with w/c=0.45 and ponded with NaCl. (ECR^{+}: Based on exposed area, four 3.2 mm (1/8 in.) diameter holes in epoxy)

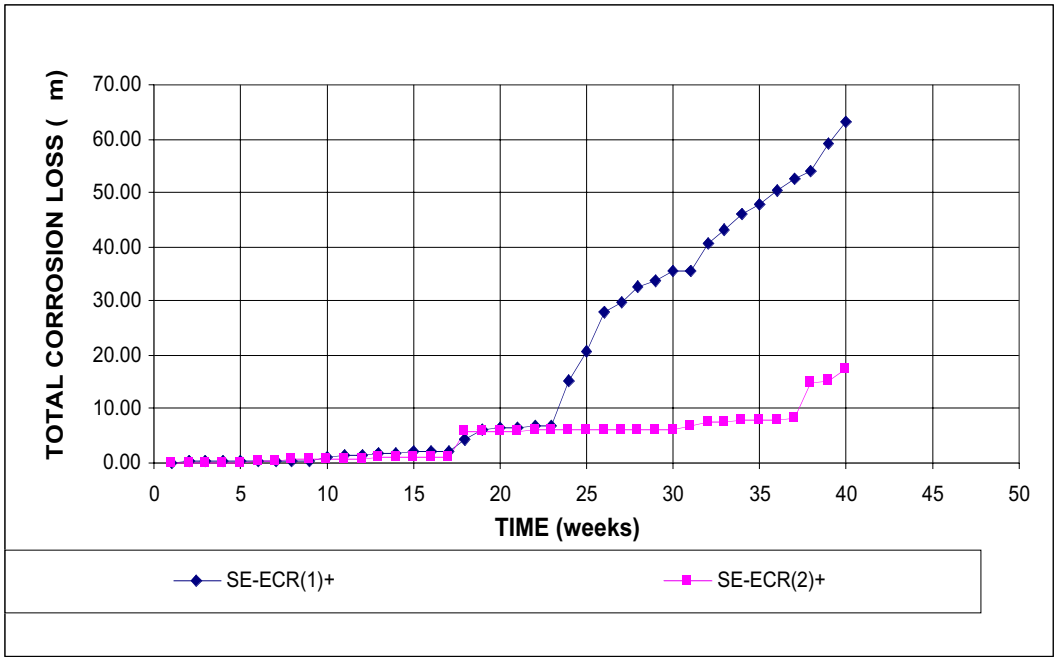

Figure 3.19 - Southern Exposure Test. Total corrosion loss, epoxy-coated bars, specimens with w/c=0.45 and ponded with NaCl. (ECR^{+}: Based on exposed area, four 3.2 mm (1/8 in.) diameter holes in epoxy)

The corrosion potentials of all bench-scale tests are measured with respect to the copper-copper sulfate electrode (CSE), which gives values that are 0.075 V more

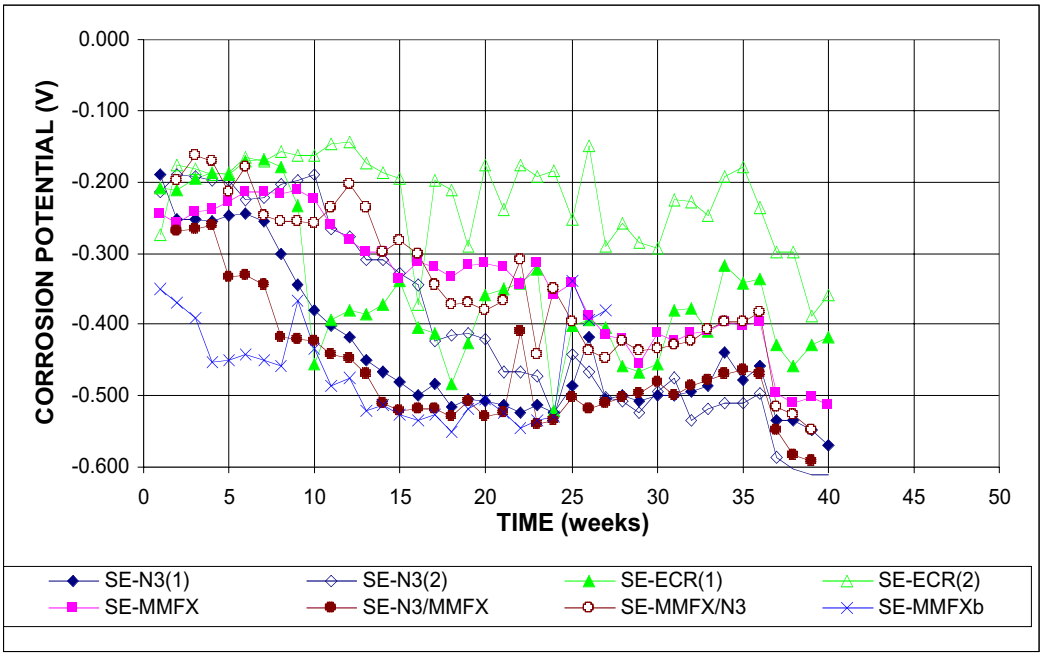

negative than those measured with the SCE. The average potentials for the top mat of steel dropped below –0.35 V at the end of the first week for the MMFX bent bars, which indicates the specimens were actively corroding. For the N3 specimens and for the N3/MMFX combination, the anode potentials were more negative than –0.35 V after eight and nine weeks, respectively. The ECR specimens exhibit fluctuating potentials, with some specimens remaining passive but some undergoing active corrosion at week 10. For the MMFX/N3 combination and for the MMFX specimens, the corrosion potentials were more negative than –0.35 V after 23 and 24 weeks, respectively. The bottom layers were under active corrosion for the N3 and ECR(1) specimens after 15 weeks, for the MMFX/N3 combination after 16 weeks, and for the MMFX and N3/MMFX specimens after 30 weeks. The corrosion potentials for the top and bottom mats are presented in Figs 3.20 and Fig 3.21, respectively.

Figure 3.20 - Southern Exposure Test. Average corrosion potential vs. CSE, top mat.

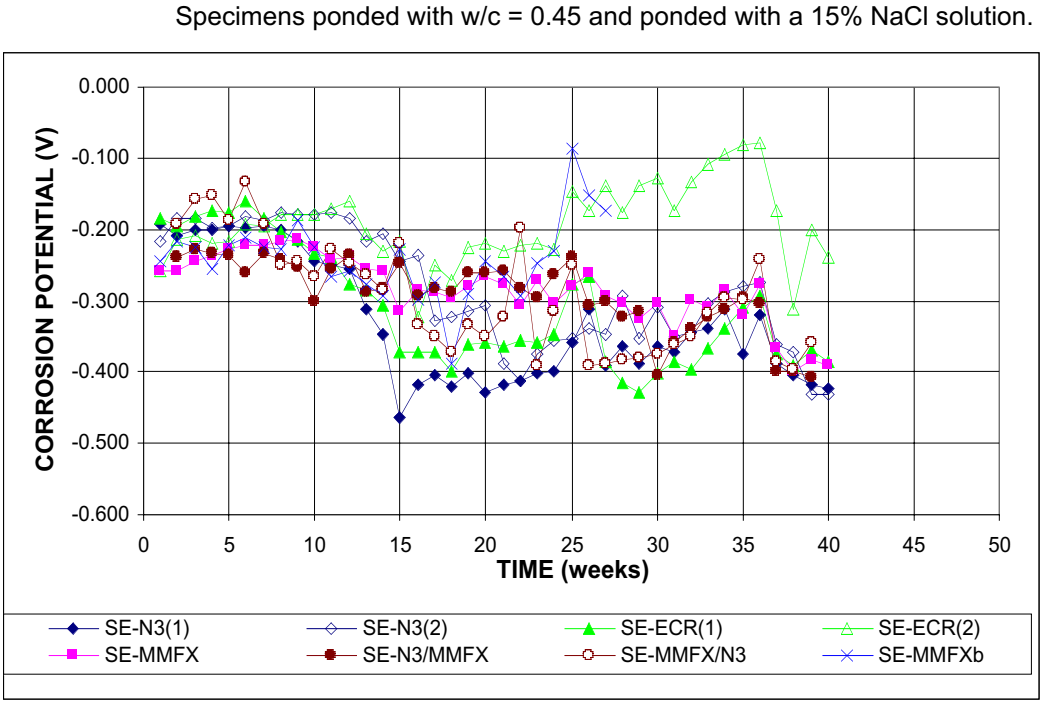

Figure 3.21 - Southern Exposure Test. Average corrosion potential vs. CSE, bottom mat. Specimens ponded with w/c = 0.45 and ponded with a 15% NaCl solution.

3.2.2 Cracked Beam Tests

The cracked beam tests include six specimens each of conventional, MMFX, and epoxy-coated reinforcement. Figures 3.22, 3.23 and 3.24 show the average corrosion rates, average total corrosion losses, and average mat-to-mat resistances for the ECR bars based on total area, N3 steel, and MMFX reinforcement. After 40 weeks, conventional, MMFX, and epoxy-coated steel exhibited average corrosion rates of 4.8 μm/yr, 2.7 μm/yr, and 0.9 μm/yr respectively. At this point, MMFX steel was corroding at a rate equal to 56% of that exhibited by conventional steel, while ECR steel exhibits a corrosion rate equal to 18.8 % of that exhibited by conventional steel. The conventional steel also exhibits the highest average total corrosion loss, which is about 6.2 μm. This is followed by MMFX steel, with an average total corrosion loss of 2.5 μm. The ECR specimens exhibit the lowest corrosion loss, about 0.7 μm, based on full bar area. The six ECR specimens exhibit a total corrosion loss equal to 11% of that exhibited by the conventional reinforcement, while the MMFX

steel exhibits a total corrosion loss equal to 40% of that exhibited by the conventional steel. The corrosion rate and total corrosion loss of the ECR bars based on the exposed surface are very high, as shown in Figs. 3.25 and 3.26. The results are similar to that observed for the ECR macrocell specimens and SE specimens.

The average corrosion potentials of the top and bottom mats are shown in Figs. 3.27 and 3.28. The specimens in group N3(1) exhibit the most negative corrosion potentials of top mats, with an average value more negative than –0.6 V, while the ECR(1) and MMFX specimens exhibit corrosion potentials of about –0.58 and –0.55 V, respectively. The bottom mat of the conventional steel specimens begins to corrode in the 8th week; this occurs for ECR(1) specimens in the 15th week, for ECR(2) specimens in the 16th week, and for the MMFX specimens in the 27th week.

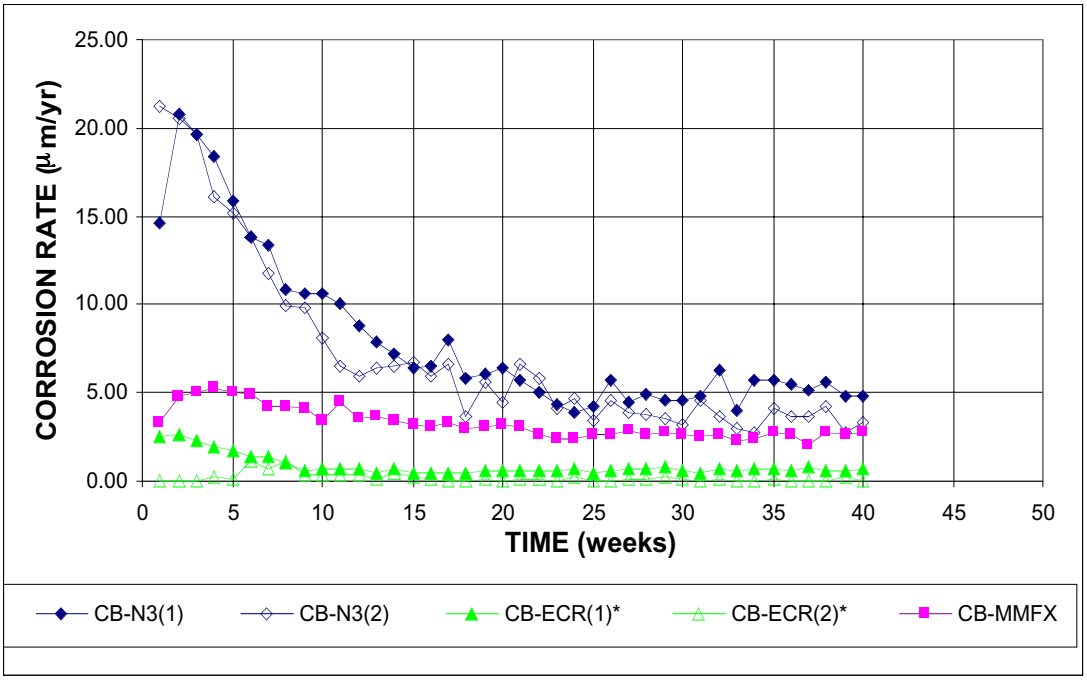

Figure 3.22 - Cracked Beam Test. Average corrosion rate, specimens with w/c=0.45 and ponded with 15% NaCl solution. (ECR*: Based on total area of bar exposed to solution)

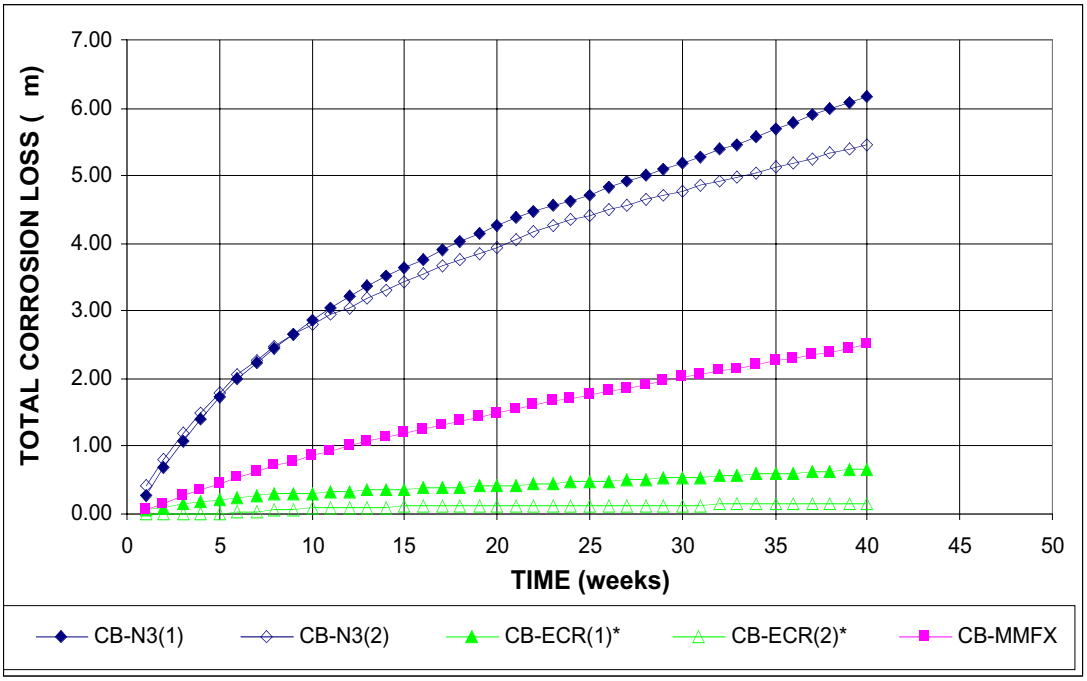

Figure 3.23- Cracked Beam Test. Average total corrosion loss, specimens with w/c=0.45, ponded with a 15% NaCl solution. (ECR*: Based on total area of bar exposed to solution)

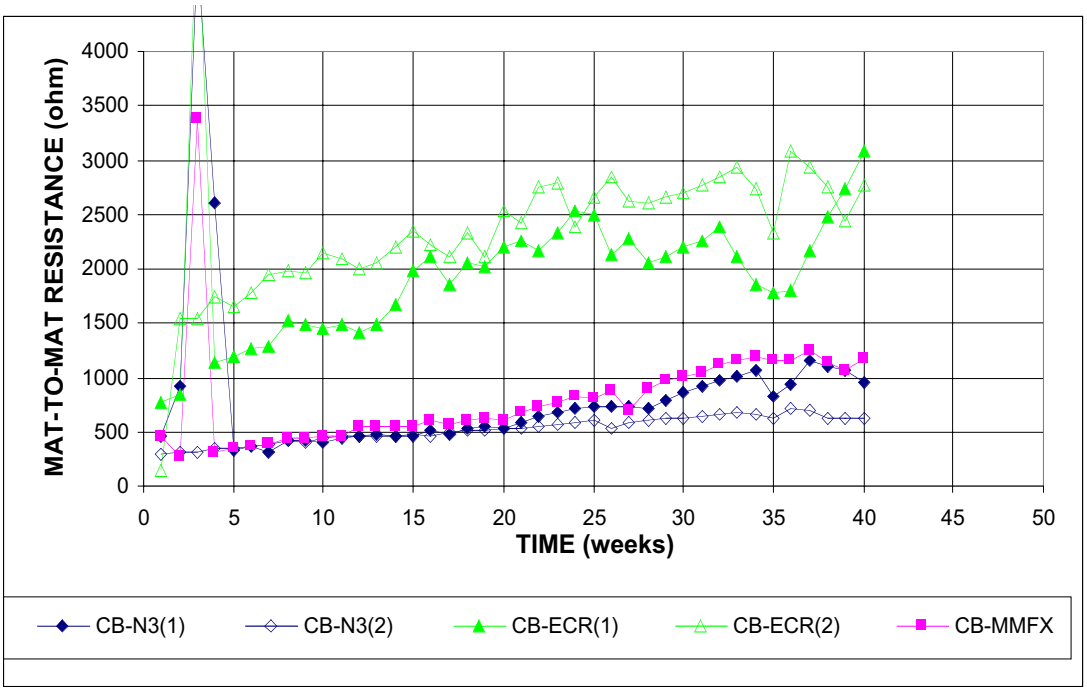

Figure 3.24 - Cracked Beam Test. Average mat-to-mat resistance. Specimens with w/c=0.45, ponded with a 15% NaCl solution.

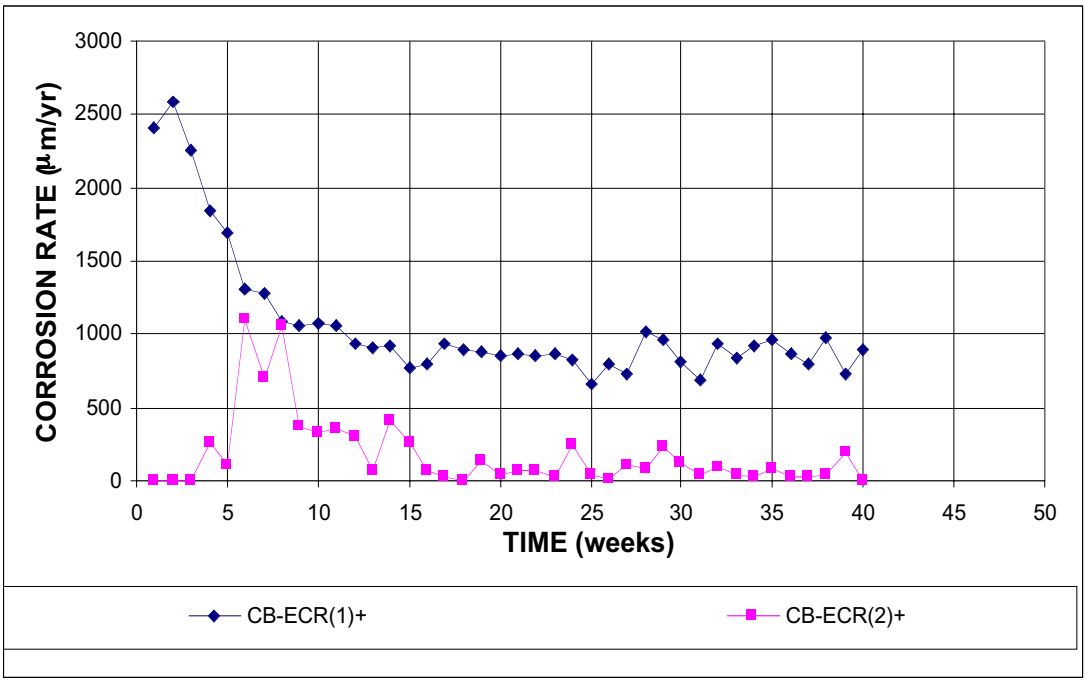

Figure 3.25 - Cracked Beam Test. Average corrosion rate, epoxy-coated bars, specimens with w/c=0.45, ponded with a 15% NaCl solution. (ECR^{+}: Based on exposed area, four 3.2 mm (1/8 in.) diameter holes in epoxy)

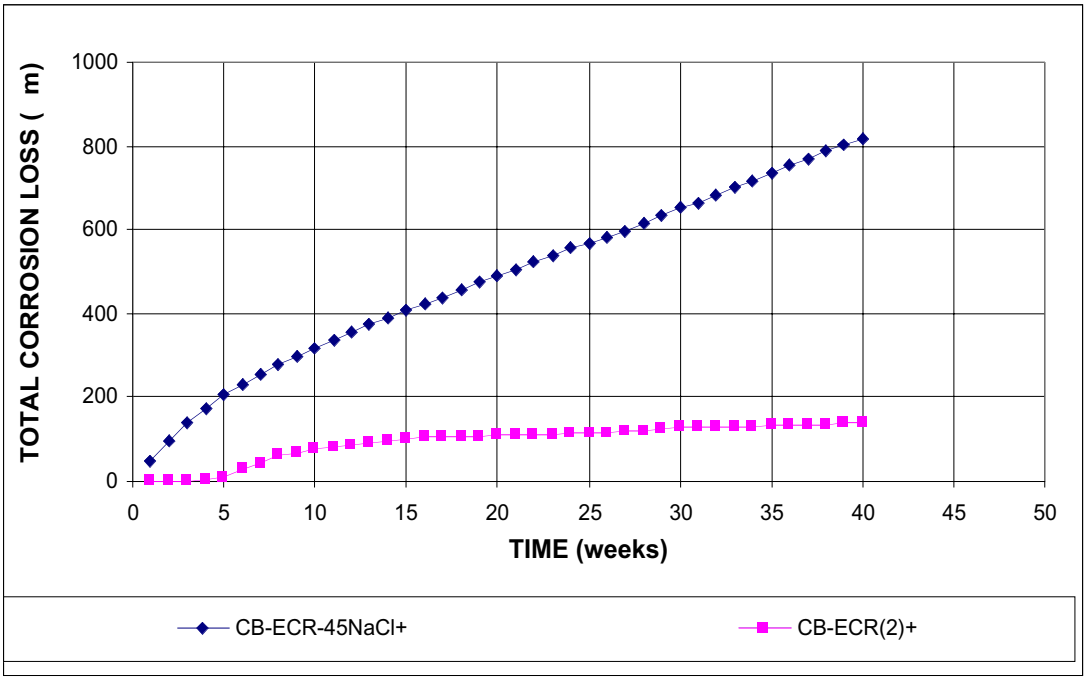

Figure 3.26 - Cracked Beam Test. Average total corrosion loss, epoxy-coated bars, specimens with w/c=0.45, ponded with a 15% NaCl solution. (ECR^{+}: Based on exposed area, four 3.2 mm (1/8 in.) diameter holes in epoxy)

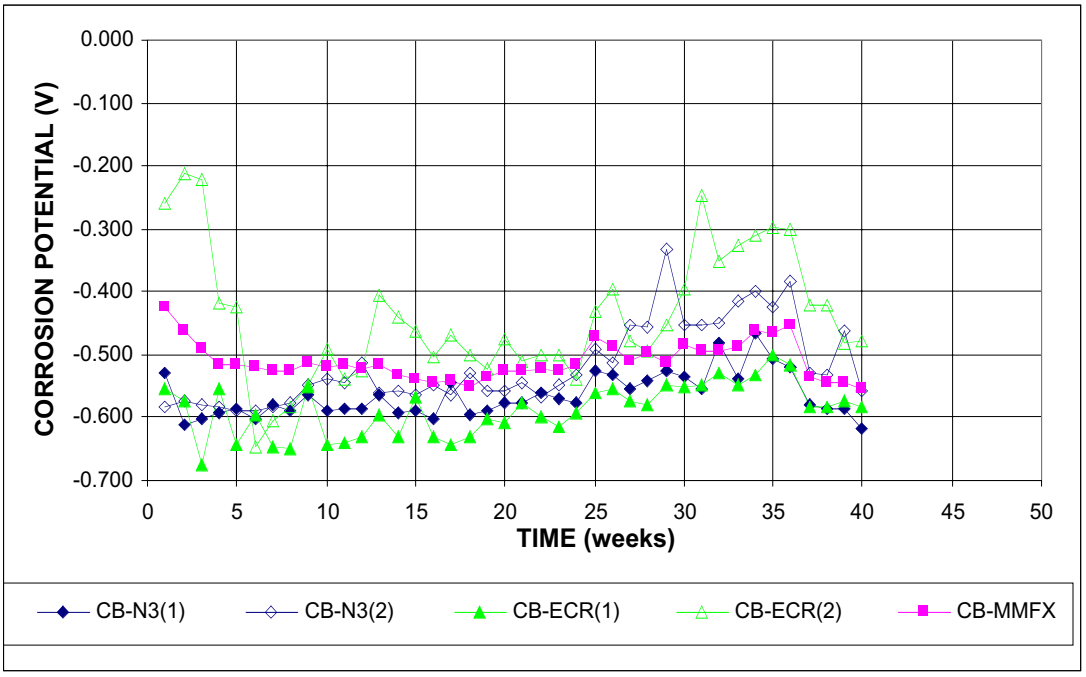

Figure 3.27- Cracked Beam Test. Average corrosion potential vs. CSE, top mat. Conventional steel, normalized, specimens ponded with NaCl.

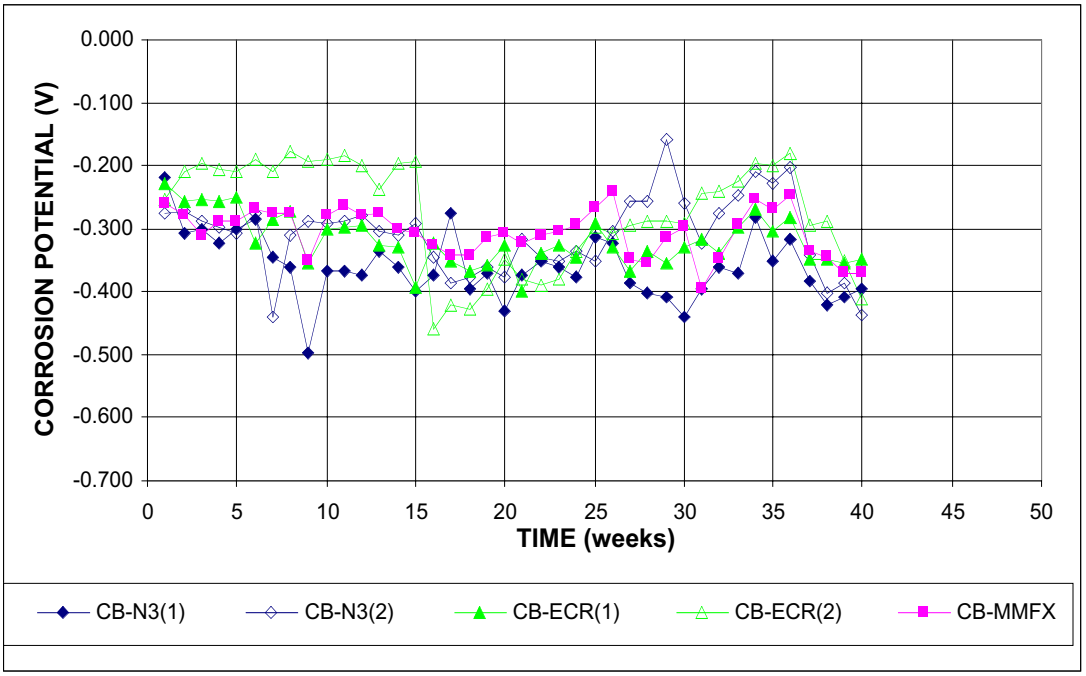

Figure 3.28- Cracked Beam Test. Average corrosion potential vs. CSE, bottom mat. Conventional steel, normalized, specimens ponded with NaCl.

Overall, from the results of rapid and bench-scale tests, the corrosion performance of ECR is superior to MMFX steel, indicating that epoxy-coated reinforcement should not be replaced by MMFX reinforcing steel without the use of a supplementary corrosion protection system.

3.3 MECHANICAL TESTING OF THE REINFORCING BARS

Both MMFX and conventional steels were tested for mechanical properties. The yield strength, tensile strength, elongation, and bending results are summarized in Table 3.3.

The yield strengths for conventional steel are obtained based on a well-defined yield point. The average yield strengths range from a low of 459.9 MPa (66.7 ksi) for a heat of No. 13 [No. 4] bars to a high of 510.9 MPa (74.1 ksi) for a heat of No. 19 [No. 6] bars. Average tensile strengths are between 749.5 MPa (108.7 ksi) and

816.3 MPa (118.4 ksi). Average elongations range from 13.6 to 16.8%, with a low of 10.9% for an individual test.

Because the MMFX steel does not have an obvious yield plateau, yield strengths are determined using the 0.2% offset method and 0.7% total strain. Based on the 0.2% offset method, the heat of No. 16 [No. 5] MMFX bars had an average yield strength of 824.6 MPa (119.6 ksi), while the two heats of No. 19 [No. 6] MMFX bars had average yield strengths of 976.3 MPa (141.6 ksi) and 913.6 MPa (132.5 ksi). Based on 0.7% total strain, yield strengths increase to 833.6 MPa (120.9 ksi), 983.9 MPa (142.7 ksi) and 931.5 MPa (135.1 ksi), respectively. The average tensile strengths for the three heats were 1104.5 MPa (160.2 ksi), 1193.5 MPa (173.1 ksi) and 1134.9 MPa (164.6 ksi), respectively. Average elongations for an 8 in. gage length were 7.2, 7.1 and 7.0%, respectively, with a low value of 6.3 %. All conventional and MMFX bars passed the bend test.

Compared to conventional steel, MMFX steel has much higher yield and tensile strengths but smaller elongation. The yield and tensile strengths of MMFX steel are closer to those specified for high-strength steel bars for prestressing concrete (ASTM A 722) than to conventional steel (ASTM A 615). The average tensile strengths for both No. 5 and No. 6 bars exceed the 1034.3 Mpa (150 ksi) minimum required for A 722 bars. Based on 0.7% total strain, the yield strengths of the individual No. 19 [No. 6] bars meet the minimum requirements for both Type I and Type II bars, which are set at 85% [879.1 Mpa (127.5 ksi)] and 80% [827.4 Mpa (120 ksi)], respectively, of the minimum tensile strength. However, values obtained based on the 0.2% offset method only satisfy the Type II bar criteria, and only for No. 19 [No. 6] bars. Values for No. 16 [No. 5] bars are lower than the requirement and would not be acceptable. To fully meet the requirement of ASTM A 722, the bars must be cold-stressed to at least 80% of the minimum tensile strength, as required by the standard.

Table 3.3 – Mechanical test results

Steel	Heat No.	Size	Sample Number	Yield Strength Mpa (ksi)		Tensile Strength (ksi)	Elongation % in 8 in.	Bending
N3[1]	S46753	No. 13 (No. 4)	1	451.6 (65.5)		733.6 (106.4)	14.1	Pass
			2	455.1 (66.0)		747.4 (108.4)	12.5	
			3	473.7 (68.7)		768.1 (111.4)	12.5	
			Average	459.9 (66.7)		749.5 (108.7)	13	
N3	S46757	No. 13 (No. 4)	1	501.2 (72.7)		790.8 (114.7)	12.5	Pass
			2	476.4 (69.1)		767.4 (111.3)	12.9	
			3	475.7 (69.0)		768.8 (111.5)	15.6	
			Average	484.7 (70.3)		775.7 (112.5)	13.7	
N3	S46760	No. 13 (No. 4)	1	495.7 (71.9)		768.8 (111.5)	12.5	Pass
			2	482.6 (70.0)		764.6 (110.9)	10.9	
			3	477.8 (69.3)		760.5 (110.3)	13.3	
			Average	485.4 (70.4)		764.6 (110.9)	12.2	
N3	S44407	No. 16 (No. 5)	1	470.2 (68.2)		761.9 (110.5)	16.4	Pass
			2	461.9 (67.0)		748.1 (108.5)	15.6	
			3	460.6 (66.8)		746.7 (108.3)	14.8	
			Average	464.0 (67.3)		752.2 (109.1)	15.6	
N3	S44420	No. 16 (No. 5)	1	469.5 (68.1)		779.8 (113.1)	12.5	Pass
			2	470.2 (68.2)		764.6 (110.9)	15.6	
			3	481.3 (69.8)		790.8 (114.7)	14.1	
			Average	473.7 (68.7)		778.4 (112.9)	14.1	
N3	S47695	No. 19 (No. 6)	1	511.6 (74.2)		819.1 (118.8)	14.1	Pass
			2	515.0 (74.7)		821.9 (119.2)	12.5	
			3	504.7 (73.2)		808.1 (117.2)	14.1	
			Average	510.2 (74.0)		816.3 (118.4)	13.6	
N3	S47790	No. 19 (No. 6)	1	508.1 (73.7)		797.0 (115.6)	12.9	Pass
			2	516.4 (74.9)		810.8 (117.6)	14.1	
			3	509.5 (73.9)		798.4 (115.8)	18.8	
			Average	510.9 (74.1)		801.9 (116.3)	15.3	
N3	S47814	No. 19 (No. 6)	1	473.0 (68.6)		759.1 (110.1)	18.4	Pass
			2	479.2 (69.5)		766.0 (111.1)	16.4	
			3	475.0 (68.9)		759.8 (110.2)	15.6	
			Average	475.7 (69.0)		761.9 (110.5)	16.8	
				0.2% offset	0.7% total			
MMFX[1]	810737	No. 16 (No. 5)	1	785.3 (113.9)	819.1	1094.2 (158.7)	7	Pass
			2	859.1 (124.6)	866.0	1113.5 (161.5)	6.6	
			3	802.5 (116.4)	868.7	1113.5 (161.5)	7.8	
			4	786.0 (114.0)	822.5	1088.0 (157.8)	8.5	
			5	888.7 (128.9)	791.5	1112.1 (161.3)	6.3	
			Average	824.6 (119.6)	833.6	1104.5 (160.2)	7.2	
MMFX	810737	No. 19 (No. 6)	1	1037.0 (150.4)	1028.0	1200.4 (174.1)	6.3	Pass
			2	923.9 (134.0)	941.8	1196.2 (173.5)	7.8	
			3	866.7 (125.7)	907.4	1196.2 (173.5)	7	
			4	1028.0 (149.1)	1020.4	1182.5 (171.5)	6.6	
			5	1027.3 (149.0)	1020.4	1190.0 (172.6)	7	
			Average	976.3 (141.6)	983.9	1193.5 (173.1)	7	
MMFX	710788	No. 19 (No. 6)	1	905.3 (131.3)	924.6	1127.3 (163.5)	7.8	Pass
			2	916.3 (132.9)	924.6	1148.0 (166.5)	7.8	
			3	909.4 (131.9)	920.5	1129.4 (163.8)	6.3	
			4	835.6 (121.2)	878.4	1121.1 (162.6)	7	
			5	999.7 (145.0)	1008.7	1148.7 (166.6)	6.6	
			Average	913.6 (132.5)	931.5	1134.9 (164.6)	7.1	

3.4 MICROANALYSIS OF THE REINFORCING BARS

The results of X-ray microanalyses are shown in Table 3.4 and include the composition of one heat of conventional steel and all three groups of MMFX steel. The variations in the individual constituents are within the scatter expected for a high quality x-ray microanalysis. The results demonstrate that the chemistry of MMFX steel is consistent for bars within the same heat and very close for the three groups analyzed.

Table 3.4 - Results of X-Ray Microanalysis of MMFX Microcomposite Steel

Steel	Bar Size	Heat No.	Sample	Locatio	Fe	Cr	Si	Mn
N3[1]	No. 16 (No.5)	S44420	1	1	98.26	0.22	0.45	1.07
				2	98.04	0.27	0.52	1.17
				3	98.17	0.23	0.45	1.15
				average	98.16	0.24	0.47	1.13
			2	1	98.16	0.28	0.42	1.14
				2	98.18	0.22	0.39	1.21
				3	98.11	0.25	0.45	1.19
				average	98.15	0.25	0.42	1.18
			average for this heat		98.15	0.25	0.45	1.16
MMFX[2]	No. 16 (No.5)	810737	1	1	89.54	9.67	0.40	0.38
				2	89.37	9.78	0.44	0.40
				3	89.36	9.86	0.45	0.34
				average	89.42	9.77	0.43	0.37
			2	1	89.39	9.59	0.34	0.68
				2	89.56	9.72	0.41	0.31
				3	90.06	9.24	0.35	0.35
				average	89.67	9.52	0.37	0.45
			average for this heat		89.55	9.64	0.40	0.41
MMFX	No. 19 (No.6)	810737	1	1	89.58	9.37	0.66	0.38
				2	89.65	9.39	0.49	0.47
				3	90.01	9.31	0.25	0.43
				average	89.75	9.36	0.47	0.43
			2	1	89.54	9.72	0.25	0.49
				2	89.54	9.64	0.43	0.39
				3	89.38	9.69	0.49	0.44
				average	89.49	9.68	0.39	0.44
			average for this heat		89.62	9.52	0.43	0.43
MMFX	No. 19 (No.6)	710788	1	1	89.62	9.41	0.66	0.32
				2	89.76	9.40	0.29	0.54
				3	89.56	9.31	0.61	0.52
				average	89.65	9.37	0.52	0.46
			2	1	89.54	9.70	0.44	0.33
				2	89.55	9.71	0.50	0.25
				3	89.58	9.54	0.49	0.39
				average	89.56	9.65	0.48	0.32
			average for this heat		89.60	9.51	0.50	0.39

[1] N2 and N3: Conventional, normalized A 615 reinforcing steel
[2] MMFX: MMFX Microcomposite steel

3.5 SEM ANALYSIS OF CORROSION PRODUCTS

The scanning electron microscope was used to obtain images of corrosion products from both conventional and MMFX steel. The selected images are shown in Figs 3.29-3.37. The images of corrosion products from MMFX steel are shown on the left (a) and the images of corrosion products from conventional steel are shown on the right (b). The following description is taken from Darwin et al. (2002):

Figures 3.29-3.33 show corrosion products on the anode bars from bare steel macrocell tests. Figure 3.29 shows the corrosion product with nodular structures covered by some short fibers. Figures 3.30 and 3.31 show corrosion products consisting of generally smooth, amorphous structures with angular crystal-like elements. Figure 3.32 shows a structure similar to that shown in Figs. 3.30 and 3.31, but with fewer crystal-like elements. Images in Fig. 3.33, taken at 85X, show the interfaces of corrosion products and steels.

Figures 3.34-3.37 show corrosion products on anodes from mortar-wrapped macrocell tests. Figure 3.34 shows nodular structures similar but smaller to those seen in Fig. 3.29. However, the corrosion product from conventional steel shown in Fig 3.34 (b) is not covered with fibers as that shown in Fig. 3.29 (b). The corrosion products shown in Fig. 3.35 are dissimilar, with the conventional steel (Fig. 3.35b) showing obviously crystal-like particles. Figure 3.36 shows an amorphous structure that is very similar for both materials. Finally, Fig. 3.37 shows corrosion products with a rather fine structure.

The images shown here only cover the structures of a part of the corrosion products. However, two conclusions can be made: (1) The structure of the corrosion products can vary widely. (2) Products with similar morphology are observed on both metals, indicating the formation of similar corrosion products.

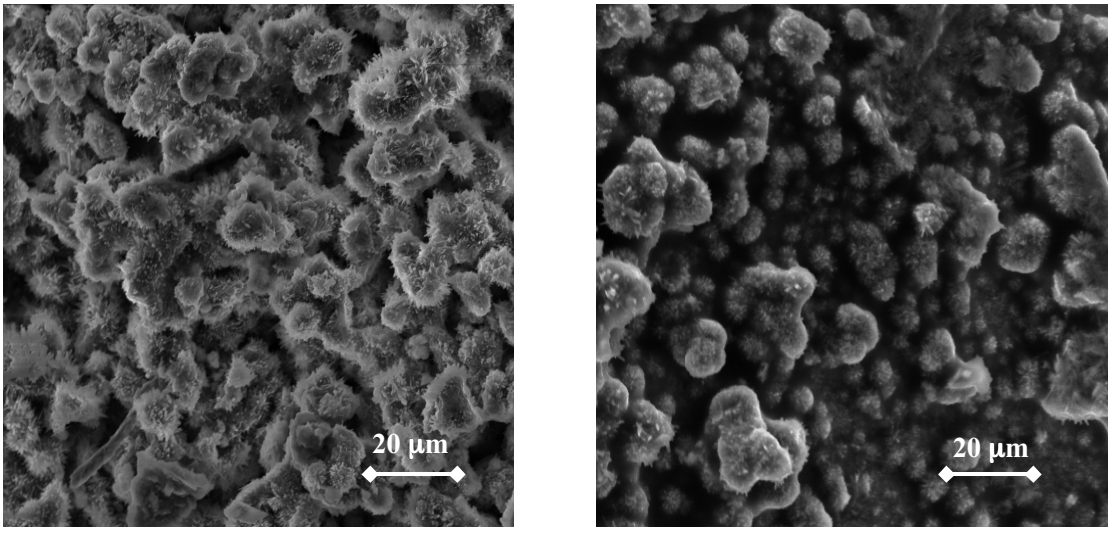

(a) (b)

Figure 3.29 - Nodular corrosion products with fibers on bare bar anodes for (a) MMFX and (b) conventional steel. 680X

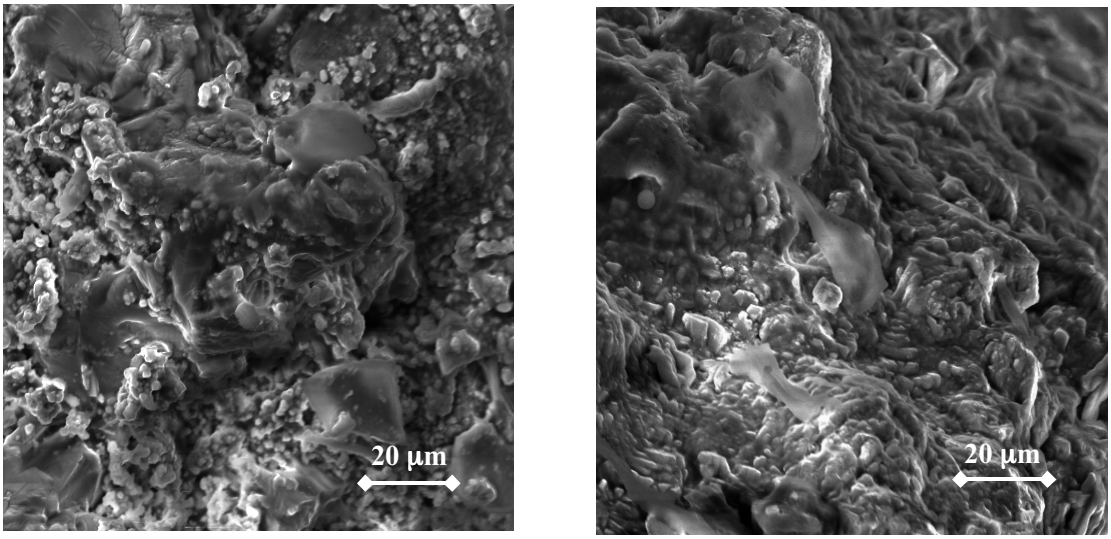

(a) (b)

Figure 3.30 - Amorphous corrosion products with small crystal-like elements on bare bar anodes for (a) MMFX and (b) conventional steel**.** 680X

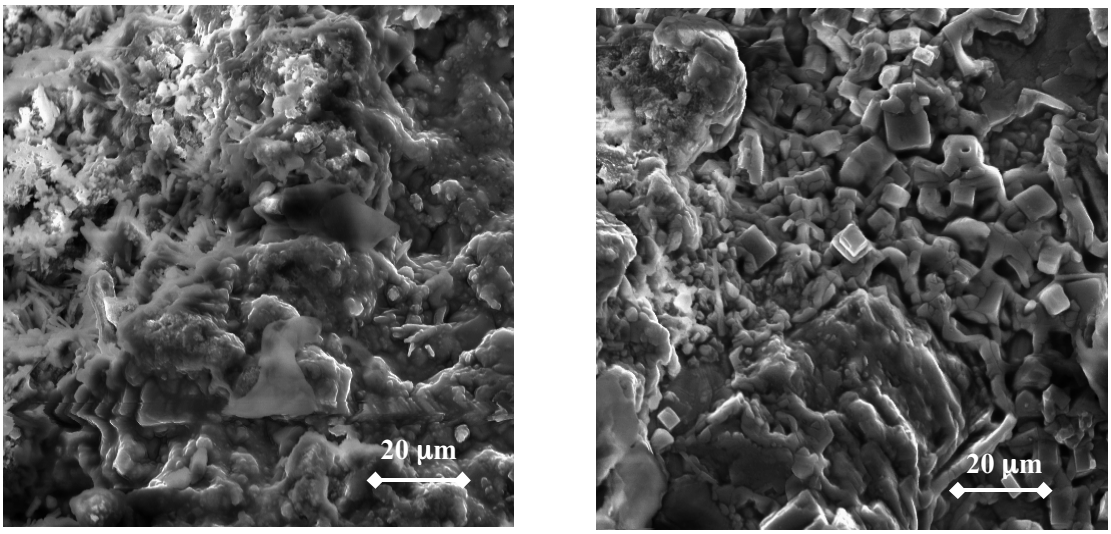

(a) (b)

Figure 3.31 - Amorphous corrosion products with small crystal-like elements on bare bar anodes for (a) MMFX and (b) conventional steel**.** 680X

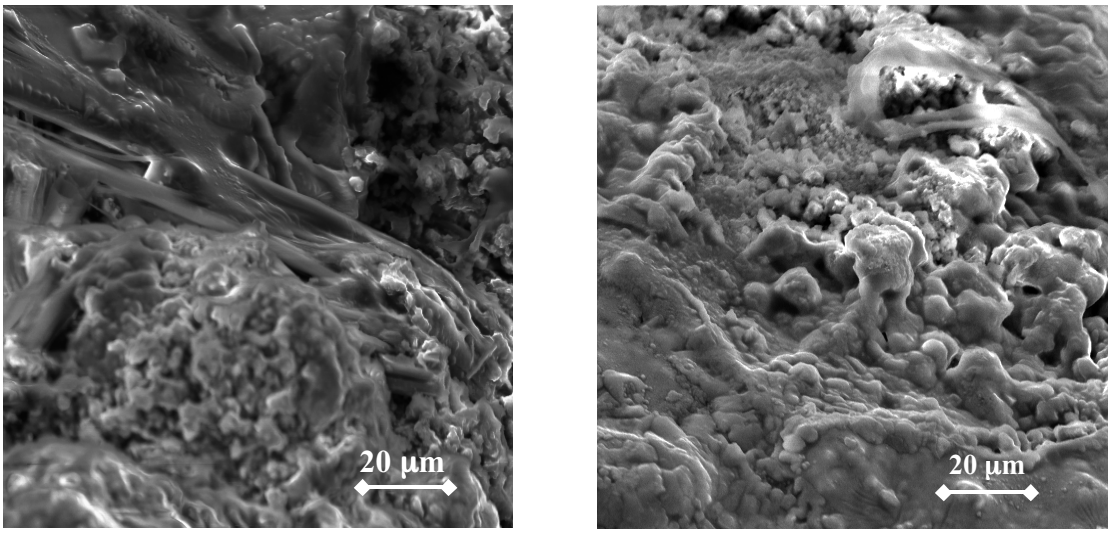

(a) (b)

Figure 3.32- Amorphous corrosion products on bare bar anodes for (a) MMFX and (b) conventional steel**.** 680X

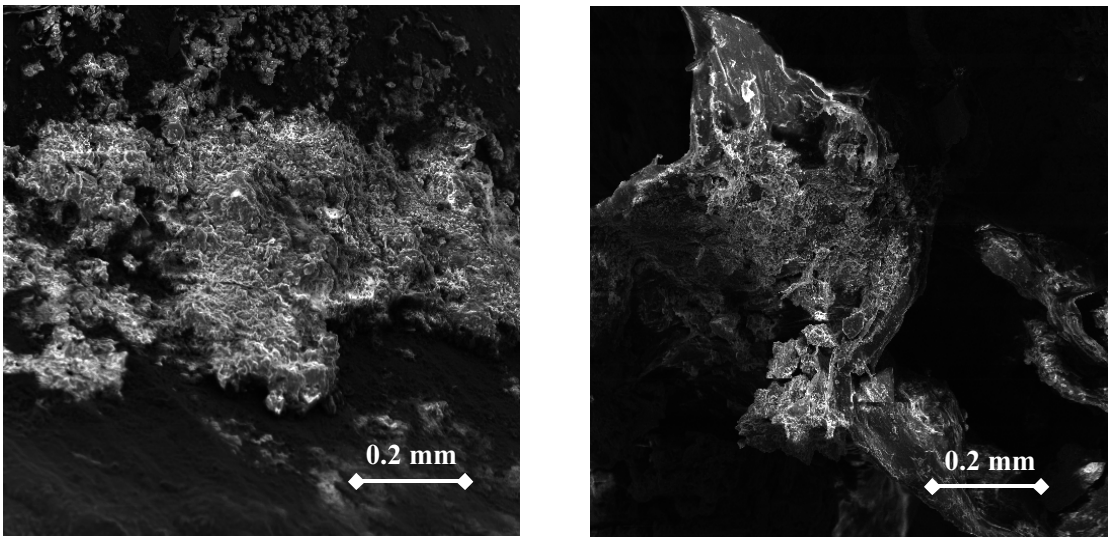

Figure 3.33 - Corrosion products on bare bar anodes for (a) MMFX and (b) conventional steel. 85X

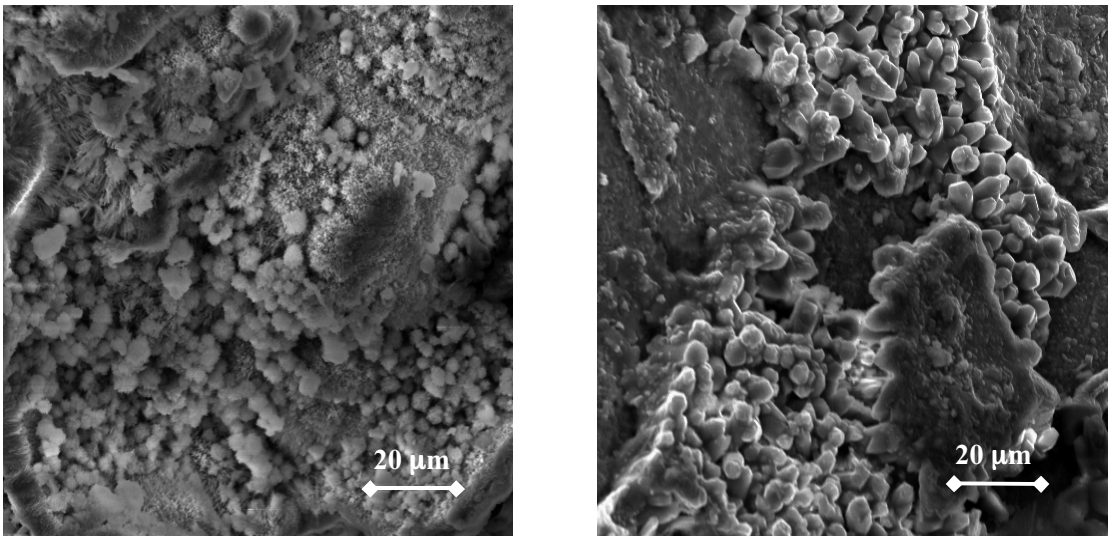

Figure 3.34 - Nodular corrosion products on anode bars in mortar-wrapped specimens for (a) MMFX and (b) conventional steel. 680X

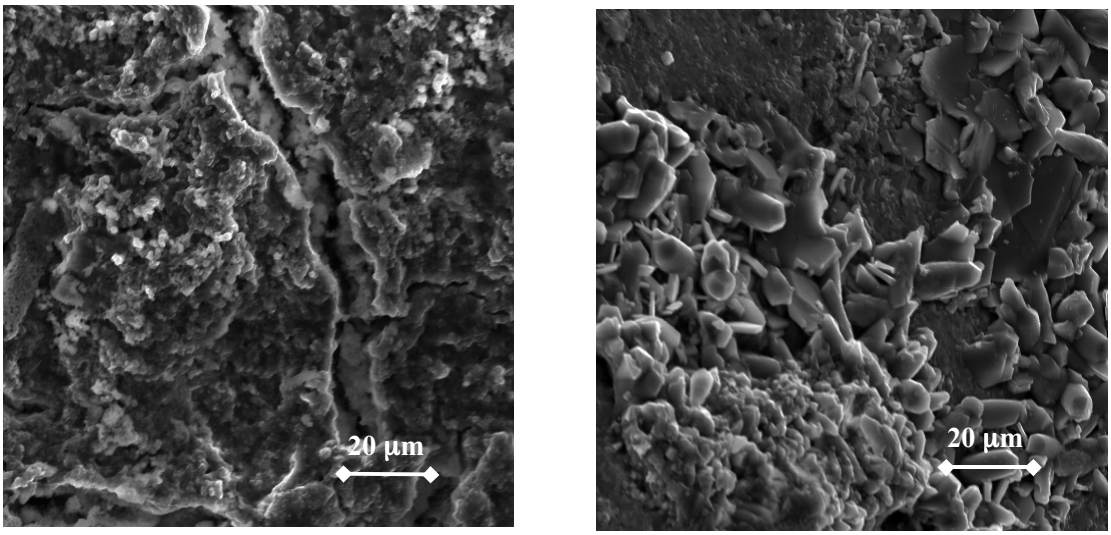

(a) (b)

Figure 3.35 - Corrosion products on anode bars in mortar-wrapped specimens showing differing structure for (a) MMFX and (b) conventional steel. 680X

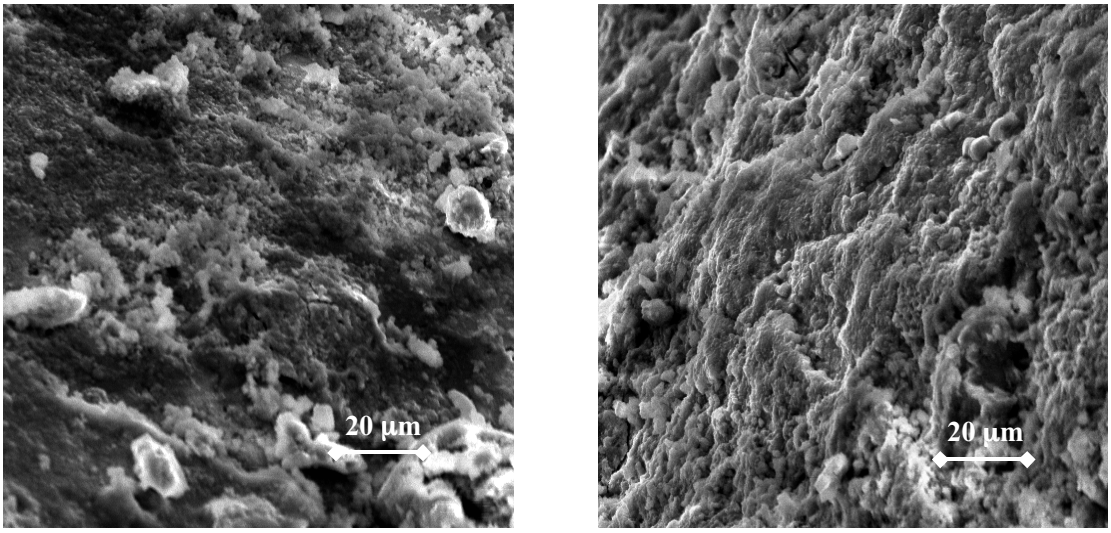

(a) (b)

Figure 3.36 - Amorphous corrosion products for anode bars in mortar-wrapped specimens for (a) MMFX and (b) conventional steel. 680X

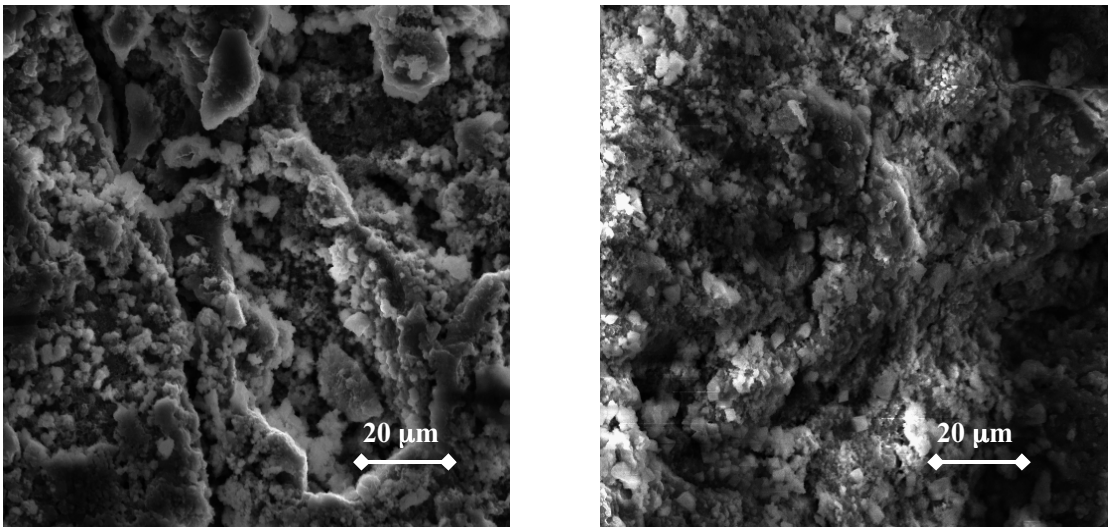

Figure 3.37 - Corrosion products with fine structure for anode bars in mortar-wrapped specimens for (a) MMFX and (b) conventional steel. 680X

3.6 COST EFFECTIVENESS

A 75-year economic life is used to compare the costs for 8.5-in. bridge decks containing conventional, epoxy-coated, or MMFX reinforcement. The total costs include the costs of a new bridge deck and repair costs over the 75-year life of the bridge. Initial construction and repair costs were obtained from SDDOT (Gilsrud 2002). The cost of MMFX steel was obtained from the MMFX Steel Corporation of America (Cano 2002). The following analysis of the steel is drawn from the work of Darwin et al. (2002).

All in-place costs considered in the analysis are listed in Table 3.5. The reinforcement costs were calculated based on an average amount of reinforcement of 210 lb/yd^3 (Gilsrud 2002).

Table 3.5 – Bridge deck construction costs in South Dakota (Gilsrud 2000)

Item	In-place Cost	Cost/m^2	Cost/yd^2	Total cost for bridge deck
Concrete	\$458/m^3 (\$350/yd^3)	\$98.9	\$82.6	
Conventional steel	\$1.30/kg (\$0.59/lb)	\$35.1	\$29.3	\$134.0/m^2 (\$111.9/yd^2)
Epoxy-coated steel	\$1.32/kg (\$0.60/lb)	\$35.6	\$29.8	\$134.5/m^2 (\$112.4/yd^2)
MMFX steel	\$1.85/kg (\$0.84/lb)	\$49.9	\$41.7	\$148.8/m^2 (\$124.3/yd^2)

* total cost for bridge deck = cost for concrete deck + cost for steel

The repair costs were calculated considering a typical bridge deck with a width of 36 ft and a total length of 150 ft (Gilsrud 2002). All repair costs considered in this analysis are shown in Table 3.6.

Table 3.6 - Repair costs for bridge decks in South Dakota (Gilsrud 2000)

Item	Unit	Cost	Cost/m^2	Cost/yd^2
Low Slump Dense Concrete Overlay	Per m^2 (Per yd^2)	\$96.00 (\$80.00)	\$96.00	\$80.00
Bridge Rail Modification	Per linear meter (Per linear ft)	148.45 (\$45.25)	\$27.00	\$23.00
Approach Guard Rail	Lump sum	\$16,000.00	\$32.00	\$27.00
Approach Pavement Work	Lump sum	\$16,500.00	\$33.00	\$28.00
Mobilization	Lump sum	\$18,600.00	\$37.00	\$31.00
Traffic Control and Misc.	Lump sum	\$9,000.00	\$18.00	\$15.00
Total Repair Costs			\$243.00	\$204.00

For bridge decks containing conventional steel, a 10-year initial life under harsh environmental conditions and a 25-year initial life under arid conditions are used to calculate the costs. For bridge decks containing epoxy-coated steel, costs are obtained using an initial life of 35 and 40 years. For bridge decks containing MMFX steel, the initial life is calculated using 27, 30, and 35 years. In all cases, additional repairs are based on 25-year cycles for the 75-year economic life used in this analysis.

The cost estimates for the different types of reinforcement are shown in Table 3.7. The lowest cost for all discount rates is the bridge deck with epoxy-coated reinforcement, with a 40-year initial life. The cost is \$261/yd^2 based on a 2% discount rate. The highest cost is the deck with conventional steel subjected to harsh exposure,

which is $444/yd^2 based on a 2% discount rate. The cost for MMFX steel ranges from $316/yd^2 using a 27-year initial life to $288/yd^2 using a 35-year initial life based on a 2% discount rate.

It is clear from this comparison that the bridge decks containing MMFX steel do not offer economic advantages when compared to decks containing epoxy-coated reinforcement.

Table 3.7 – Cost estimates for bridge decks containing conventional, epoxy-coated and MMFX steel (Darwin et al. 2002)

Reinforcement in deck	**New cost ($/m^2)**	**Repair 1 cost ($/m^2)**	**Time to repair 1 (years)**	**Repair 2 cost ($/m^2)**	**Time to repair 2 (years)**	**Repair 3 cost ($/m^2)**	**Time to repair 3 (years)**	**Present value of costs at 2% ($/m^2)**	**Present value of costs at 2% ($/m^2)**	**Present value of costs at 2% ($/m^2)**
South Dakota Decks										
Conventional- Harsh exposure	$134	$244	10	$244	35	$244	60	$530	$384	$309
Conventional - Arid exposure	$134	$244	25	$244	50			$373	$260	$204
Epoxy-coated	$134	$244	35	$244	60			$330	$219	$173
	$134	$244	40	$244	65			$312	$204	$163
MMFX	$148	$244	27	$244	52			$378	$265	$211
	$148	$244	30	$244	55			$365	$252	$201
	$148	$244	35	$244	60			$345	$233	$187

Reinforcement in deck	**New cost ($/yd^2)**	**Repair 1 cost ($/yd^2)**	**Time to repair 1 (years)**	**Repair 2 cost ($/yd^2)**	**Time to repair 2 (years)**	**Repair 3 cost ($/yd^2)**	**Time to repair 3 (years)**	**Present value of costs at 2% ($/yd^2)**	**Present value of costs at 4% ($/yd^2)**	**Present value of costs at 6% ($/yd^2)**
South Dakota Decks										
Conventional- Harsh exposure	$112	$204	10	$204	35	$204	60	$444	$321	$259
Conventional - Arid exposure	$112	$204	25	$204	50			$312	$217	$171
Epoxy-coated	$112	$204	35	$204	60			$276	$183	$145
	$112	$204	40	$204	65			$261	$170	$136
MMFX	$124	$204	27	$204	52			$316	$221	$176
	$124	$204	30	$204	55			$305	$210	$168
	$124	$204	35	$204	60			$288	$195	$157

CHAPTER 4
CONCLUSIONS AND RECOMMENDATIONS

4.1 SUMMARY

The corrosion performance of a new reinforcing steel (MMFX) is compared with that of epoxy-coated and uncoated conventional steel. The steels are evaluated using rapid macrocell tests developed at the University of Kansas, plus two bench-scale techniques, the Southern Exposure (SE) and cracked beam (CB) tests. Macrocell corrosion rate and corrosion potential are measured for both rapid and bench-scale tests. Macrocell mat-to-mat resistance is measured only for bench-scale tests. The test specimens of corrosion tests consisted of bare bars and bars cast in mortar for the rapid tests, and bars cast in concrete for the SE and CB tests. A water-cement ratio of 0.5 was used for rapid tests and 0.45 for SE and CB tests. Combinations of conventional steel and MMFX steel were tested in both rapid and bench-scale tests.

Mechanical properties are compared with the requirements of ASTM A 615 and ASTM A 722. Composition is analyzed for each steel to evaluate the uniformity of bars within the same heat, as well as between bars from different heats. The microstructure of corrosion products are observed and compared for both steels. Also, the cost effectiveness of MMFX steel in concrete bridge decks is evaluated and compared with that of epoxy-coated and uncoated conventional steel.

4.2 CONCLUSIONS

The following conclusions are based on the test results and analyses presented in this report:

1. The MMFX steel exhibits a macrocell corrosion rate between one-third and two-thirds that of conventional reinforcing bars in the rapid and bench-scale

tests. However, epoxy-coated reinforcement with the coating penetrated, corrodes at a rate between 5% and 25% that of conventional steel and provides superior corrosion performance to MMFX reinforcing steel.

2. It is not recommended that MMFX steel be combined with conventional steel in reinforced concrete structures. Although the corrosion rates were lower than conventional steel when MMFX was placed at either the anode or the cathode in rapid and SE tests, they were higher than that exhibited by MMFX steel alone.
3. The MMFX steel is a high-strength material with properties similar to those specified under ASTM A 722.
4. The chemistry of MMFX steel is consistent for bars within the same heat and very close for the two heats analyzed.
5. Corrosion products with similar morphology are observed on both conventional and MMFX steel, suggesting that products have similar composition.

4.3 RECOMMEDATIONS

1. MMFX reinforcing steel should not be used to replace epoxy-coated reinforcement unless it is used with a supplementary corrosion protection system.
2. MMFX reinforcing steel meets or comes close to meeting the requirements for high-strength steel bars for prestressing concrete as specified in ASTM A 722. To fully meet the requirements of ASTM A722, the bars must be cold-stressed to at least 80% of the minimum tensile strength, as required by the standard.

REFERENCES

ASTM A 615/A 615M-00 (2001). "Standard Specification for Deformed and Plain Billet-steel Bars for Concrete Reinforcement," *Annual Book of ASTM Standards, 2001*, American Society for Testing and Materials, West Conshohocken, PA, Vol. 01.04, pp. 296-300.

ASTM A 722/A 722M-98 (2001). "Standard Specification for Uncoated High-Strength Steel Bars for Prestressing Concrete," *Annual Book of ASTM Standards, 2001*, American Society for Testing and Materials, West Conshohocken, PA, Vol. 01.04, pp. 344-347.

ASTM C 305-99 (2001). "Standard Practice for Mechanical Mixing of Hydraulic Cement Pastes and Mortars of plastic Consistency," *Annual Book of ASTM Standards, 2001*, American Society for Testing and Materials, West Conshohocken, PA, Vol. 04.01, pp. 220-222.

ASTM C 778-00 (2001). "Standard Specification for Standard Sand," *Annual Book of ASTM Standards, 2001*, American Society for Testing and Materials, West Conshohocken, PA, Vol. 04.01, pp. 368-370.

ASTM E 8-00b (2001). "Standard Test Methods for Tension Testing of Metallic Materials", *Annual Book of ASTM Standards, 2001*, American Society for Testing and Materials, West Conshohocken, PA, Vol. 03.01, pp. 56-72.

Axelsson, H., Darwin, D., and Locke, C. E, Jr. (1999). "Influence of Adhesion at Steel/Mortar Interface on Corrosion Characteristics of Reinforcing Steel," *SL Report* 99-4, University of Kansas Center for Research, Lawrence, Kansas, 55 pp

Cano, O. (2002). MMFX Steel Corporation of America. Personal communication.

Darwin, D., Browning, J. P., Nguyen, T. V. Locke, C. E., (2002). " Mechanical and Corrosion Properties of a High-Strength, High Chromium Reinforcing Steel for Concrete," *SM Report* No. 66, University of Kansas Center for Research, Lawrence, KS, March, 169 pp.

Farzammehr, H. (1985). "Pore Solution Analysis of Sodium Chloride and Calcium Chloride Containing Cement Pastes," *Master of Science Thesis,* University of Oklahoma, Norman, OK, 101 pp.

Fliz, J., Akshey, S., Li, D., Kyo, Y., Sabol, S., Pickering, H., and Osseo-Asare, K. (1992). "Condition Evaluation of Concrete Bridges Relative to Reinforcement Corrosion – Volume 2 – Method for Measuring the Corrosion Rate of Steel in Concrete," Strategic Highway Research Program.

Gilsrud, T. (2002). South Dakota Department of Transportation. Personal communication.

Hausmann, D. A. (1967). "Steel Corrosion in Concrete - How Does it Occur?", Material Protection, Nov., pp.19-23

Martinez, S. L., Darwin, D., McCabe, S. L., and Locke, C. E. (1990). "Rapid Test for Corrosion Effects of Deicing Chemicals in Reinforced Concrete," *SL Report* 90-4, University of Kansas Center for Research, Lawrence, KS, Aug., 61 pp.

McDonald, D. B., Pfeifer, D. W., Krauss, P., and Sherman, M. R. (1994). "Test Methods for New Breeds of Reinforcing Bars," Corrosion and Corrosion Protection of Steel in Concrete, Vol. II, July, pp.1155-1171

MMFX Steel Corporation of America website - http://www.mmfxsteel.com/

Perenchio, William F. (1992). "Corrosion of Reinforcing Bars in Concrete," Annual Seminar, Master Builders Technology, Cleveland, OH, Dec.

Pfeifer, D. W., Landgren, R. J., and Zoob, A. (1987). "Protective Systems for New Prestressed and Substructure Concrete," *Report* No. FHWA/RD-86/193, Federal Highway Administration, McLean, VA, April, 133 pp.

Steinbach, O. F., and King, C. V. (1950). *Experiments in Physical Chemistry*, American Book Co., New York, 250 pp.

Ulig, H. H., and Revie, R. R. (1985). *Corrosion and Corrosion Control: An Introduction to Corrosion Science and Engineering*, John Wiley & Sons, New York, 441 pp.

APPENDIX A

CORRODION TEST RESULTS FOR INDIVIDUAL SPECIMENS

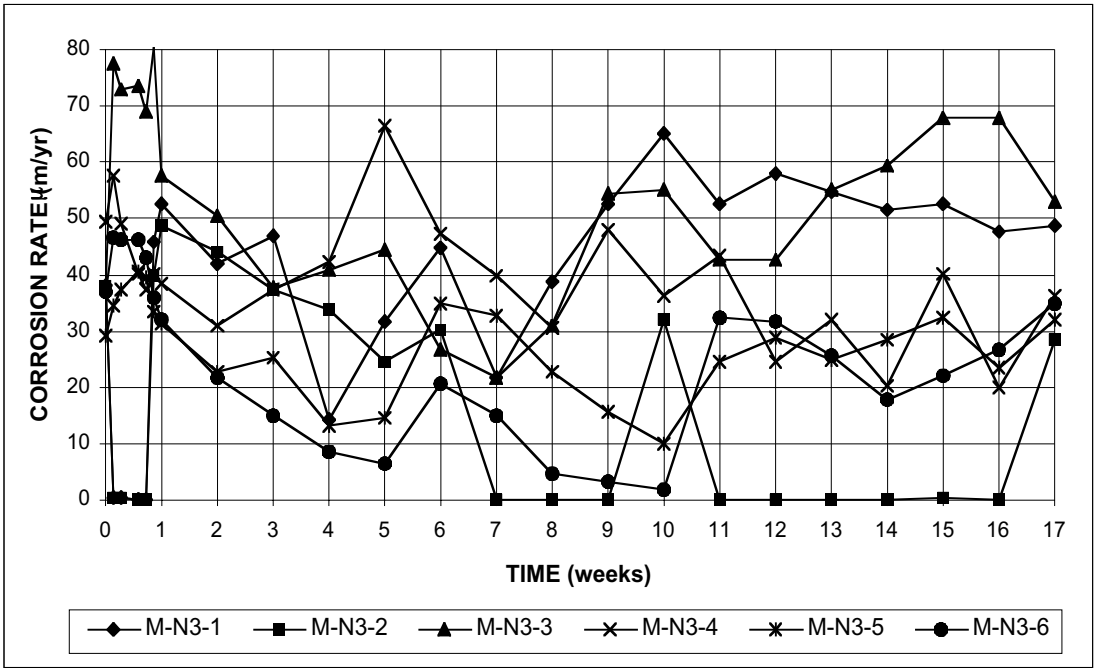

Figure A.1 - Macrocell Test. Corrosion rate. Bare conventional, normalized steel in 1.6 m ion NaCl and simulated concrete pore solution.

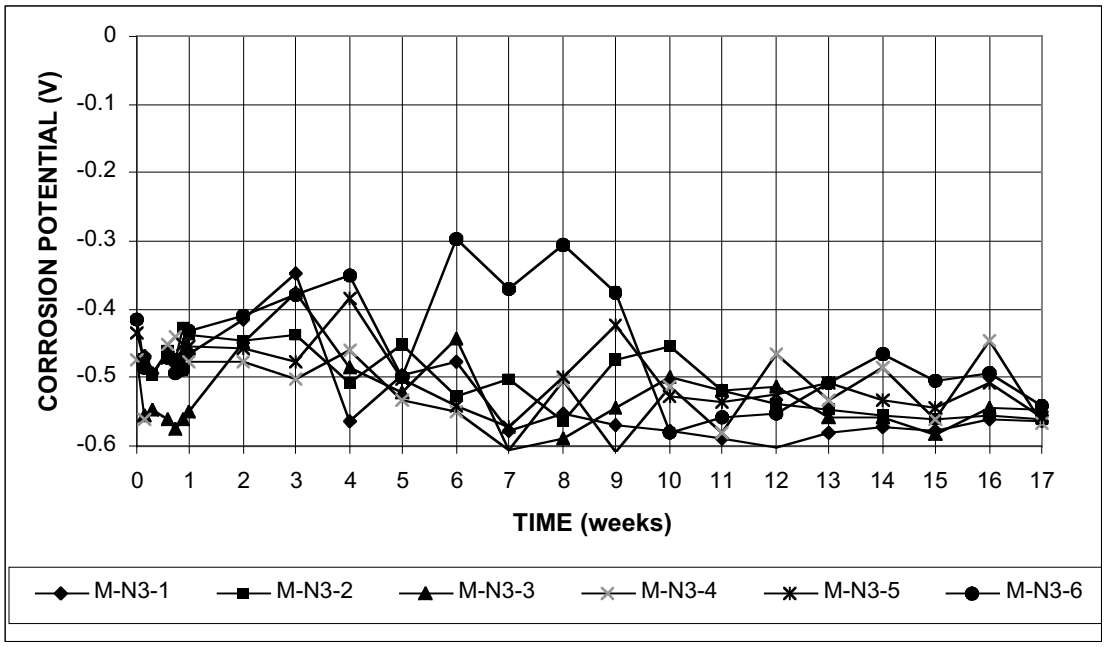

Figure A.2a - Macrocell Test. Corrosion potential vs. saturated calomel electrode, anode. Bare conventional, normalized steel in 1.6 m ion NaCl and simulated concrete pore solution.

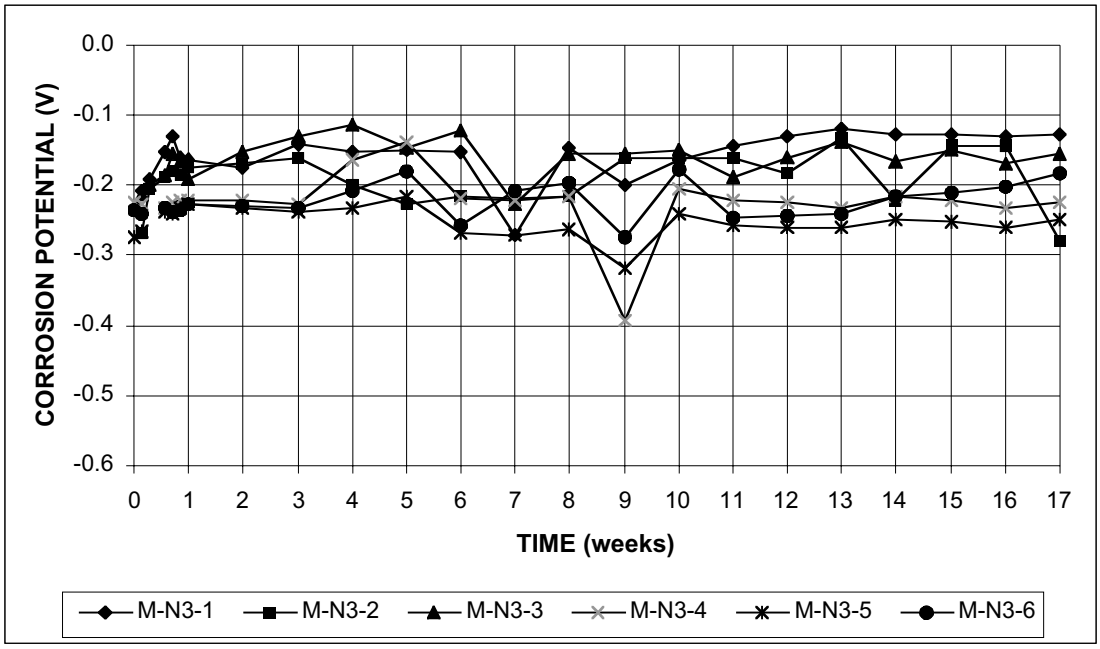

Figure A.2b - Macrocell Test. Corrosion potential vs. saturated calomel electrode, cathode. Bare conventional, normalized steel in 1.6 m ion NaCl and simulated concrete pore solution.

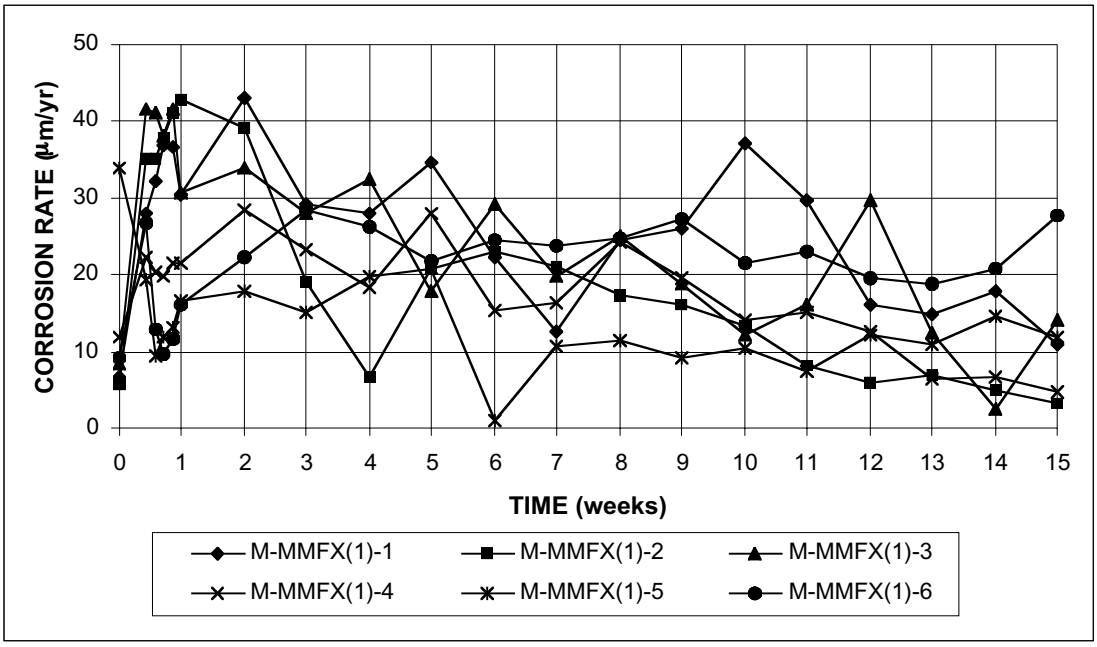

Figure A.3 - Macrocell Test. Corrosion rate. Bare MMFX steel in 1.6 m ion NaCl and simulated concrete pore solution.

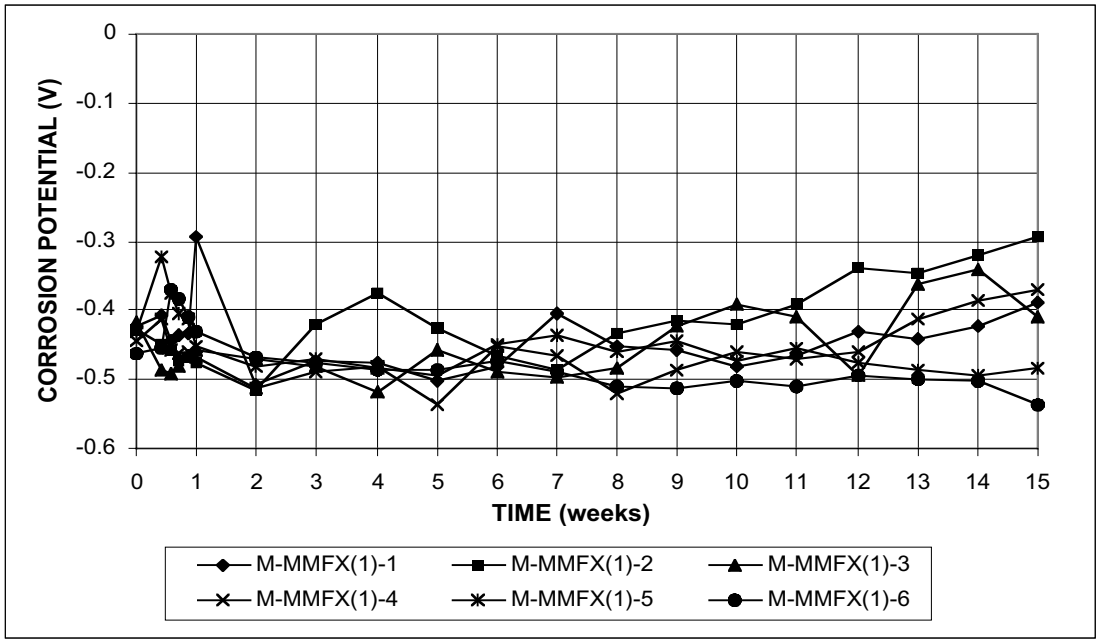

Figure A.4a - Macrocell Test. Corrosion potential vs. saturated calomel electrode, anode. Bare MMFX steel in 1.6 m ion NaCl and simulated concrete pore solution.

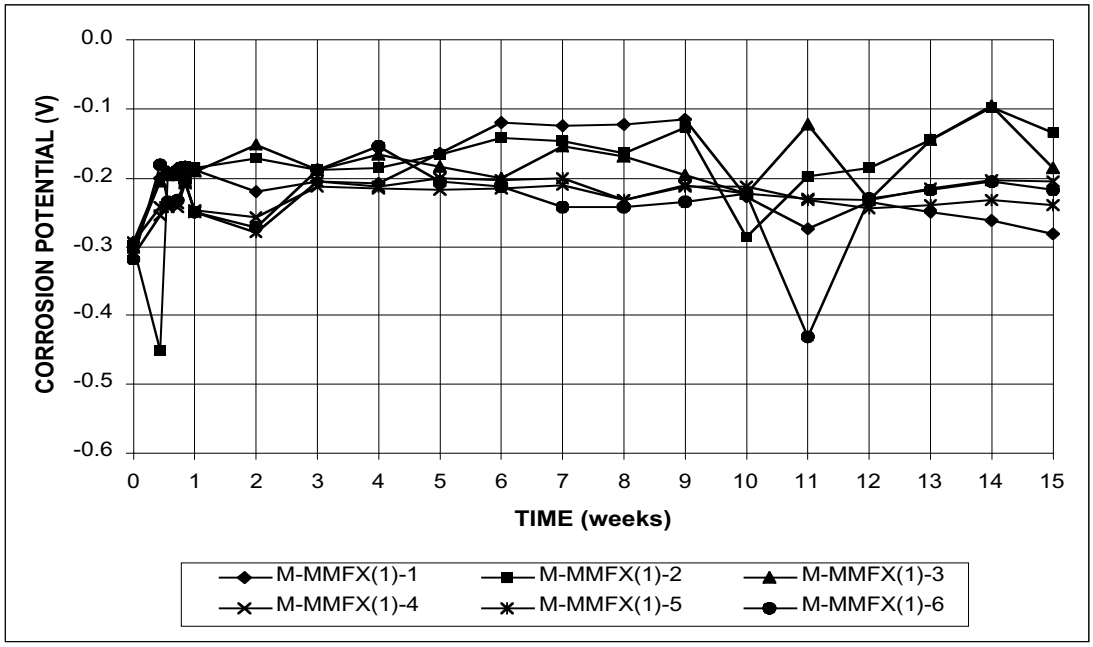

Figure A.4b - Macrocell Test. Corrosion potential vs. saturated calomel electrode, cathode. Bare MMFX steel in 1.6 m ion NaCl and simulated concrete pore solution.

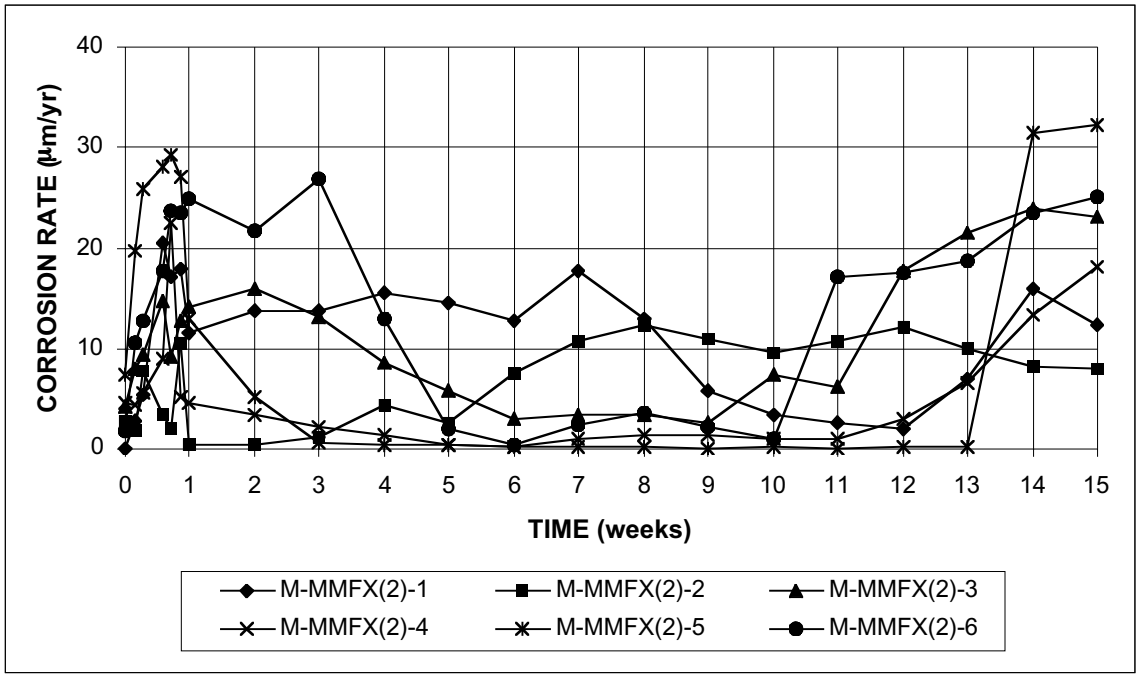

Figure A.5 - Macrocell Test. Corrosion rate. Bare MMFX steel in 1.6 m ion NaCl and simulated concrete pore solution.

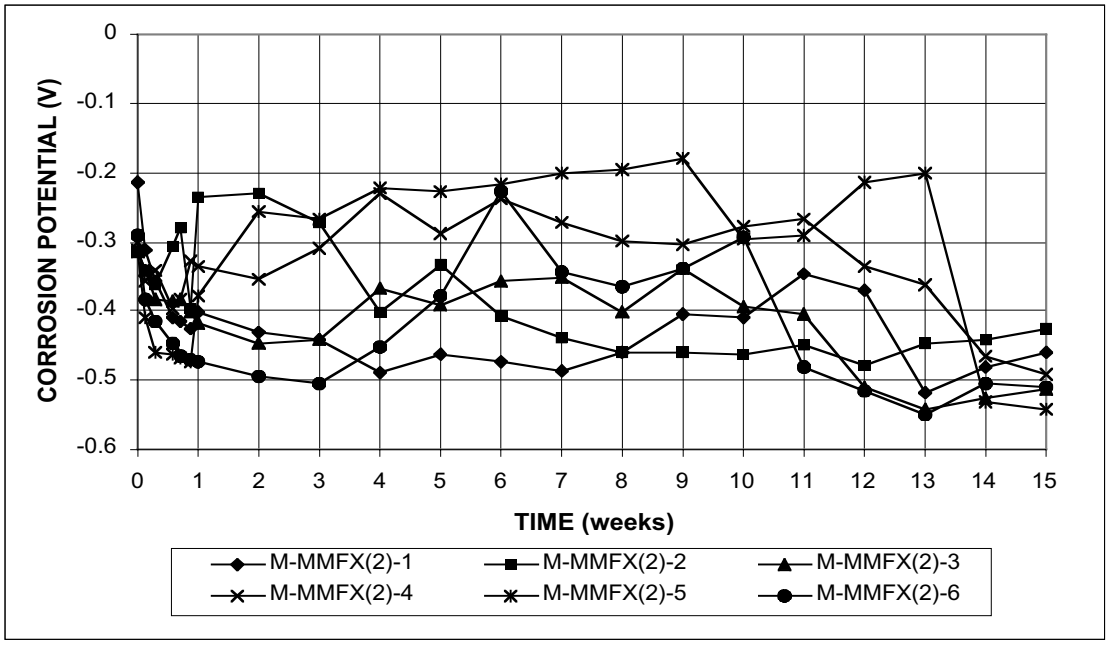

Figure A.6a - Macrocell Test. Corrosion potential vs. saturated calomel electrode, anode. Bare MMFX steel in 1.6 m ion NaCl and simulated concrete pore solution.

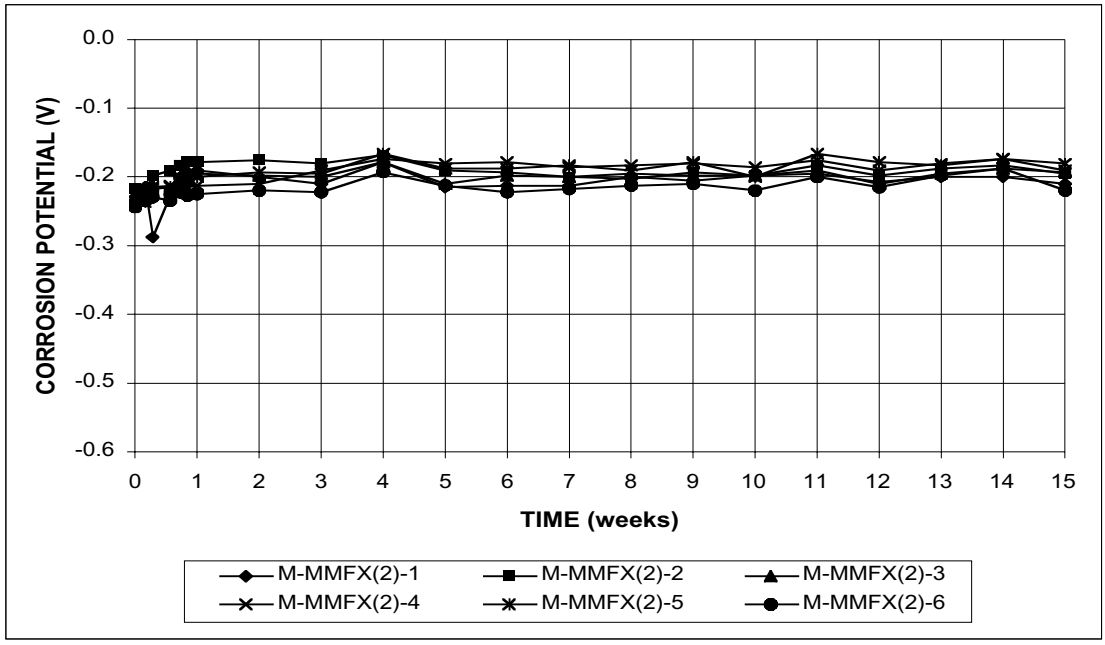

Figure A.6b - Macrocell Test. Corrosion potential vs. saturated calomel electrode, cathode. Bare MMFX steel in 1.6 m ion NaCl and simulated concrete pore solution.

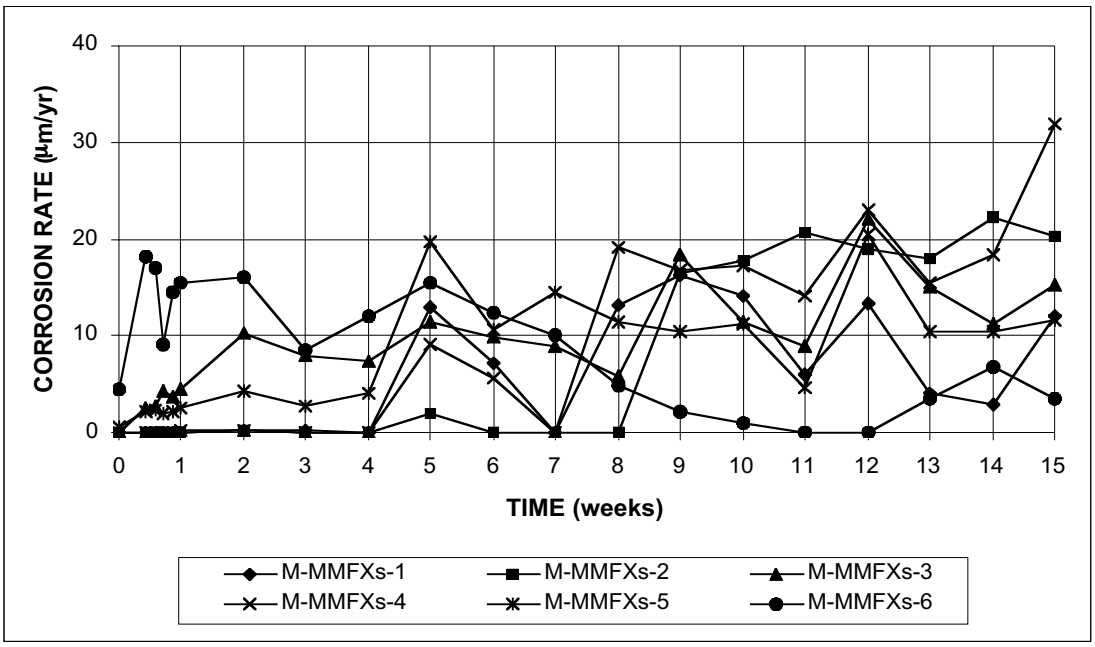

Figure A.7 - Macrocell Test. Corrosion rate. Bare, sandblasted MMFX steel in 1.6 m ion NaCl and simulated concrete pore solution.

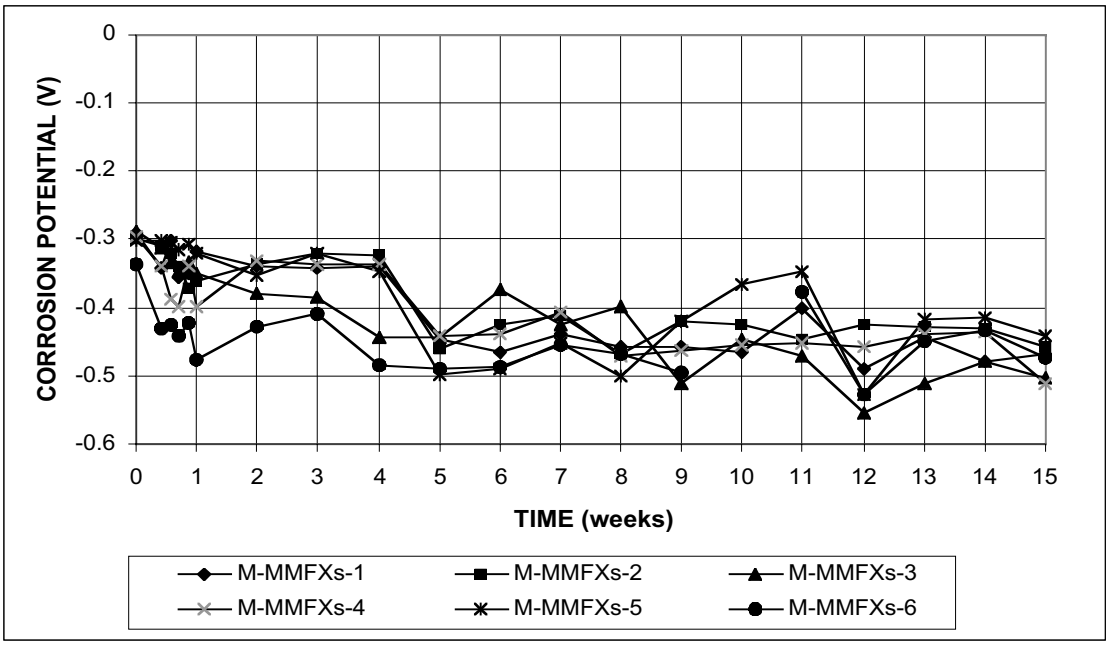

Figure A.8a - Macrocell Test. Corrosion potential vs. saturated calomel electrode, anode. Bare, sandblasted MMFX steel in 1.6 m ion NaCl and simulated concrete pore solution.

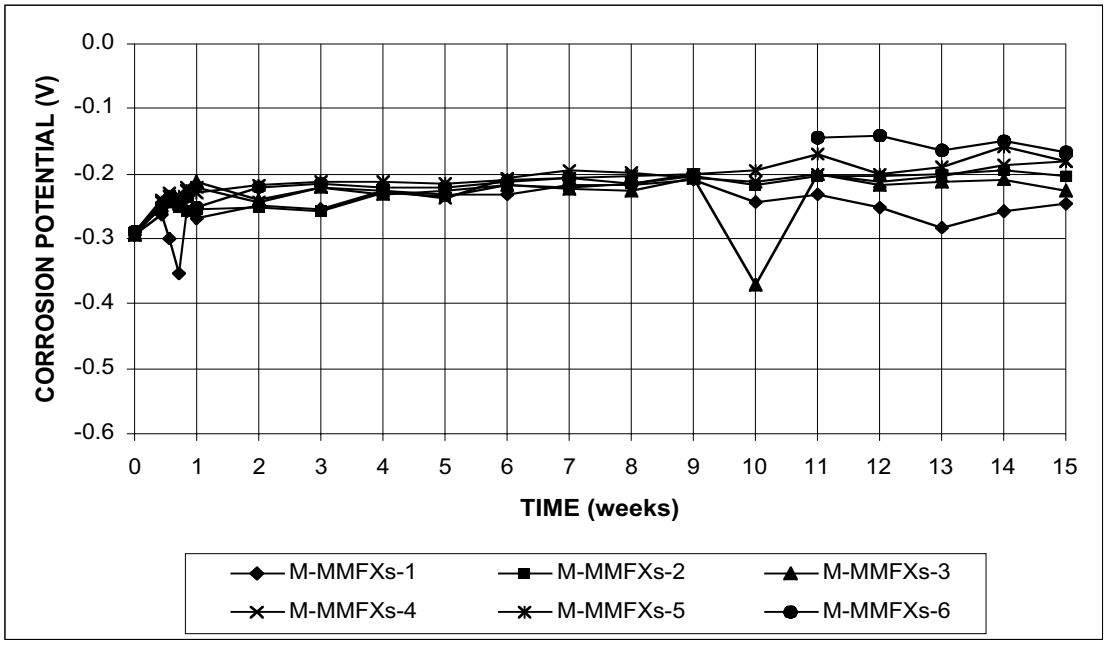

Figure A.8b - Macrocell Test. Corrosion potential vs. saturated calomel electrode, cathode. Bare, sandblasted MMFX steel in 1.6 m ion NaCl and simulated concrete pore solution.

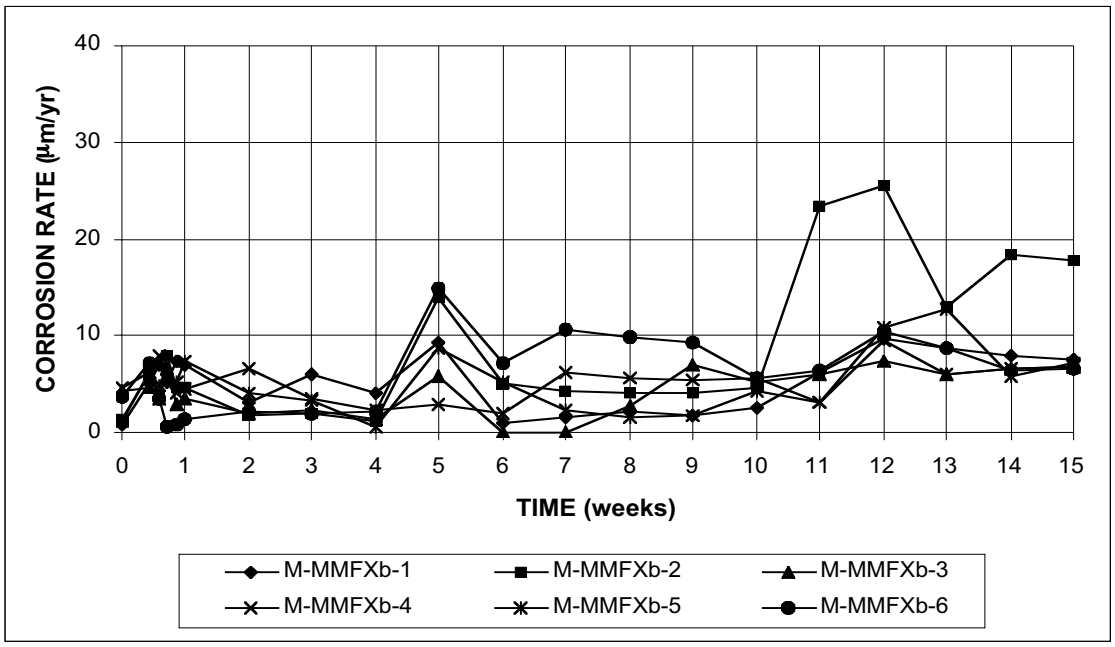

Figure A.9 - Macrocell Test. Corrosion rate. Bare MMFX steel, bent bar at the anode, in 1.6 m ion NaCl and simulated concrete pore solution.

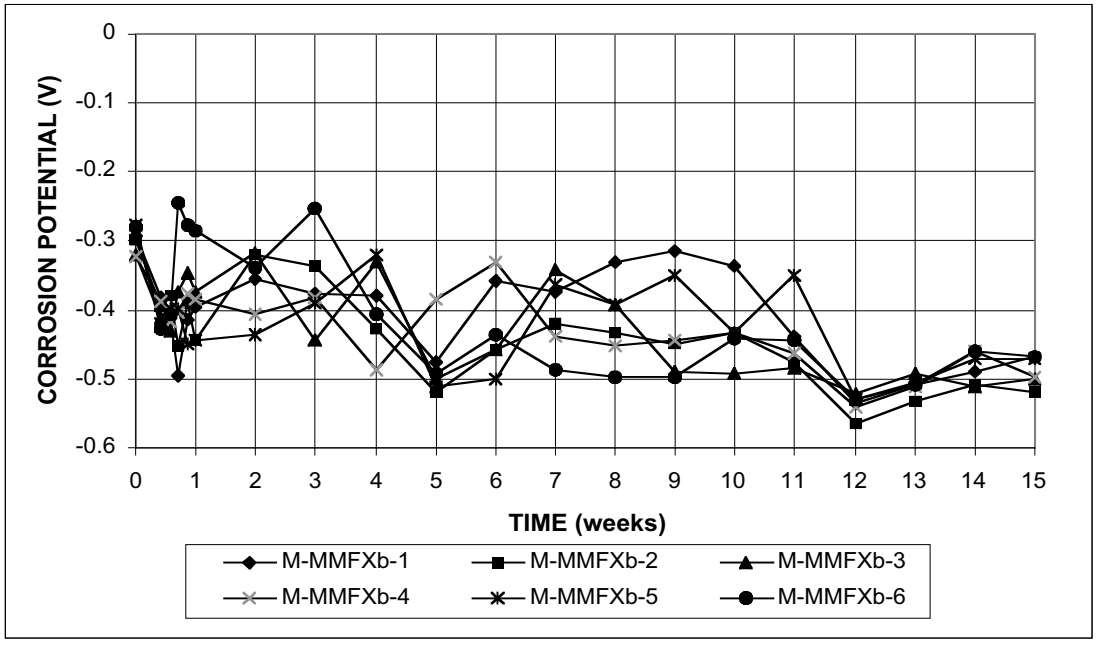

Figure A.10a - Macrocell Test. Corrosion potential vs. saturated calomel electrode, anode. Bare MMFX steel, bent bar at the anode, in 1.6 m ion NaCl and simulated concrete pore solution.

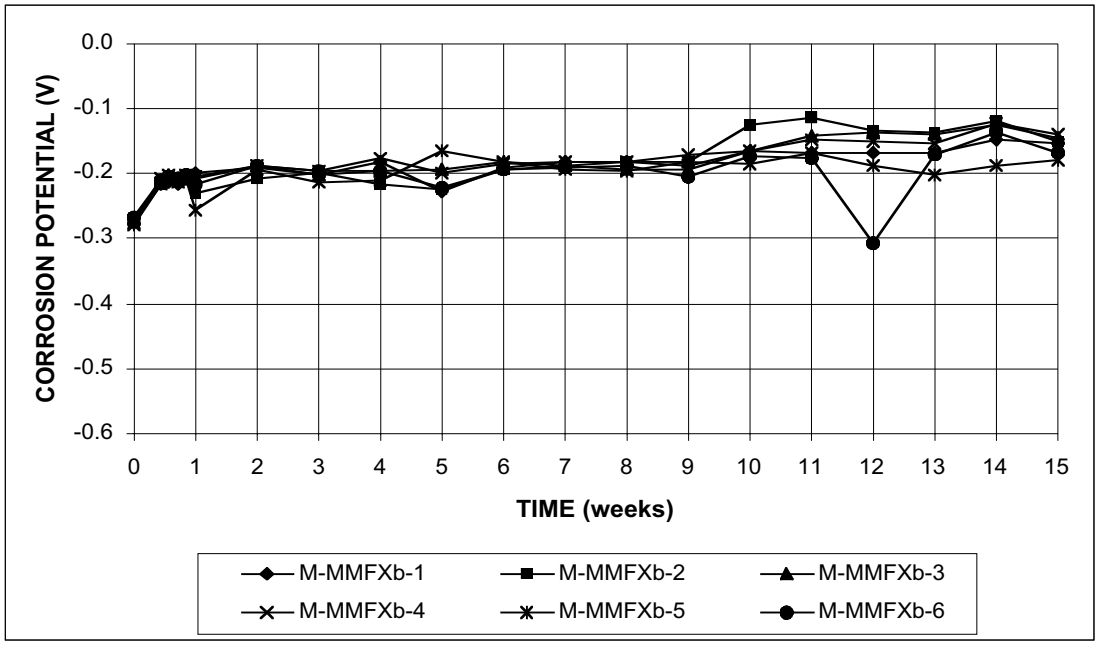

Figure A.10b - Macrocell Test. Corrosion potential vs. saturated calomel electrode, cathode. Bare MMFX steel, bent bar at the anode, in 1.6 m ion NaCl and simulated concrete pore solution.

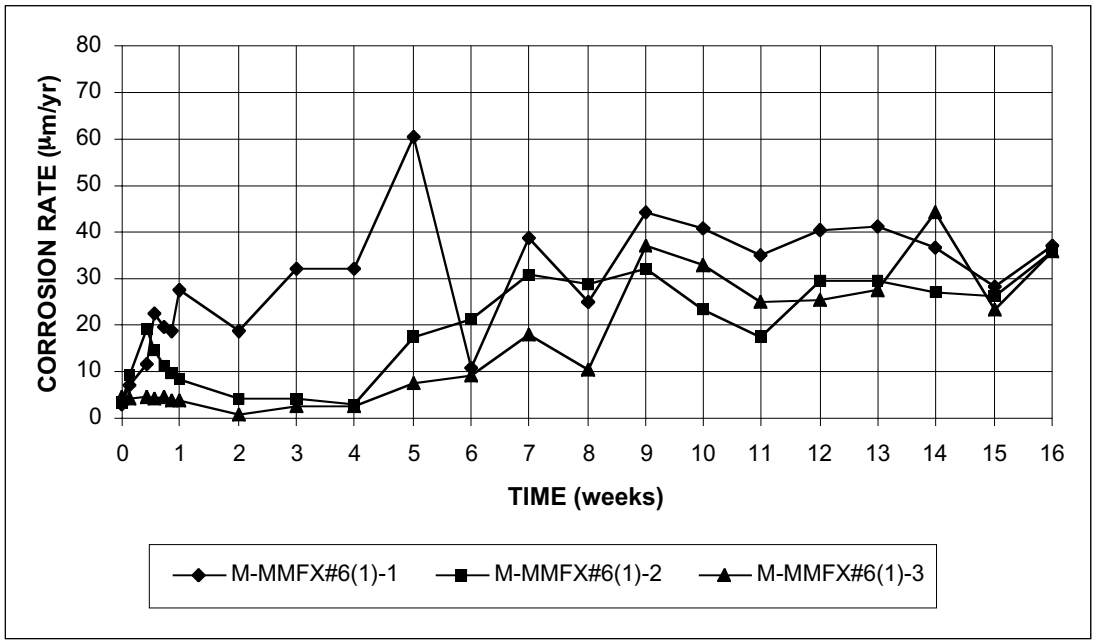

Figure A.11 - Macrocell Test. Corrosion rate. Bare #6 MMFX steel in 1.6 m ion and simulated concrete pore solution.

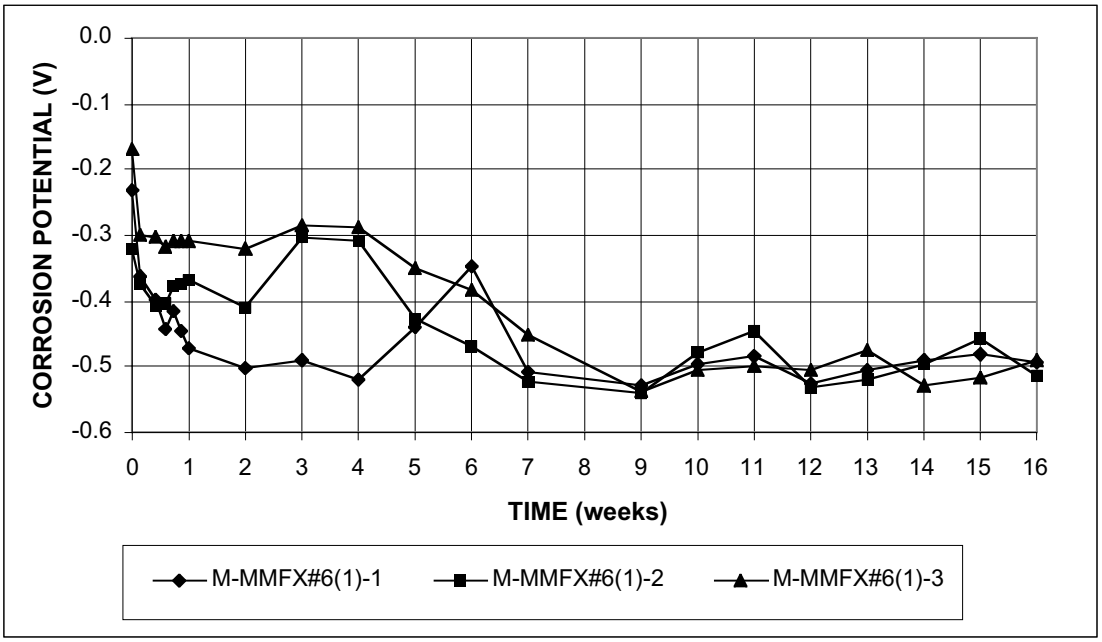

Figure A.12a - Macrocell Test. Corrosion potential vs. saturated calomel electrode, anode. Bare #6 MMFX steel in 1.6 m ion NaCl and simulated concrete pore solution.

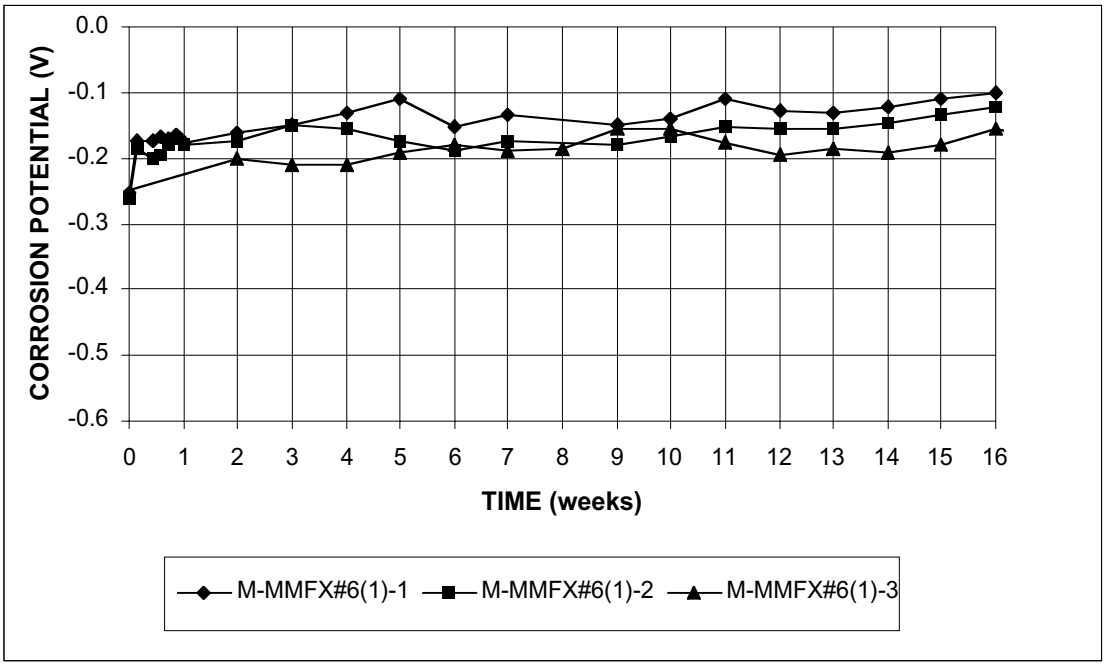

Figure A.12b - Macrocell Test. Corrosion potential vs. saturated calomel electrode, cathode. Bare #6 MMFX steel in 1.6 m ion NaCl and simulated concrete pore solution.

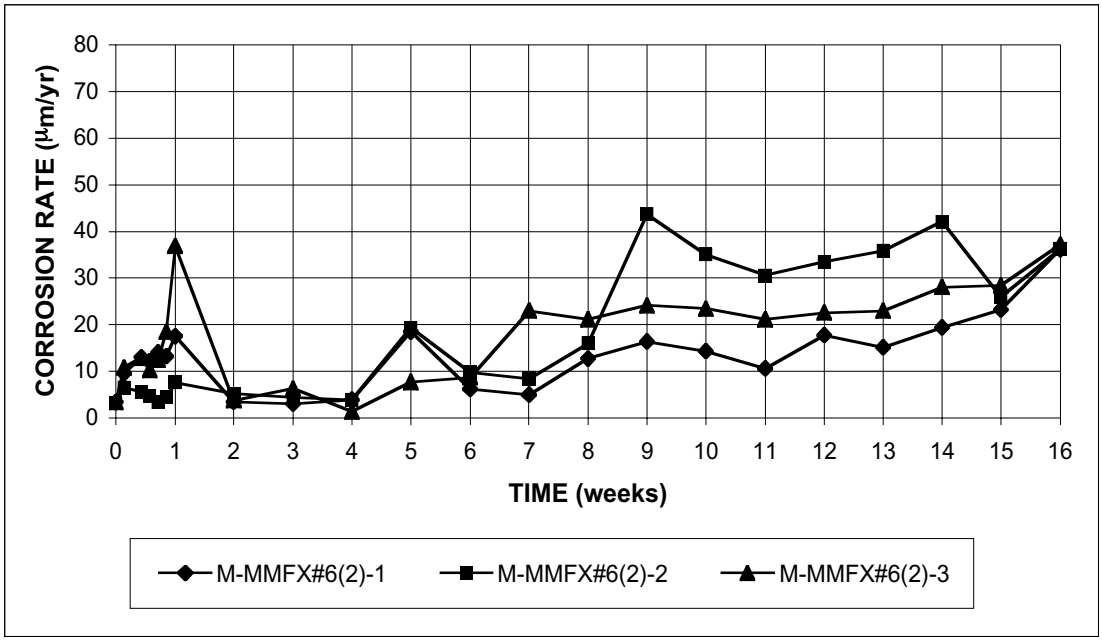

Figure A.13 - Macrocell Test. Corrosion rate. Bare #6 MMFX steel in 1.6 m ion NaCl and simulated concrete pore solution.

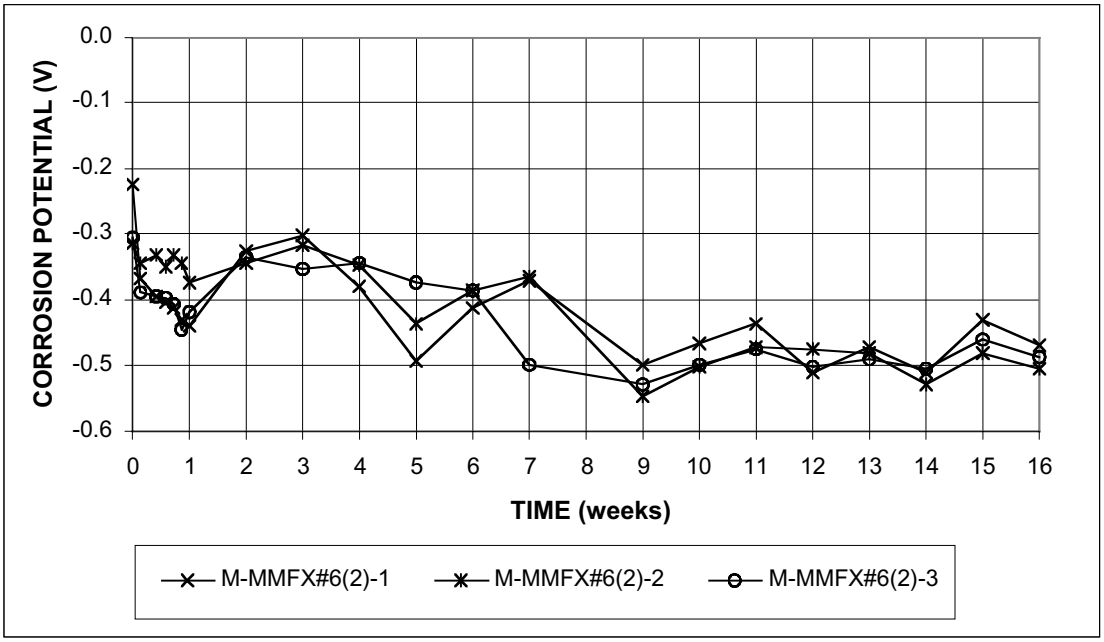

Figure A.14a - Macrocell Test. Corrosion potential vs. saturated calomel electrode, anode. Bare #6 MMFX steel in 1.6 m ion NaCl and simulated concrete pore solution.

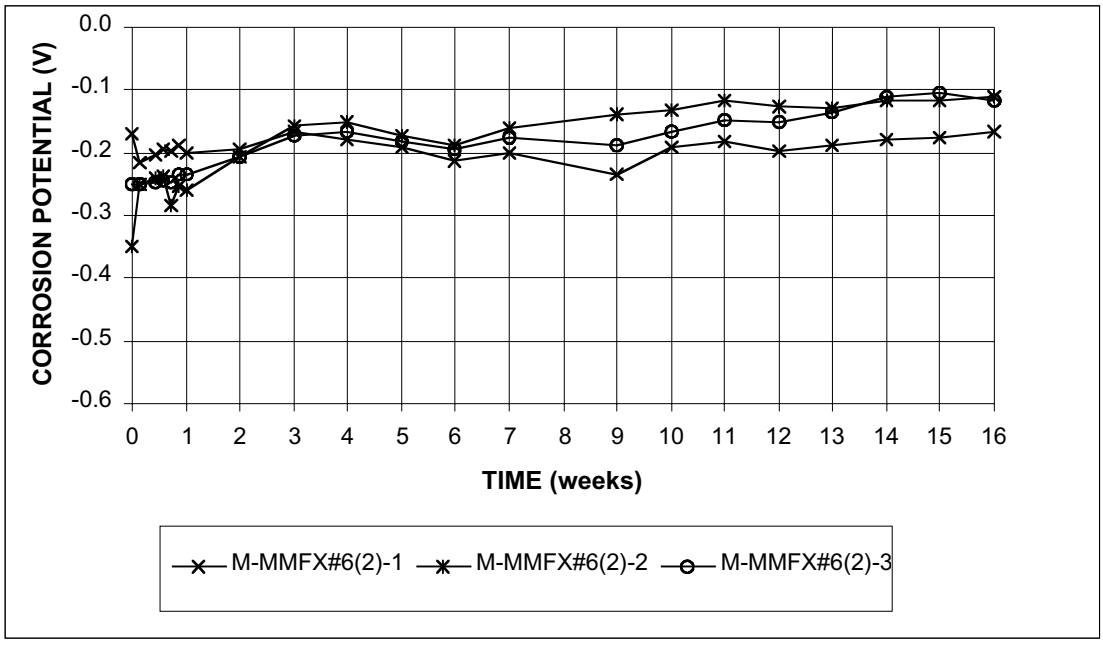

Figure A.14b - Macrocell Test. Corrosion potential vs. saturated calomel electrode, cathode. Bare #6 MMFX steel in 1.6 m ion NaCl and simulated concrete pore solution.

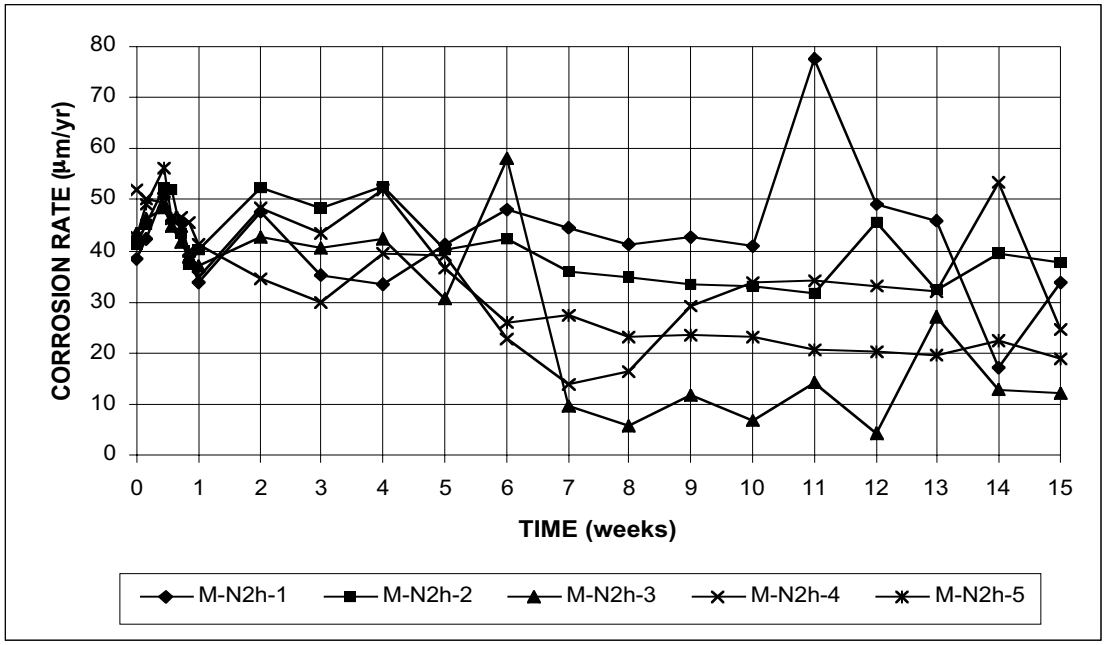

Figure A.15 - Macrocell Test. Corrosion rate. Bare conventional, normalized steel in 6.04 m ion (15%) NaCl and simulated concrete pore solution.

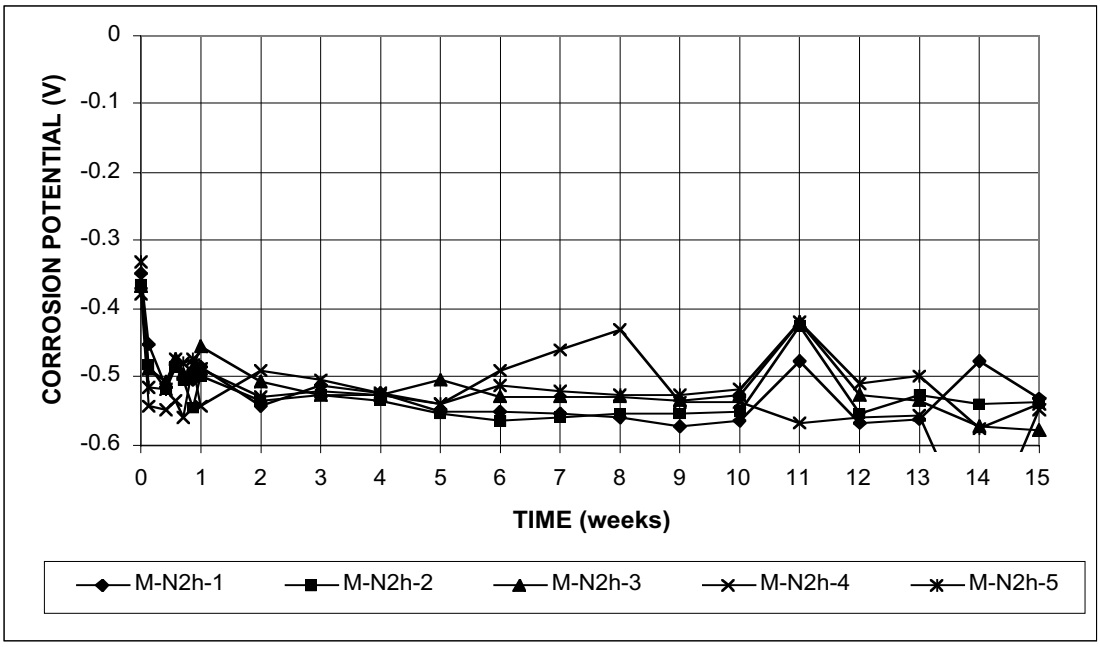

Figure A.16a - Macrocell Test. Corrosion potential vs. saturated calomel electrode, anode. Bare conventional, normalized steel in 6.04m ion (15%) NaCl and simulated concrete pore solution.

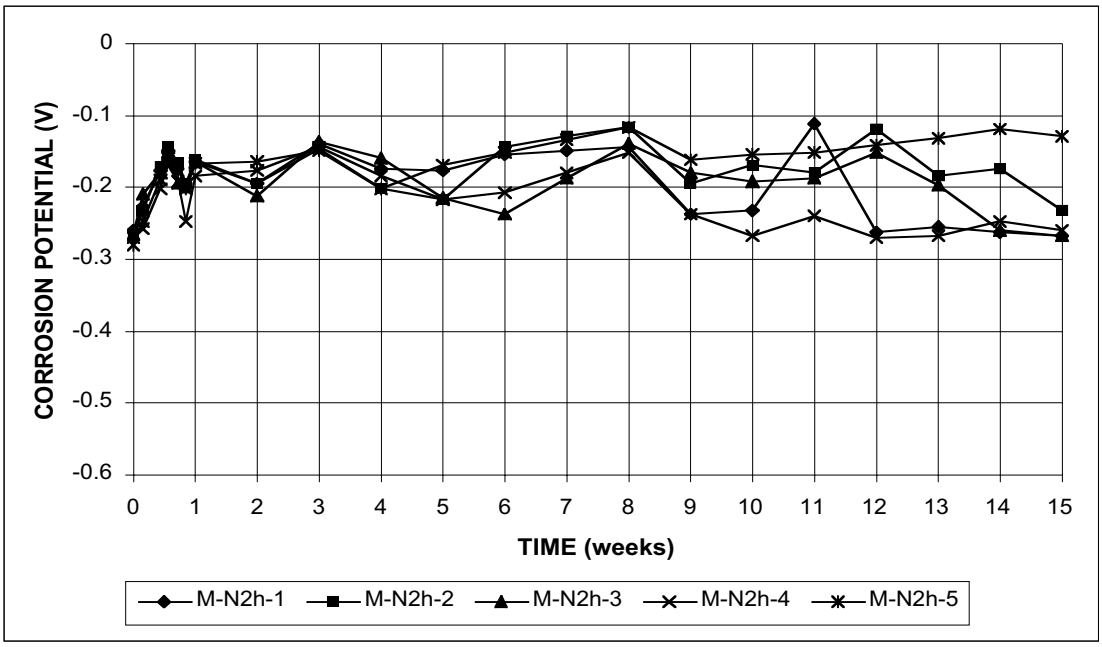

Figure A.16b - Macrocell Test. Corrosion potential vs. saturated calomel electrode, cathode. Bare conventional, normalized steel in 6.04 m ion (15%) NaCl and simulated concrete pore solution.

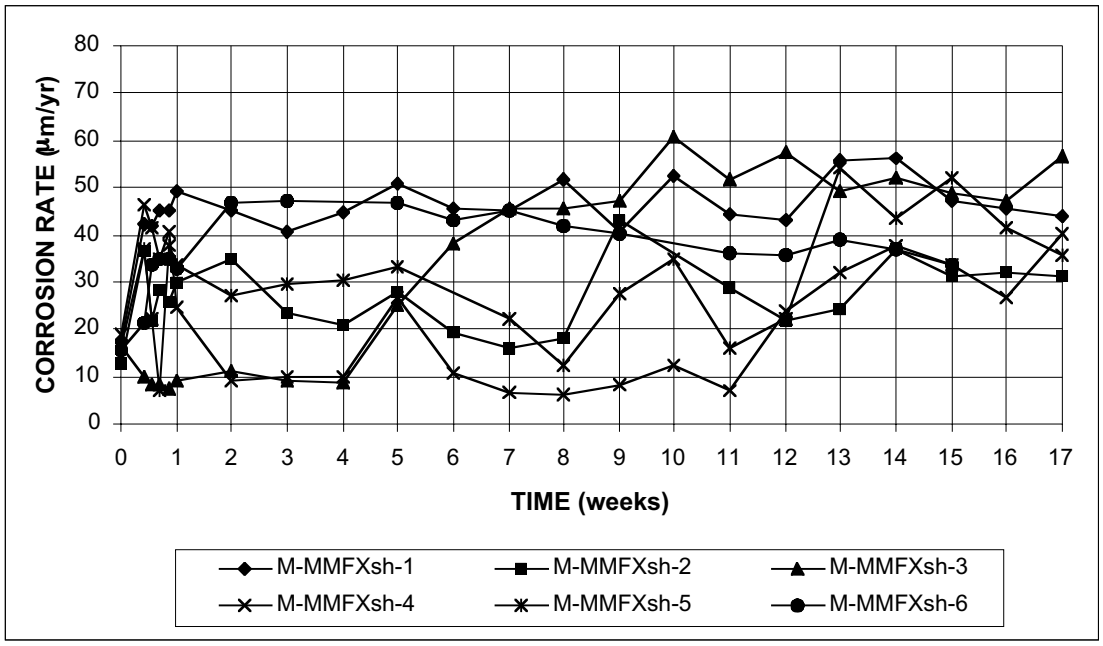

Figure A.17 - Macrocell Test. Corrosion rate. Bare sandblasted MMFX steel in 6.04 m ion (15%) NaCl and simulated concrete pore solution.

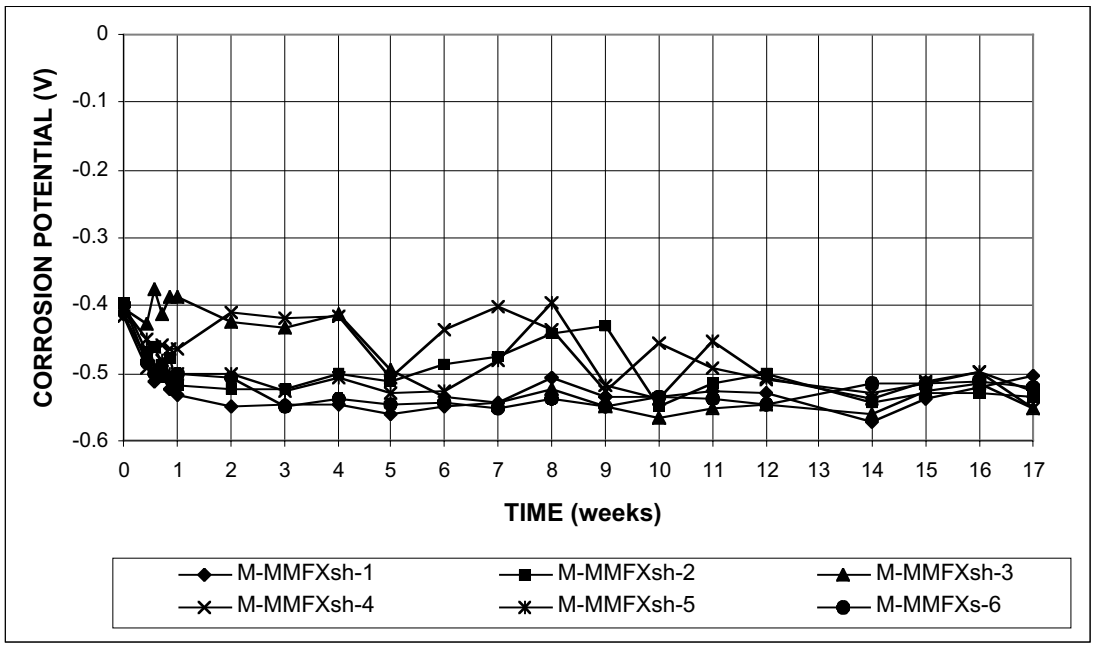

Figure A.18a - Macrocell Test. Corrosion potential vs. saturated calomel electrode, anode. Bare sandblasted MMFX steel in 6.04 m ion (15%) NaCl and simulated concrete pore solution.

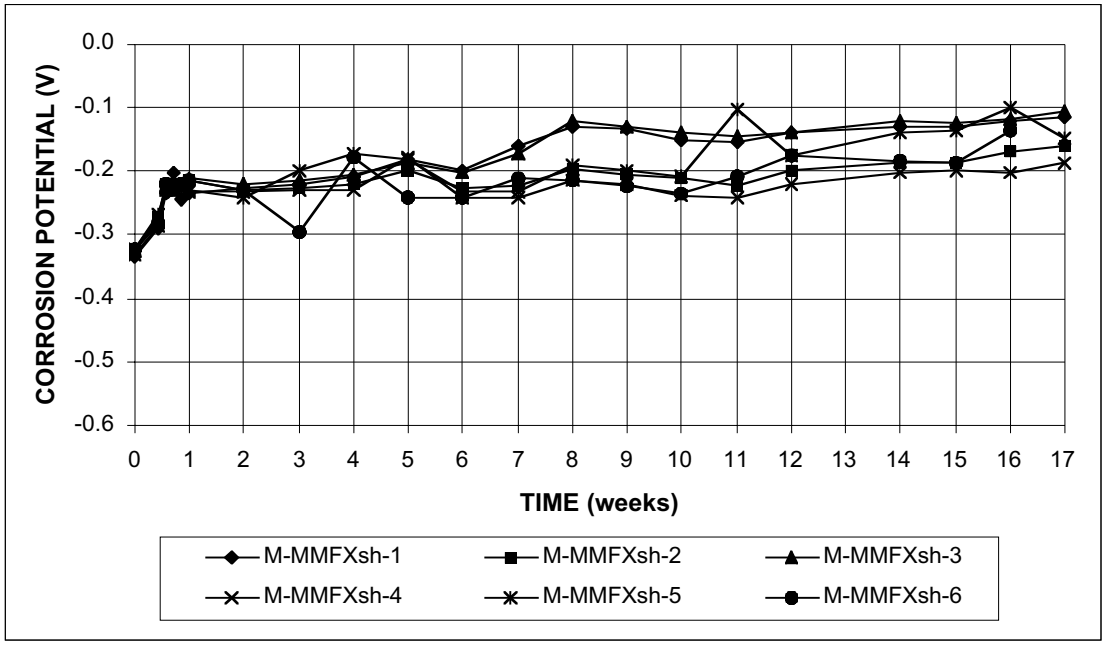

Figure A.18b - Macrocell Test. Corrosion potential vs. saturated calomel electrode, cathode. Bare sandblasted MMFX steel in 6.04 m ion (15%) NaCl and simulated concrete pore solution.

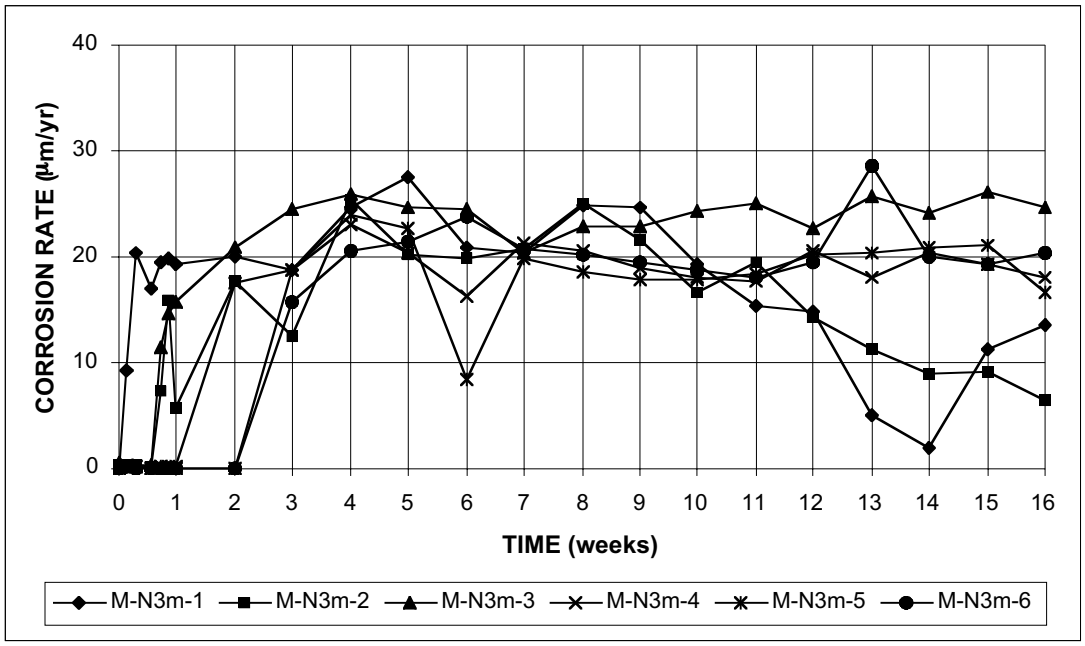

Figure A.19 - Macrocell Test. Corrosion rate. Mortar-wrapped conventional, normalized steel in 1.6 m ion NaCl and simulated concrete pore solution.

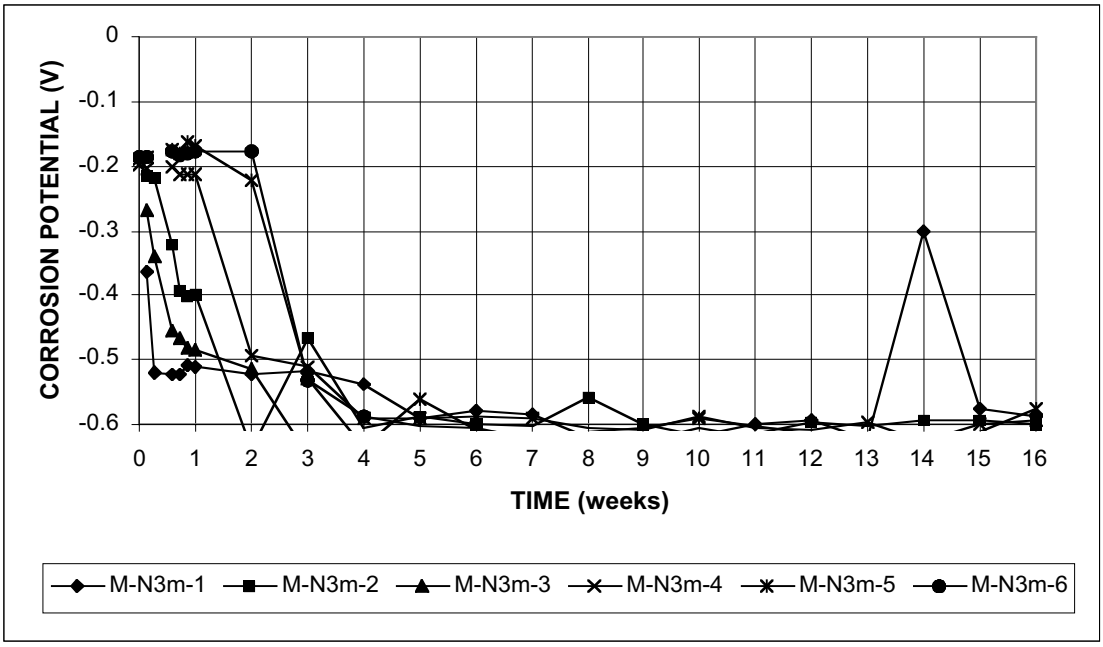

Figure A.20a - Macrocell Test. Corrosion potential vs. saturated calomel electrode, anode. Mortar-wrapped conventional, normalized steel in 1.6 m ion NaCl and simulated concrete pore solution.

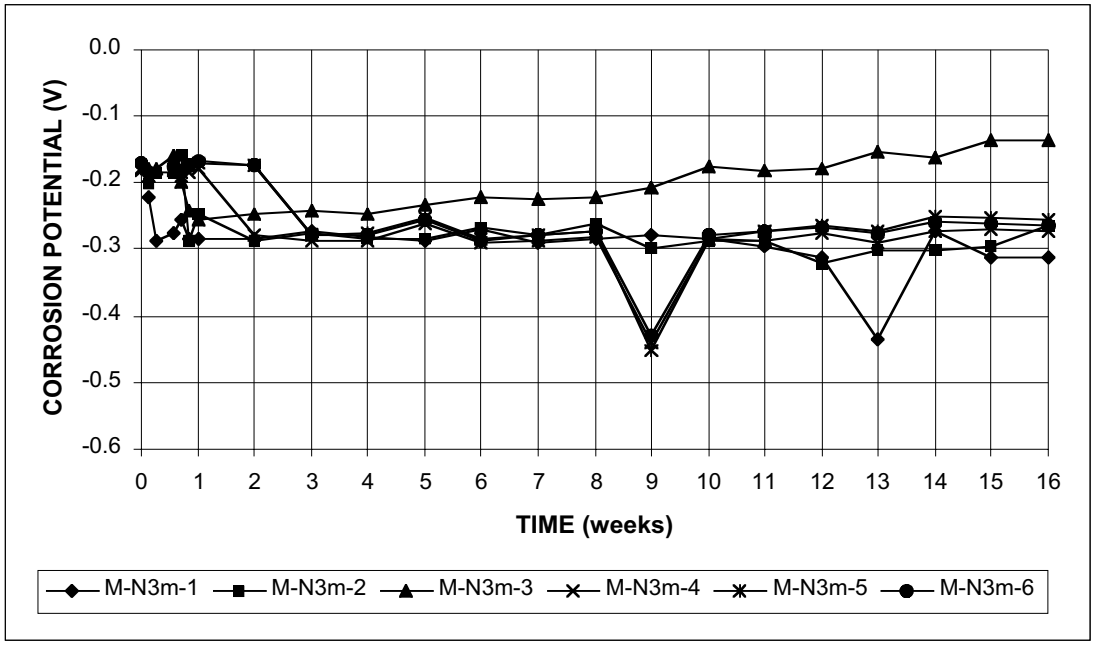

Figure A.20b - Macrocell Test. Corrosion potential vs. saturated calomel electrode, cathode. Mortar-wrapped conventional, normalized steel in 1.6 m ion NaCl and simulated concrete pore solution.

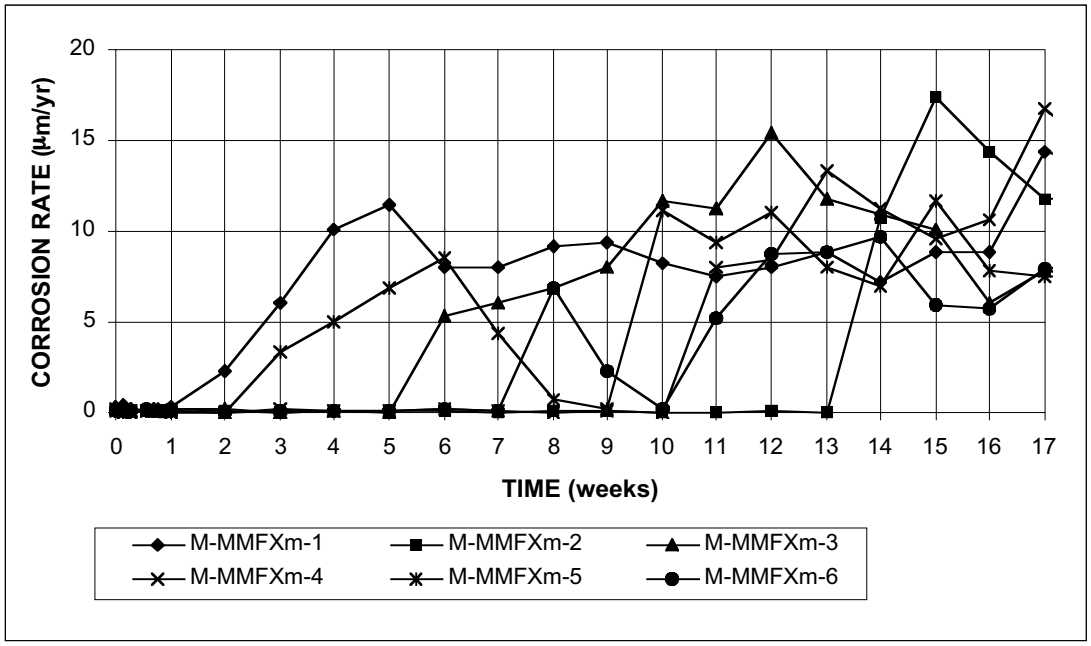

Figure A.21 - Macrocell Test. Corrosion rate. Mortar-wrapped MMFX steel in 1.6 m ion NaCl and simulated concrete pore solution.

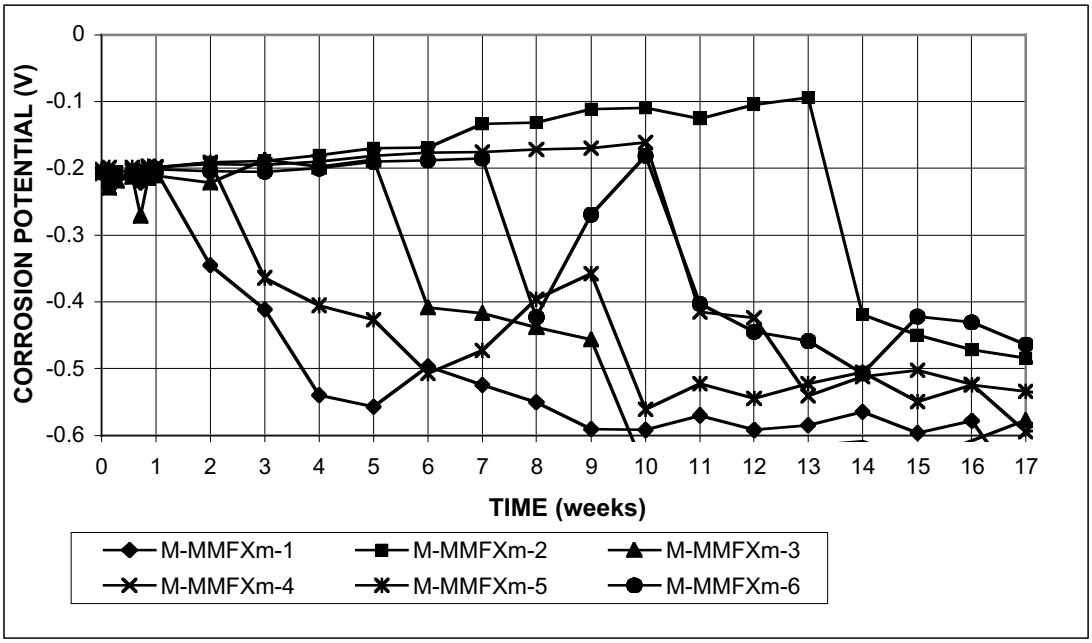

Figure A.22a - Macrocell Test. Corrosion potential vs. saturated calomel electrode, anode. Mortar-wrapped MMFX steel in 1.6 m ion NaCl and simulated concrete pore solution.

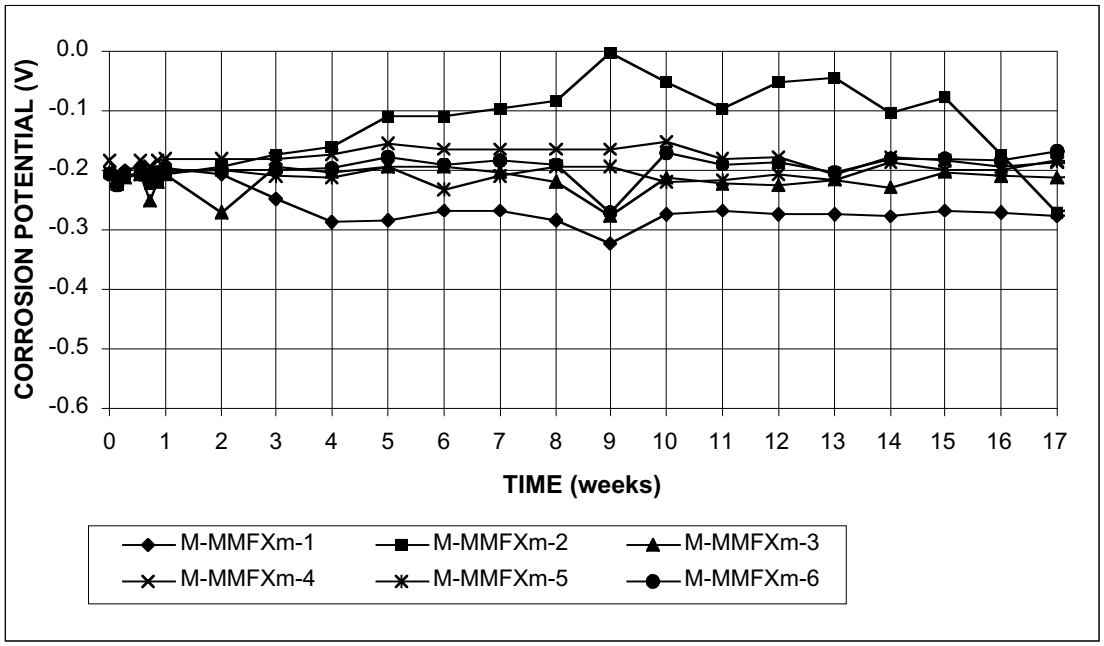

Figure A.22b - Macrocell Test. Corrosion potential vs. saturated calomel electrode, anode. Mortar-wrapped MMFX steel in 1.6 m ion NaCl and simulated concrete pore solution.

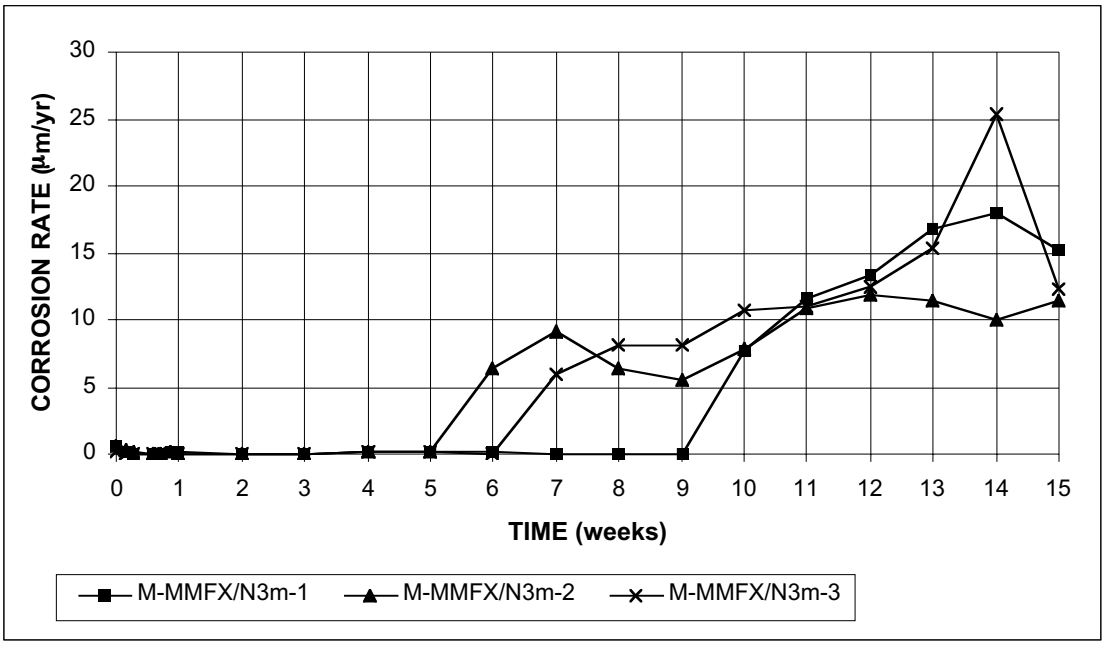

Figure A.23 - Macrocell Test. Corrosion rate. Cathode = mortar-wrapped conventional, normalized steel. Anode = mortar-wrapped MMFX steel in 1.6 m ion NaCl and simulated concrete pore solution.

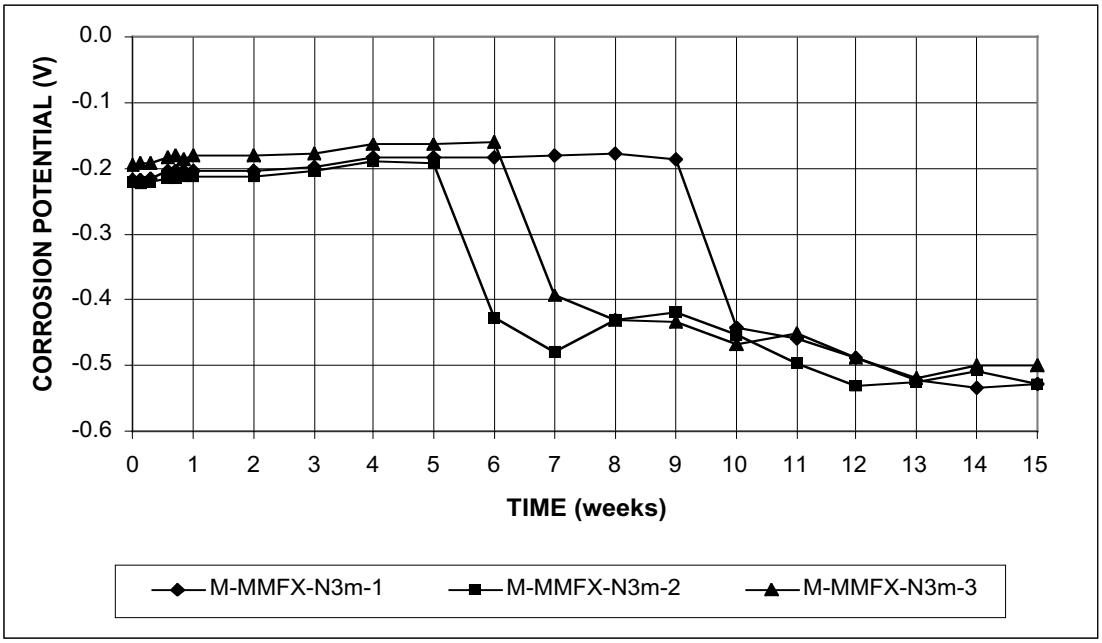

Figure A.24a - Macrocell Test. Corrosion potential vs. saturated calomel electrode, anode. Cathode = mortar-wrapped conventional, normalized steel. Anode = mortar-wrapped MMFX steel in 1.6 m ion NaCl and simulated concrete pore solution.

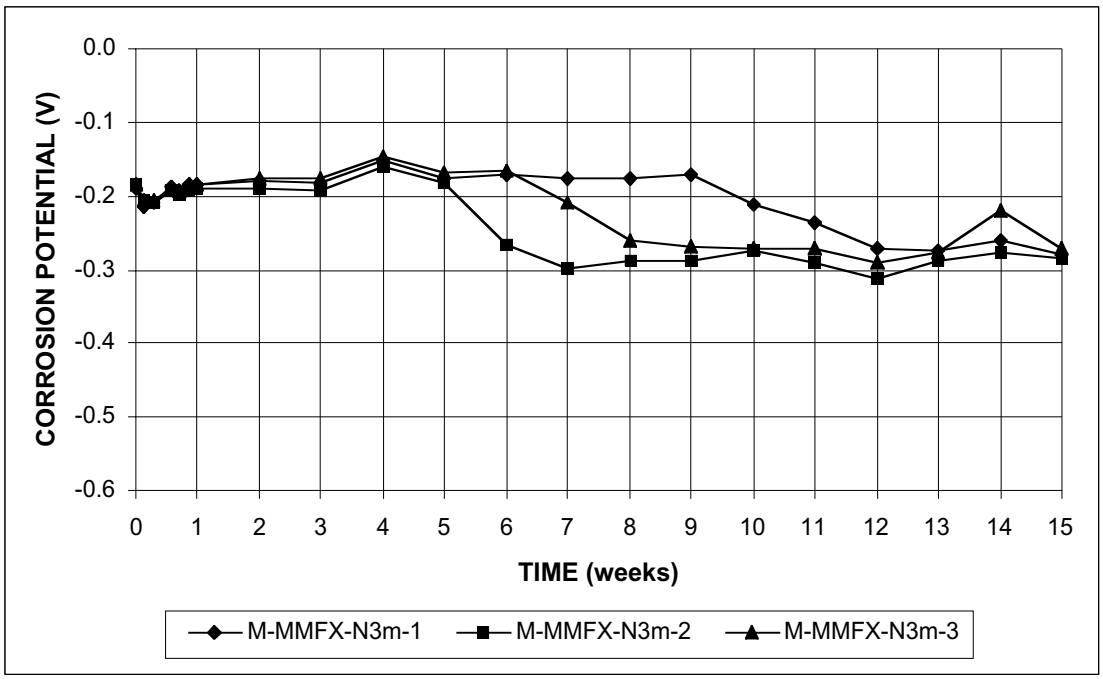

Figure A.24b - Macrocell Test. Corrosion potential vs. saturated calomel electrode, cathode. Cathode = mortar-wrapped conventional, normalized steel. Anode = mortar-wrapped MMFX steel in 1.6 m ion NaCl and simulated concrete pore solution.

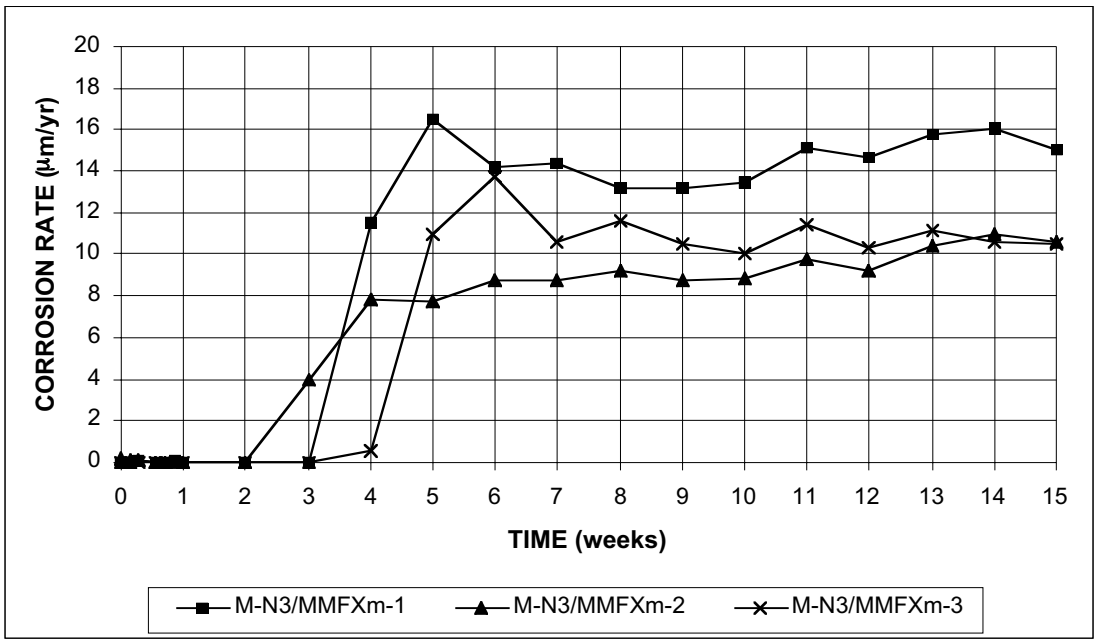

Figure A.25 - Macrocell Test. Corrosion rate. Cathode = mortar-wrapped MMFX steel. Anode = mortar-wrapped conventional, normalized steel in 1.6 m ion NaCl and simulated concrete pore solution.

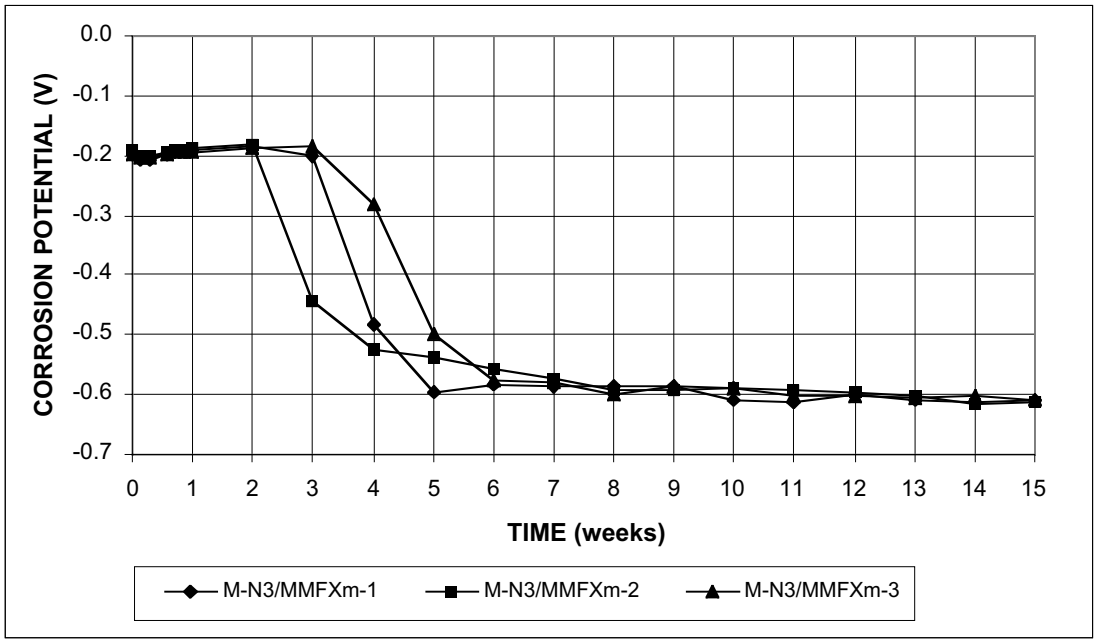

Figure A.26a - Macrocell Test. Corrosion potential vs. saturated calomel electrode, anode. Cathode = mortar-wrapped MMFX steel. Anode = mortar-wrapped conventional, normalized steel in 1.6 m ion NaCl and simulated concrete pore solution

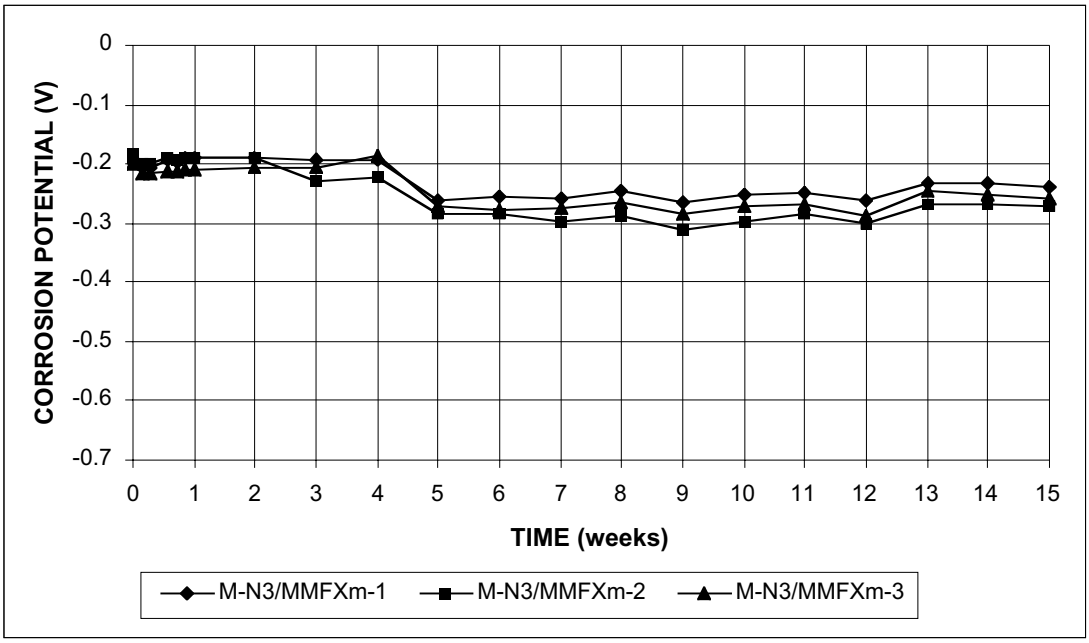

Figure A.26b - Macrocell Test. Corrosion potential vs. saturated calomel electrode, cathode. Cathode = mortar-wrapped MMFX steel. Anode = mortar-wrapped conventional, normalized steel in 1.6 m ion NaCl and simulated concrete pore solution

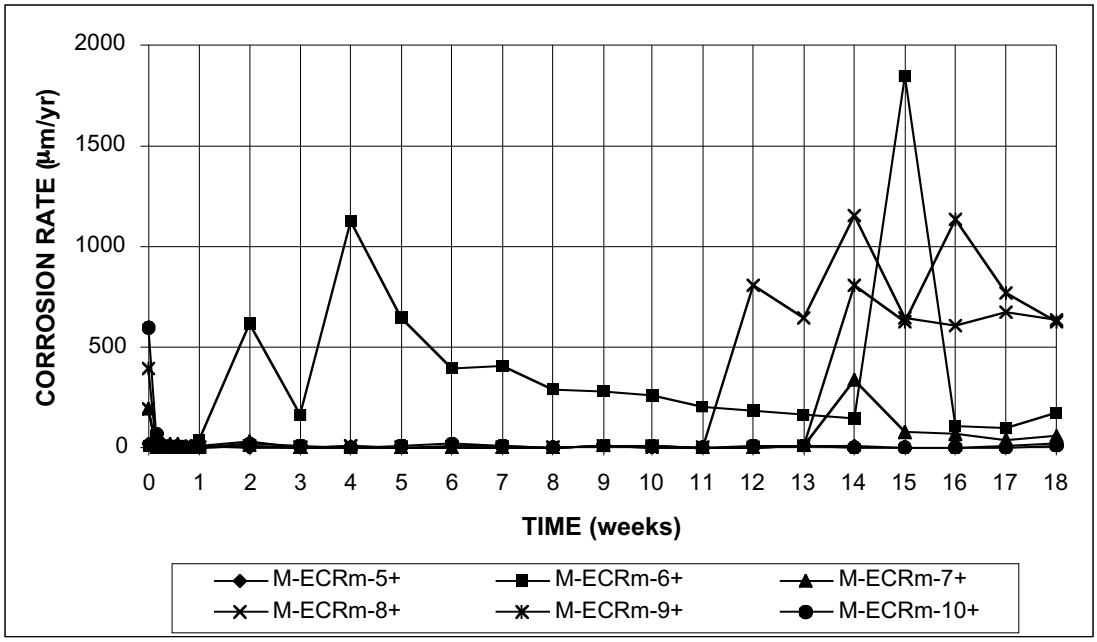

Figure A.27 - Macrocell Test. Corrosion rate based on exposed area of steel (four $^{1}/_{8}$-in. holes in epoxy). Epoxy-coated steel in 1.6 m ion NaCl and simulated concrete pore solution.

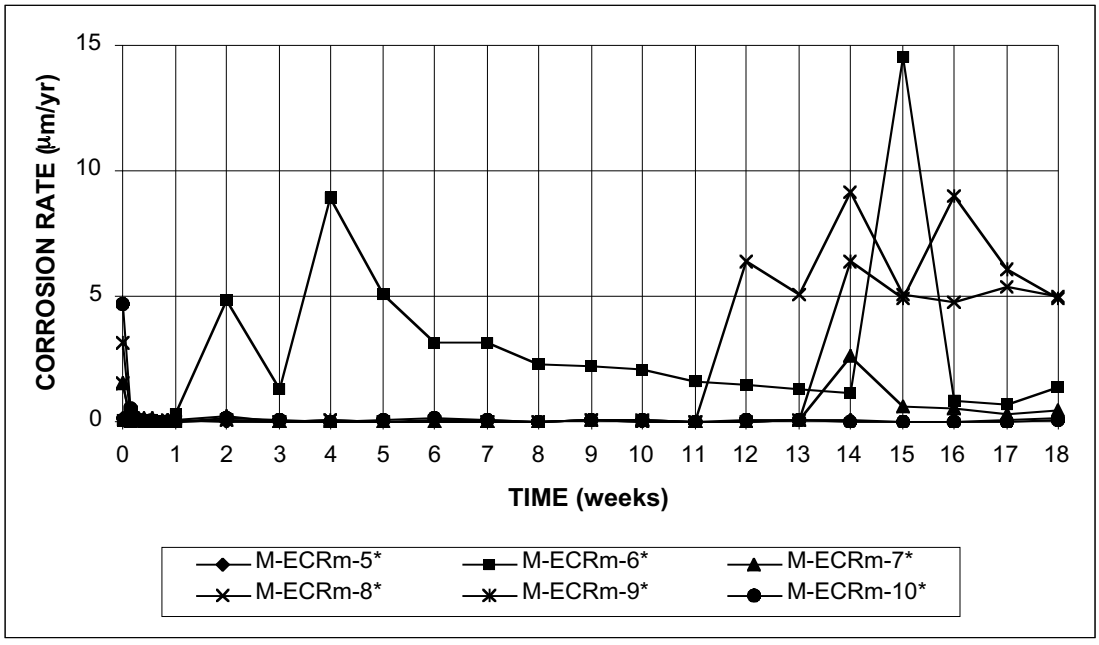

Figure A.28 - Macrocell Test. Corrosion rate based on total area of bar exposed to solution. Epoxy-coated steel in 1.6 m ion NaCl and simulated concrete pore solution.

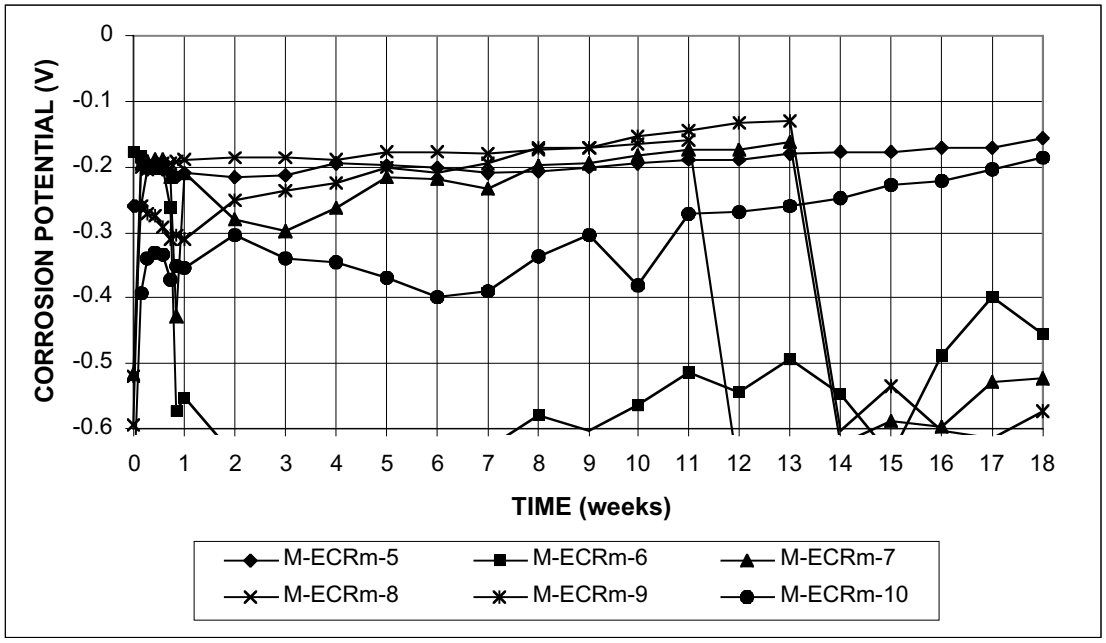

Figure A.29a - Macrocell Test. Corrosion potential vs. saturated calomel electrode, anode. Epoxy-coated steel in 1.6 m ion NaCl and simulated concrete pore solution.

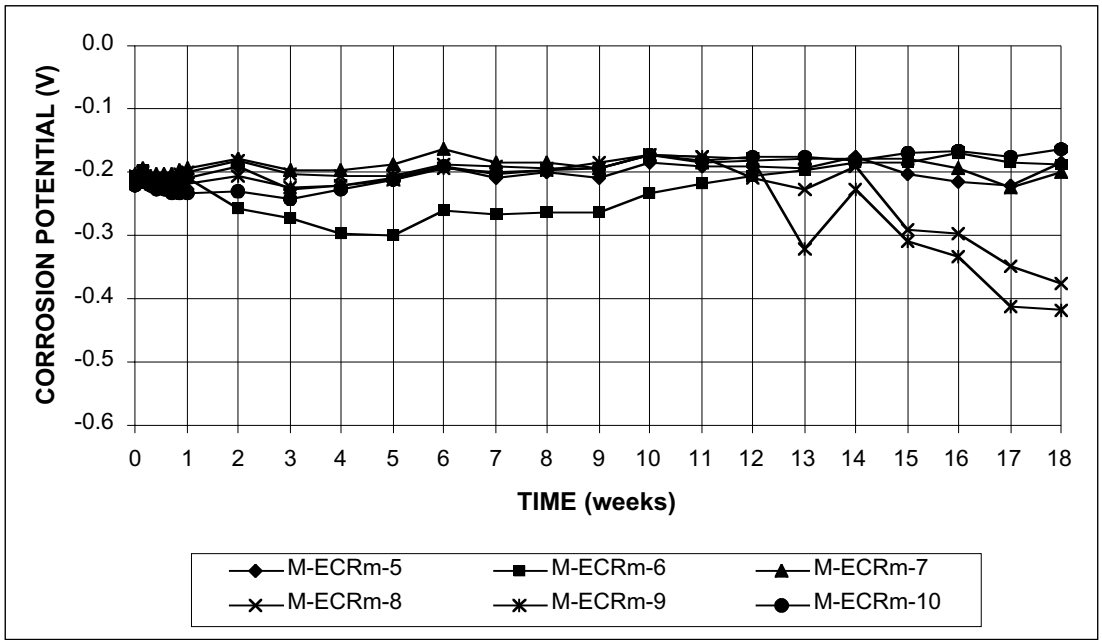

Figure A.29b - Macrocell Test. Corrosion potential vs. saturated calomel electrode, cathode. Epoxy-coated steel in 1.6 m ion NaCl and simulated concrete pore solution

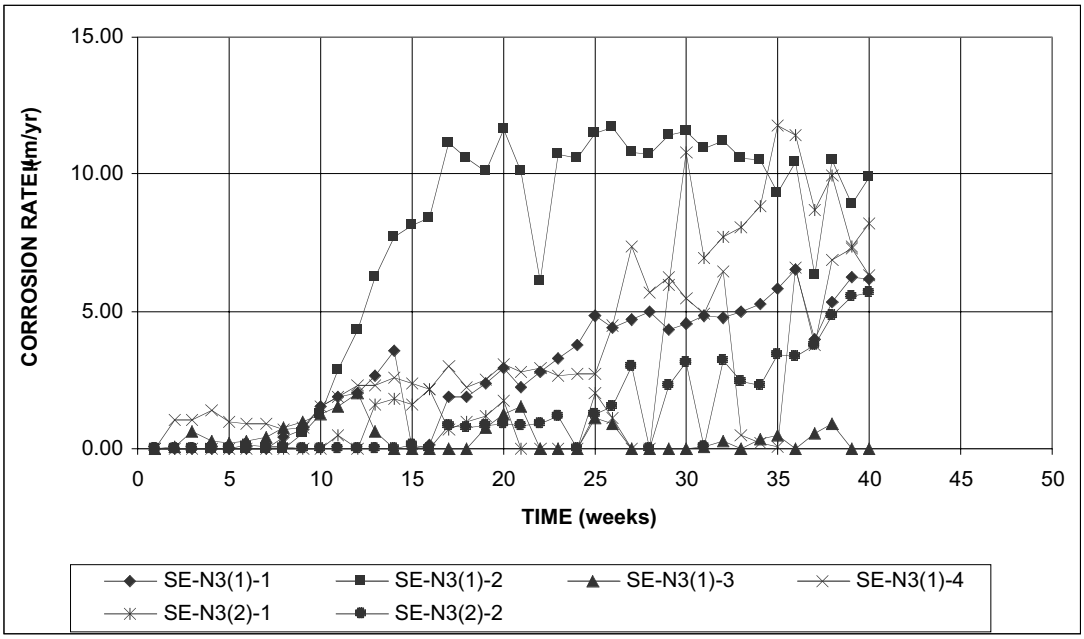

Figure A.30 - Southern Exposure Test. Corrosion rate. Conventional, normalized steel, w/c=0.45, ponded with 15% NaCl solution.

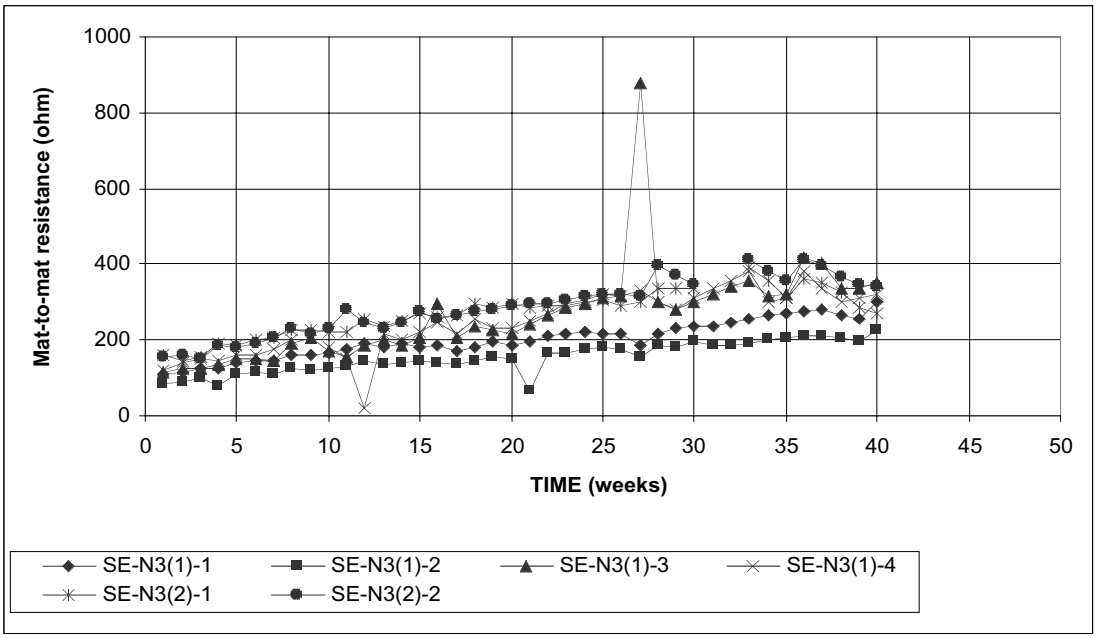

Figure A.31 - Southern Exposure Test. Mat-to-mat resistance. Conventional, normalized steel, w/c=0.45, ponded with 15% NaCl solution.

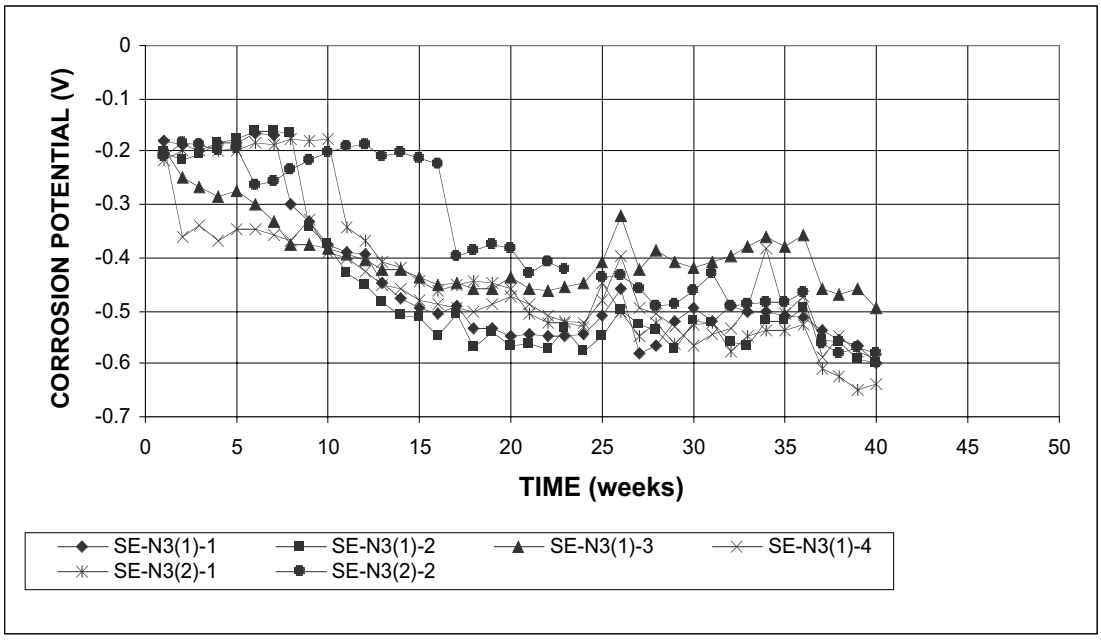

Figure A.32a - Southern Exposure Test. Corrosion potential vs. CSE, top mat. Conventional, normalized steel, w/c=0.45, ponded with 15% NaCl solution.

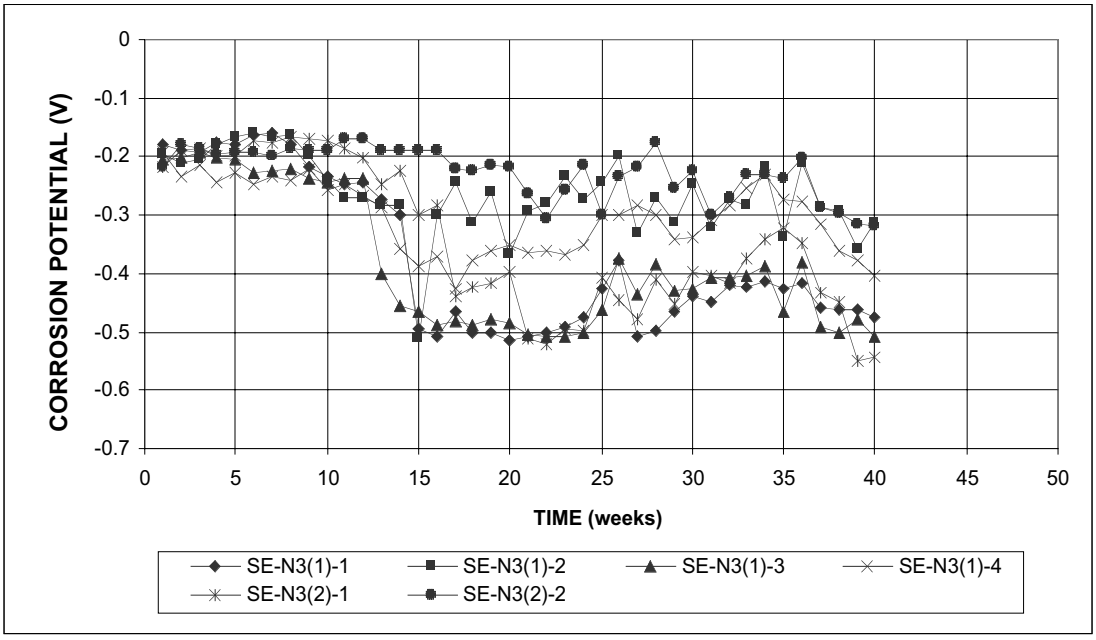

Figure A.32b - Southern Exposure Test. Corrosion potential vs. CSE, bottom mat. Conventional, normalized steel, w/c=0.45, ponded with 15% NaCl solution.

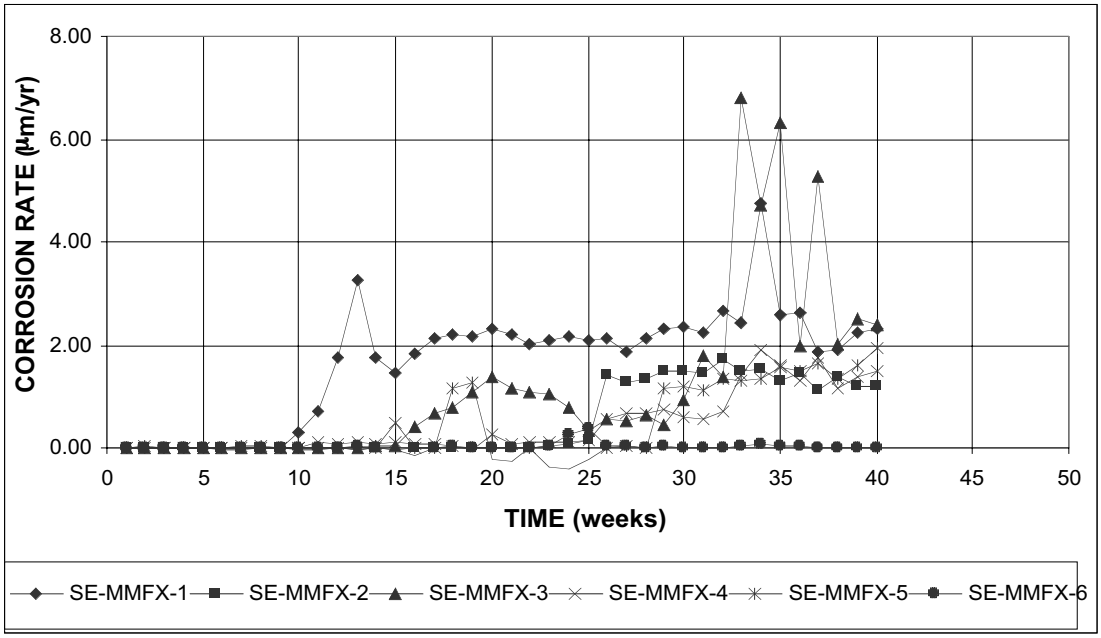

Figure A.33 - Southern Exposure Test. Corrosion rate. MMFX steel, w/c=0.45, ponded with 15% NaCl solution.

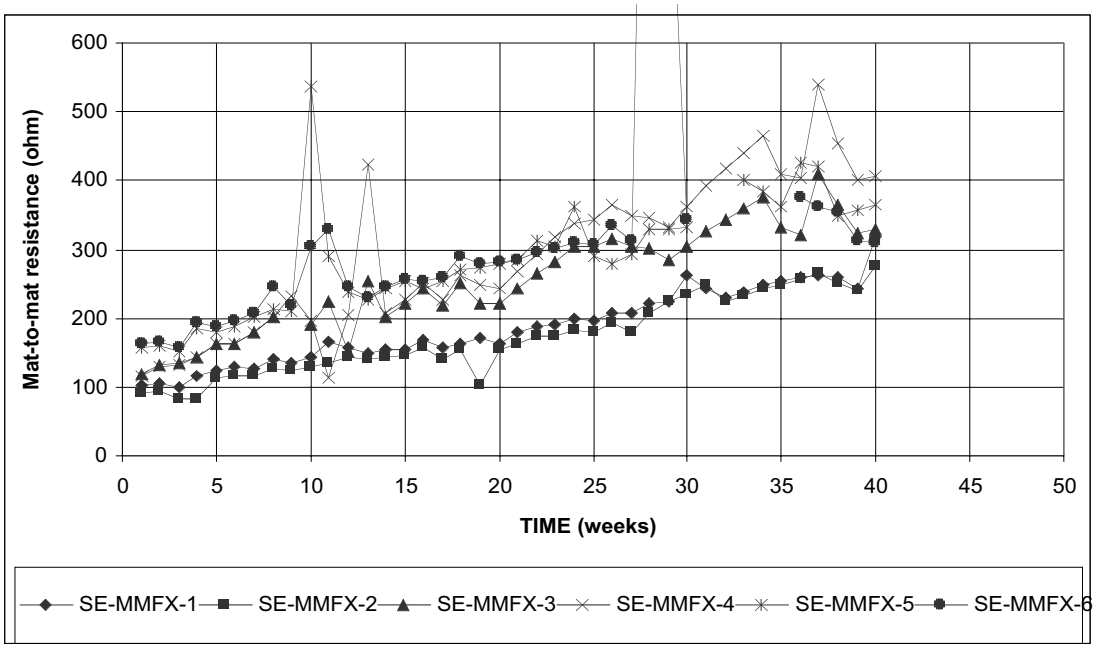

Figure A.34 - Southern Exposure Test. Mat-to-mat resistance. MMFX steel, w/c=0.45, ponded with 15% NaCl solution.

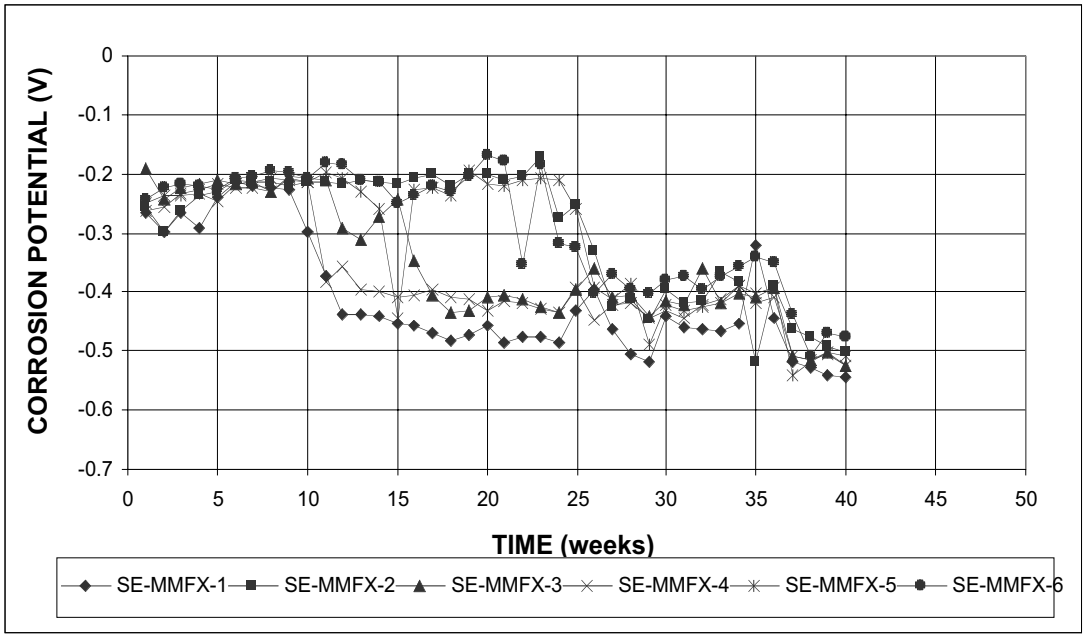

Figure A.35a - Southern Exposure Test. Corrosion potential vs. CSE, top mat. MMFX steel, w/c=0.45, ponded with 15% NaCl solution.

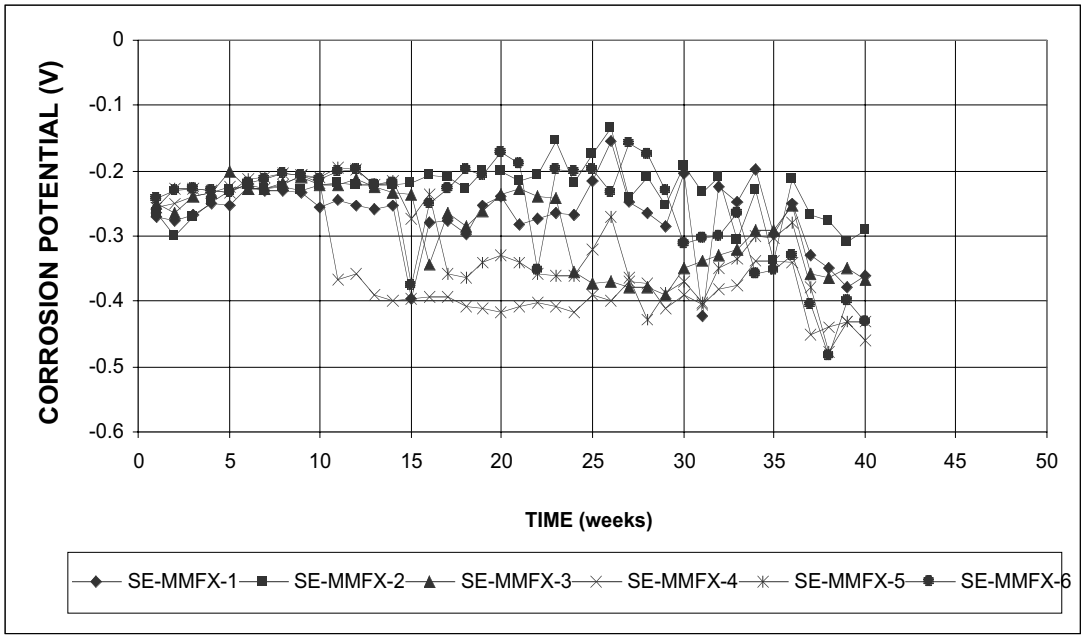

Figure A.35b - Southern Exposure Test. Corrosion potential vs. CSE, bottom mat. MMFX steel, w/c=0.45, ponded with 15% NaCl solution.

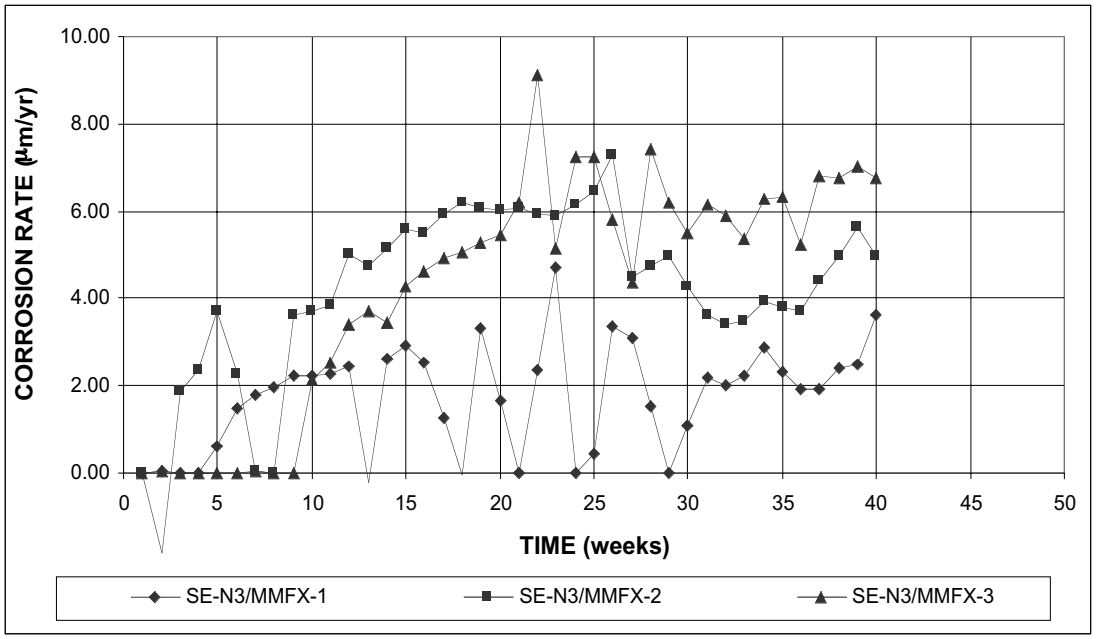

Figure A.36 - Southern Exposure Test. Corrosion rate. Top mat = conventional, normalized steel, bottom mat = MMFX steel, w/c=0.45, ponded with 15% NaCl solution.

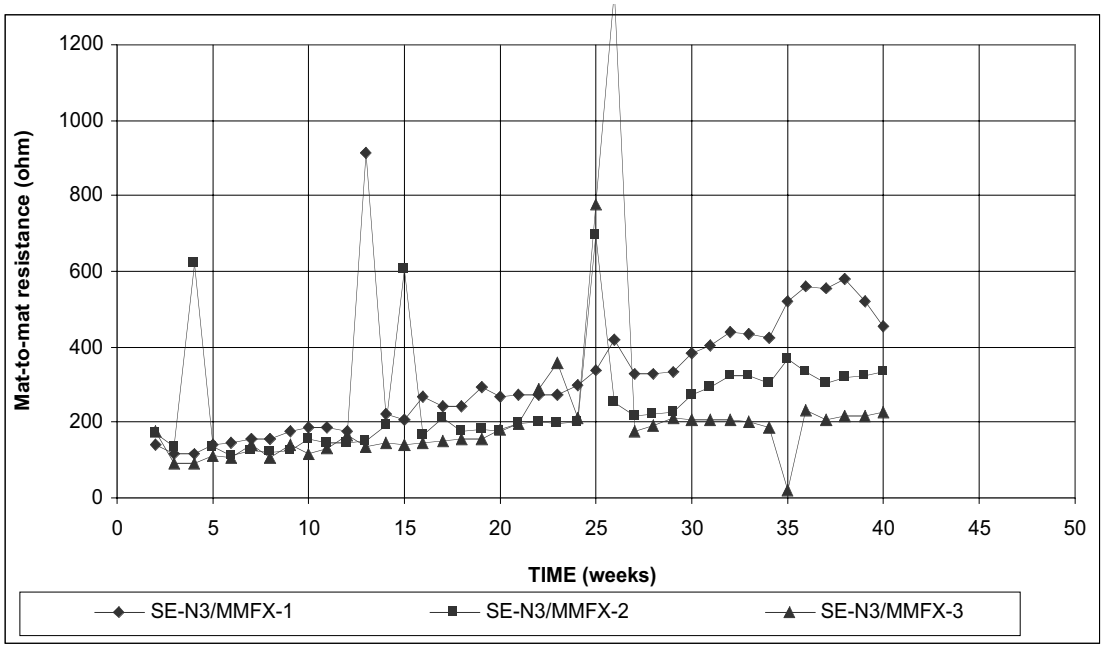

Figure A.37 - Southern Exposure Test. Mat-to-mat resistance. Top mat = conventional, normalized steel, bottom mat = MMFX steel, w/c=0.45, ponded with 15% NaCl solution.

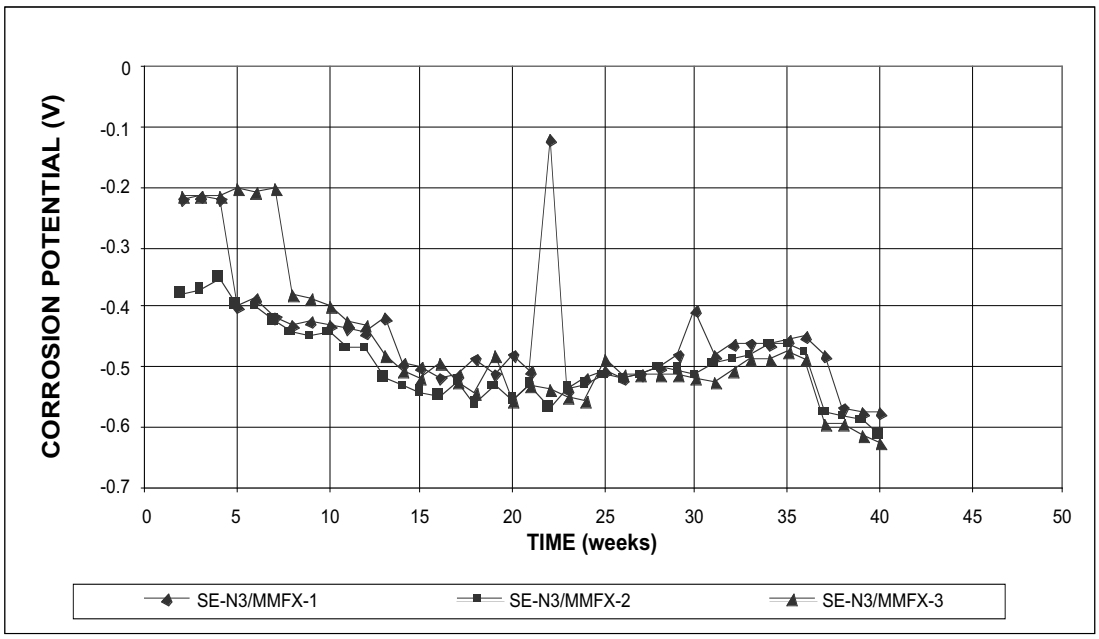

Figure A.38a - Southern Exposure Test. Corrosion potential vs. CSE, top mat. Top mat = conventional, normalized steel, bottom mat = MMFX steel, w/c=0.45, ponded with 15% NaCl solution.

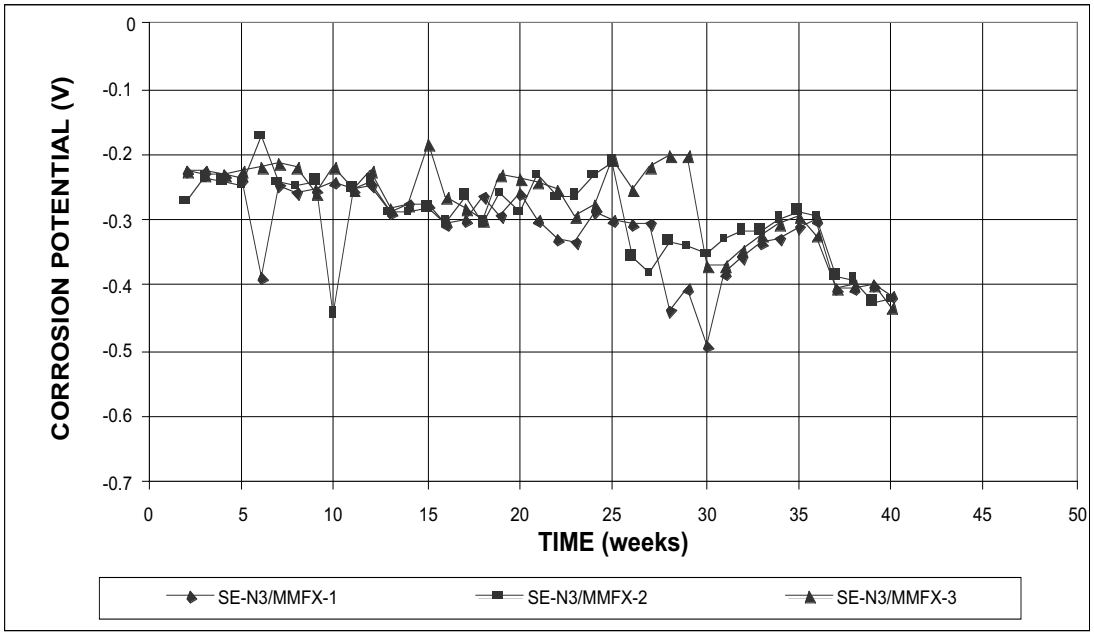

Figure A.38b - Southern Exposure Test. Corrosion potential vs. CSE, bottom mat. Top mat = conventional, normalized steel. Bottom mat = MMFX steel, w/c=0.45, ponded with 15% NaCl solution.

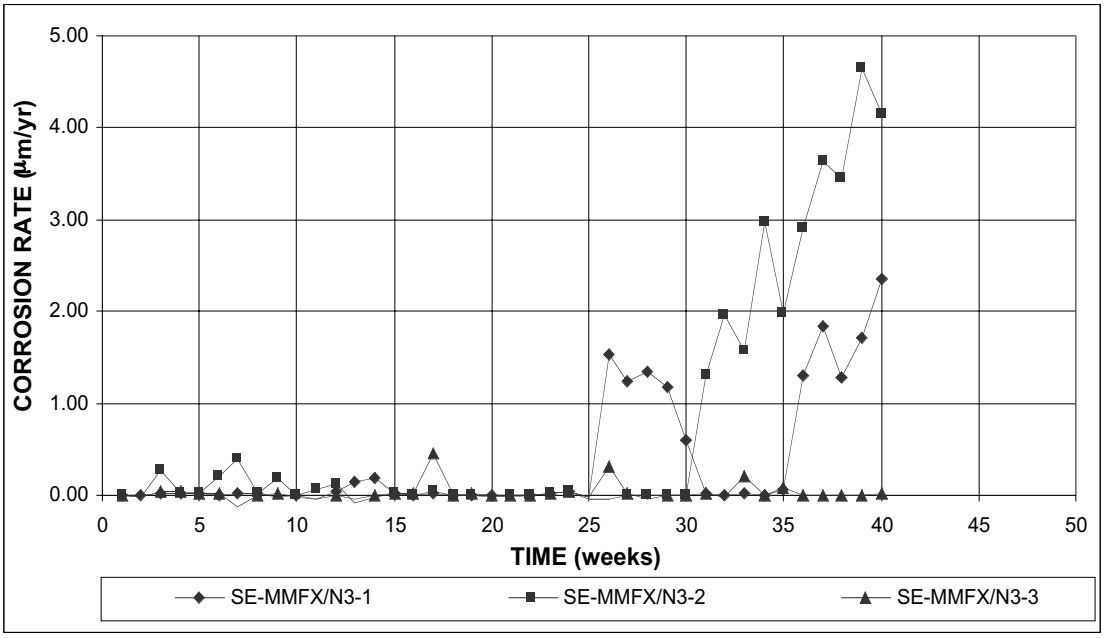

Figure A.39 - Southern Exposure Test. Corrosion rate. Top mat = MMFX steel, bottom mat = conventional steel, normalized, w/c=0.45, ponded with 15% NaCl solution.

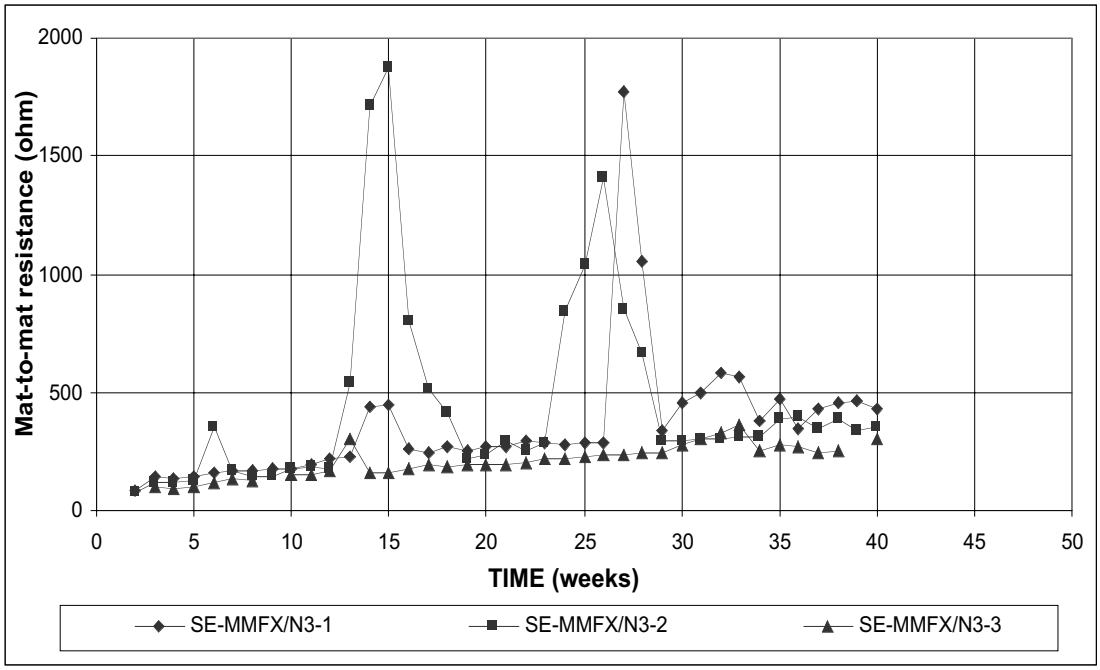

Figure A.40 - Southern Exposure Test. Mat-to-mat resistance. Top mat = MMFX steel, bottom mat = conventional steel, normalized, w/c=0.45, ponded with 15% NaCl solution.

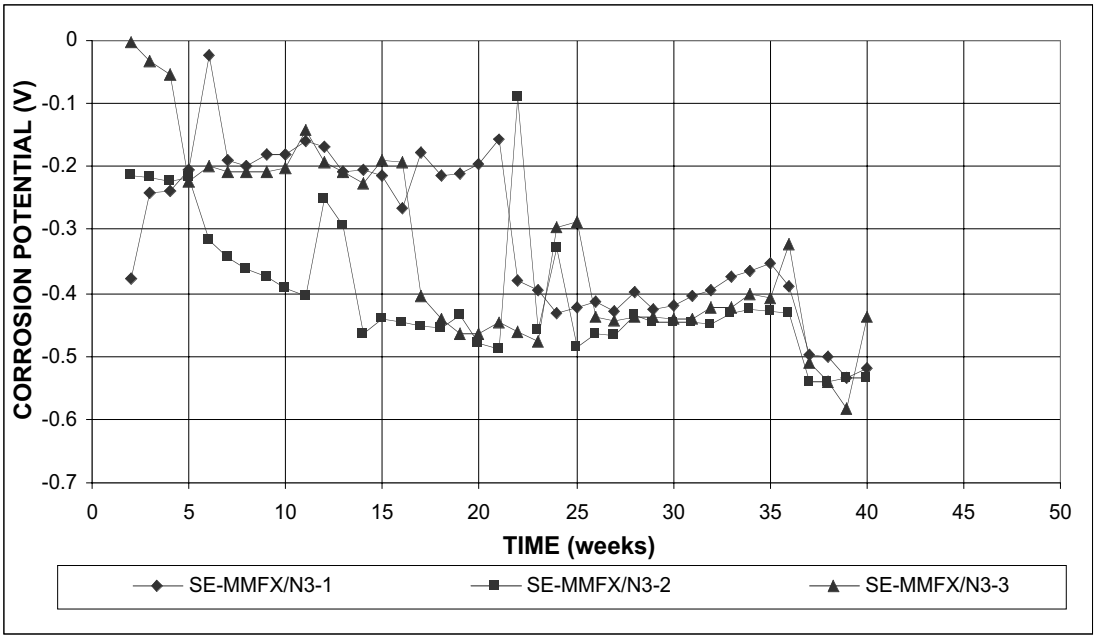

Figure A.41a - Southern Exposure Test. Corrosion potential vs. CSE, top mat. Top mat = MMFX steel, bottom mat = conventional, normalized steel, w/c=0.45, ponded with 15% NaCl solution.

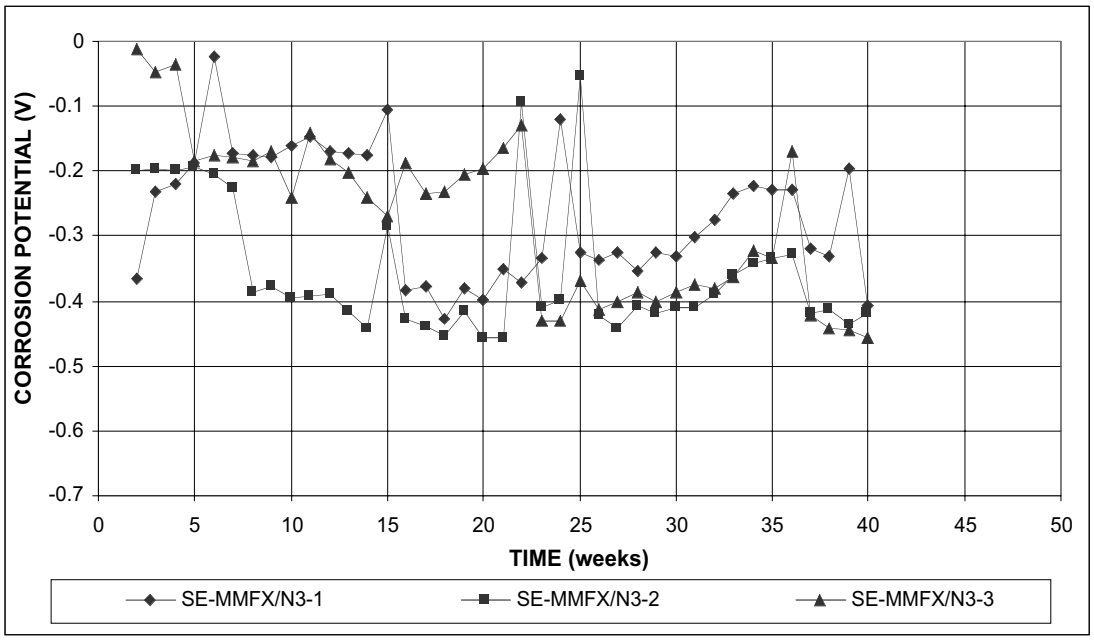

Figure A.41b - Southern Exposure Test – Corrosion potential vs. CSE, bottom mat. Top mat = MMFX steel, bottom mat = conventional, normalized steel, w/c=0.45, ponded with 15% NaCl solution.

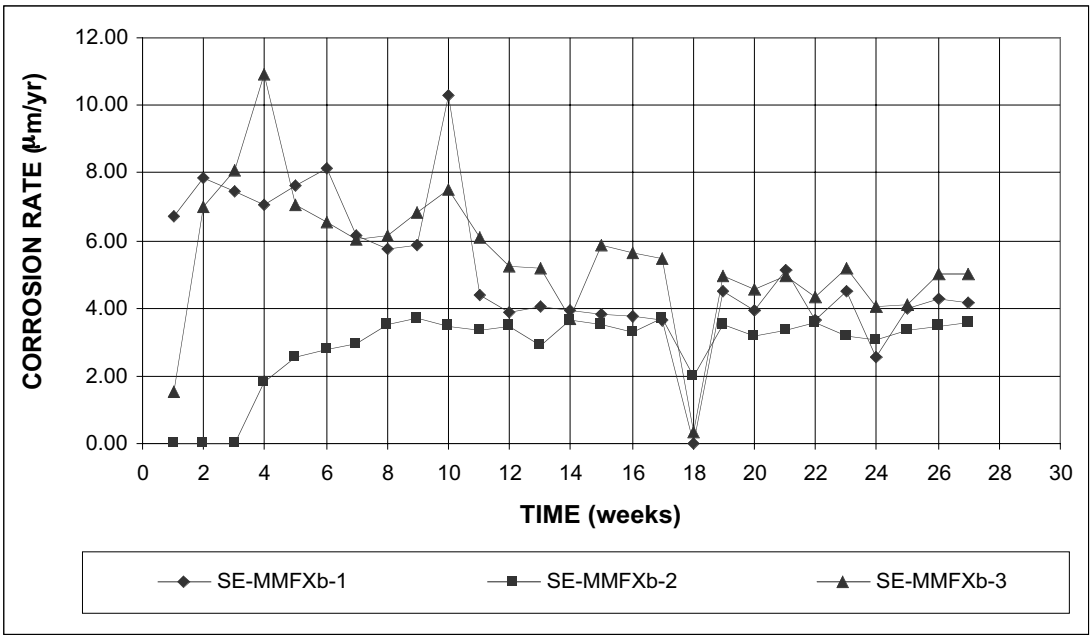

Figure A.42 - Southern Exposure Test. Corrosion rate. MMFX steel, bent bar at anode, w/c=0.45, ponded with 15% NaCl solution.

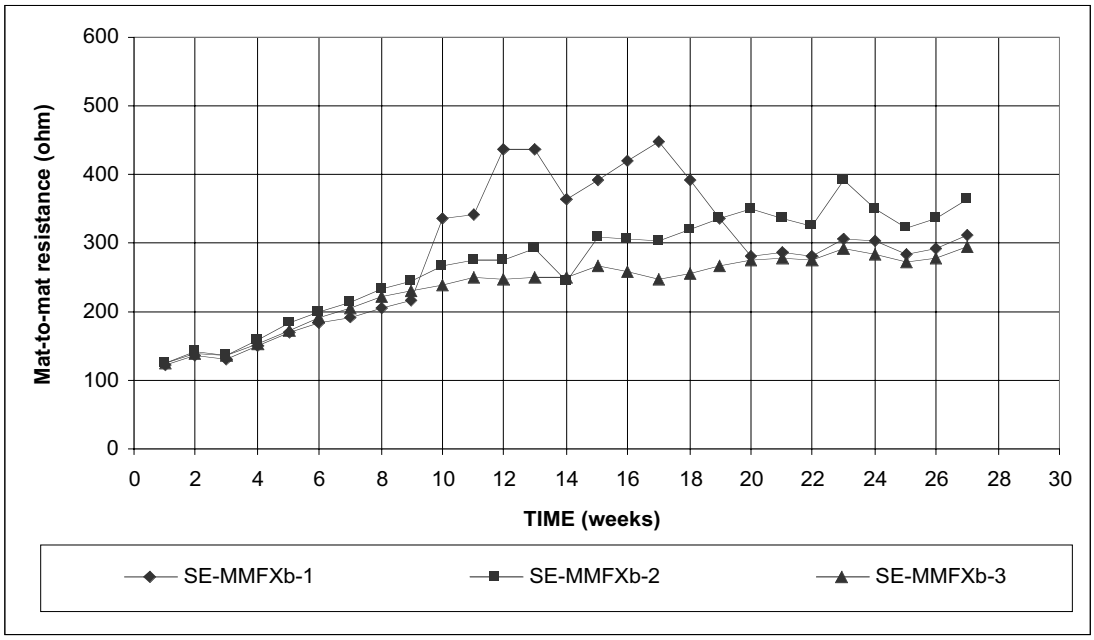

Figure A.43 - Southern Exposure Test. Mat-to-mat resistance. MMFX steel, bent bar at anode, w/c=0.45, ponded with 15% NaCl solution.

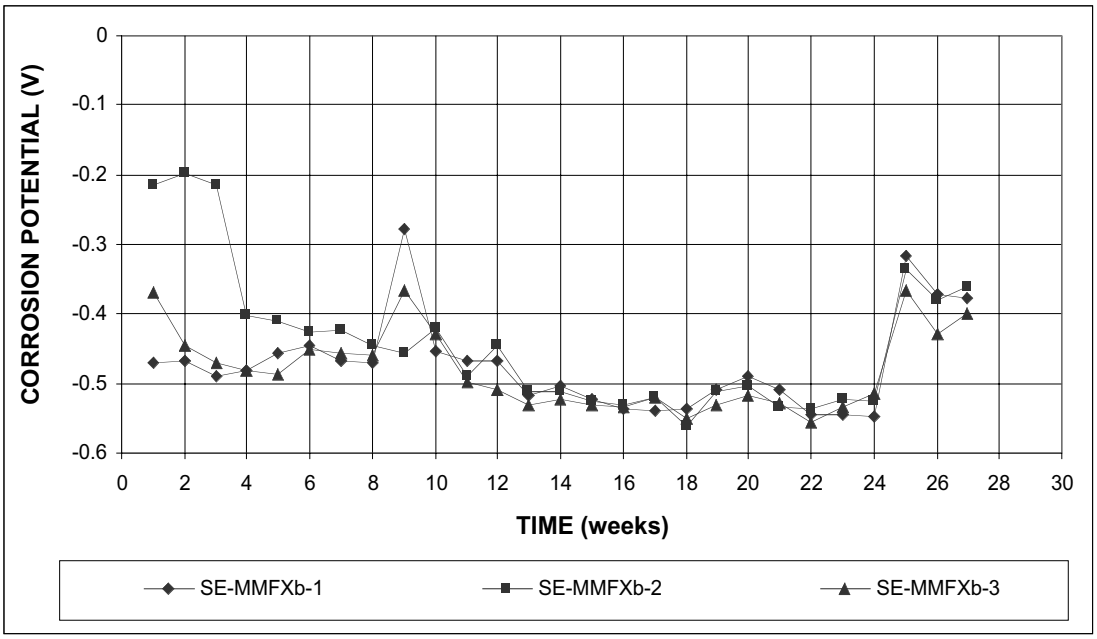

Figure A.44a - Southern Exposure Test – Corrosion potential vs. CSE, top mat. MMFX steel, bent bar at anode, w/c=0.45, ponded with 15% NaCl solution.

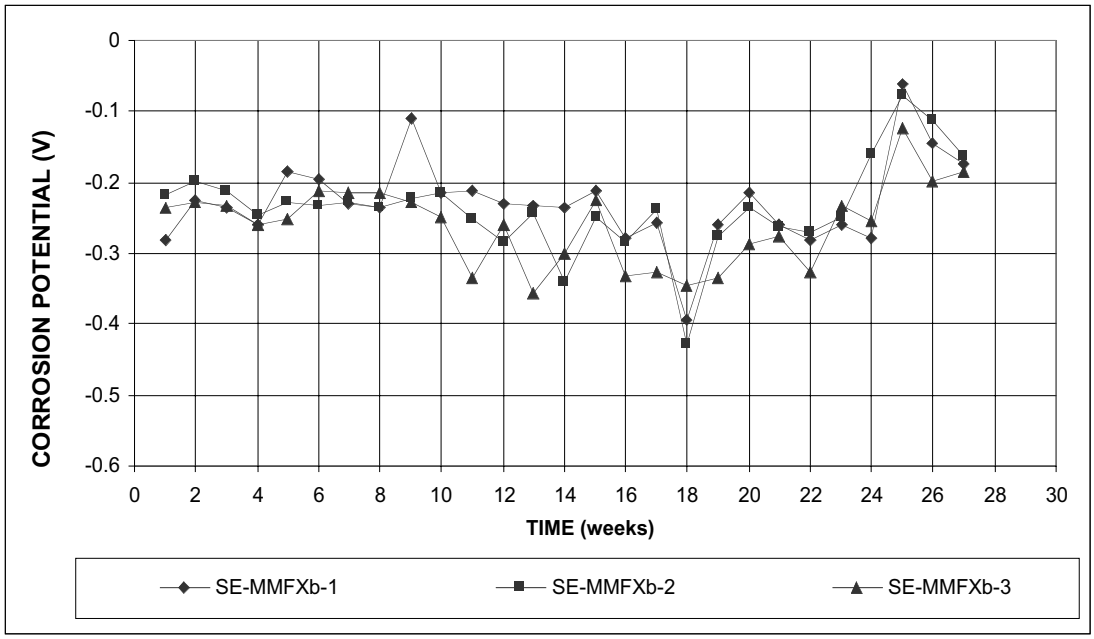

Figure A.44b - Southern Exposure Test – Corrosion potential vs. CSE, bottom mat. MMFX steel, bent bar at anode, w/c=0.45, ponded with 15% NaCl solution.

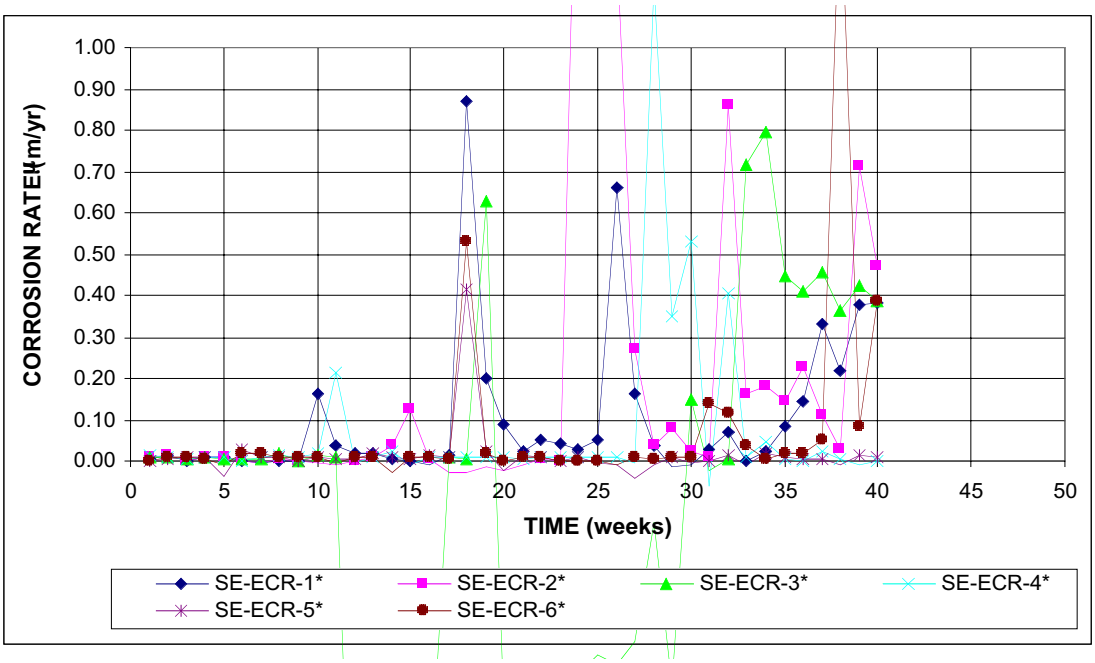

Figure A.45 - Southern Exposure Test. Corrosion rate based on total bar area exposed to solution. Epoxy-coated bars, w/c=0.45, ponded with 15% NaCl solution.

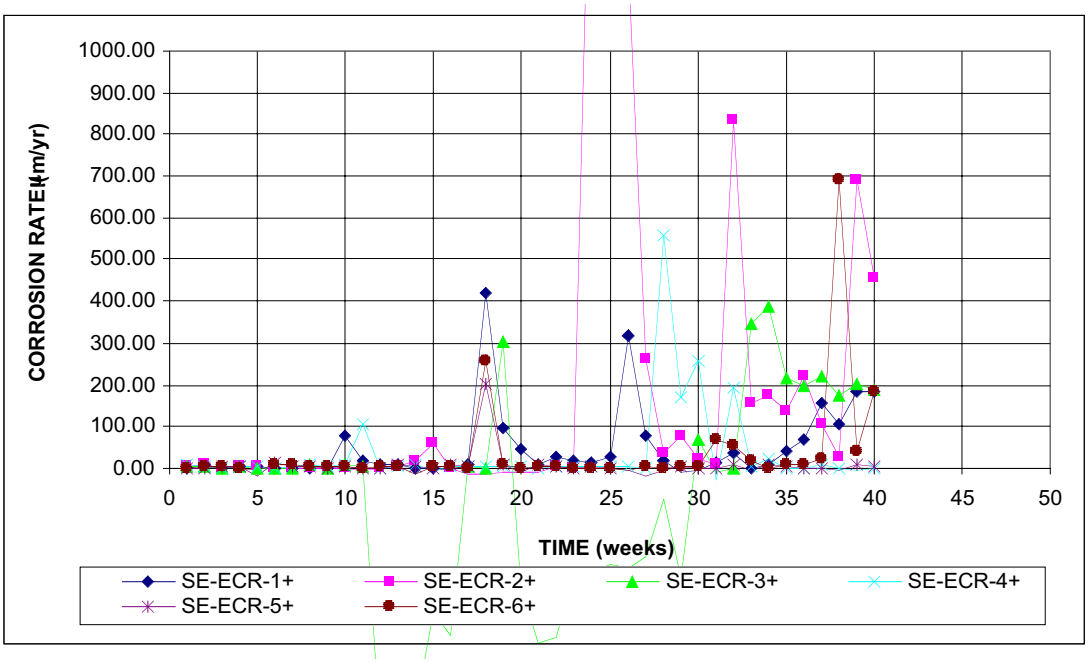

Figure A.46 - Southern Exposure Test. Corrosion rate based on exposed area of steel (four $^{1}/_{8}$-in. diameter holes in epoxy). Epoxy-coated steel, w/c=0.45, ponded with 15% NaCl solution.

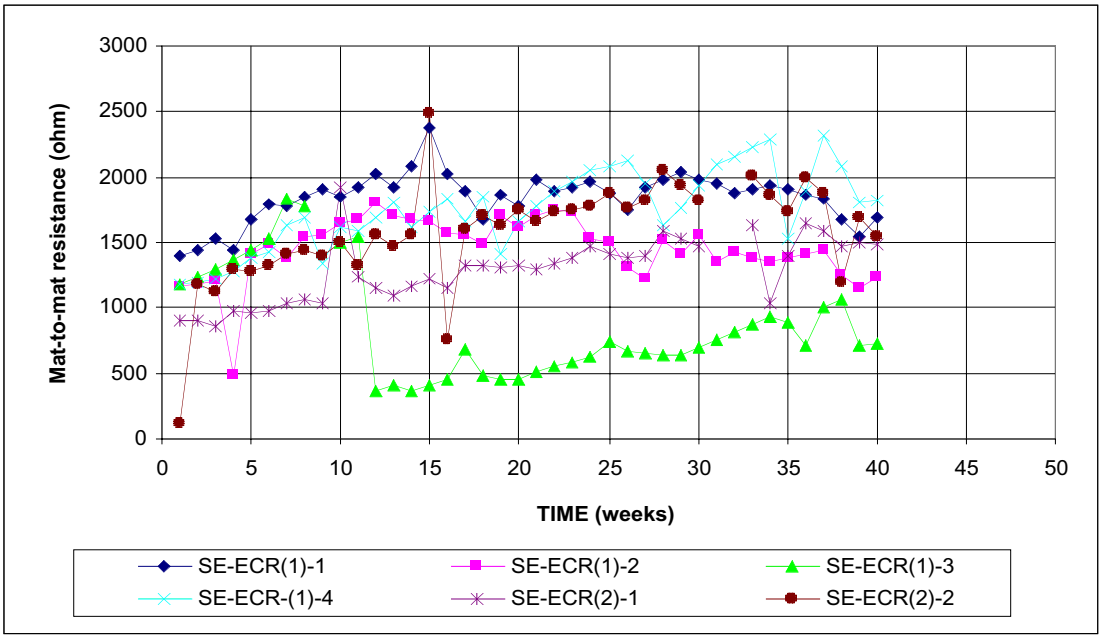

Figure A.47 - Southern Exposure Test. Mat-to-mat resistance. Epoxy-coated steel, w/c=0.45, ponded with 15% NaCl solution.

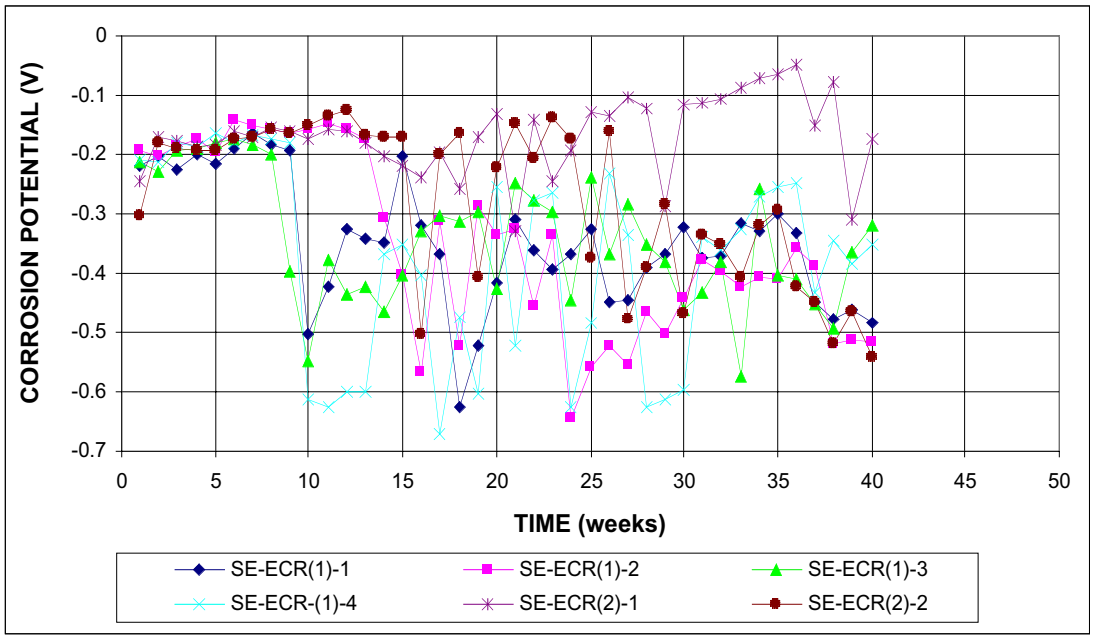

Figure A.48a - Southern Exposure Test. Corrosion potential vs. CSE, top mat. Epoxy-coated steel, w/c=0.45, ponded with 15% NaCl solution.

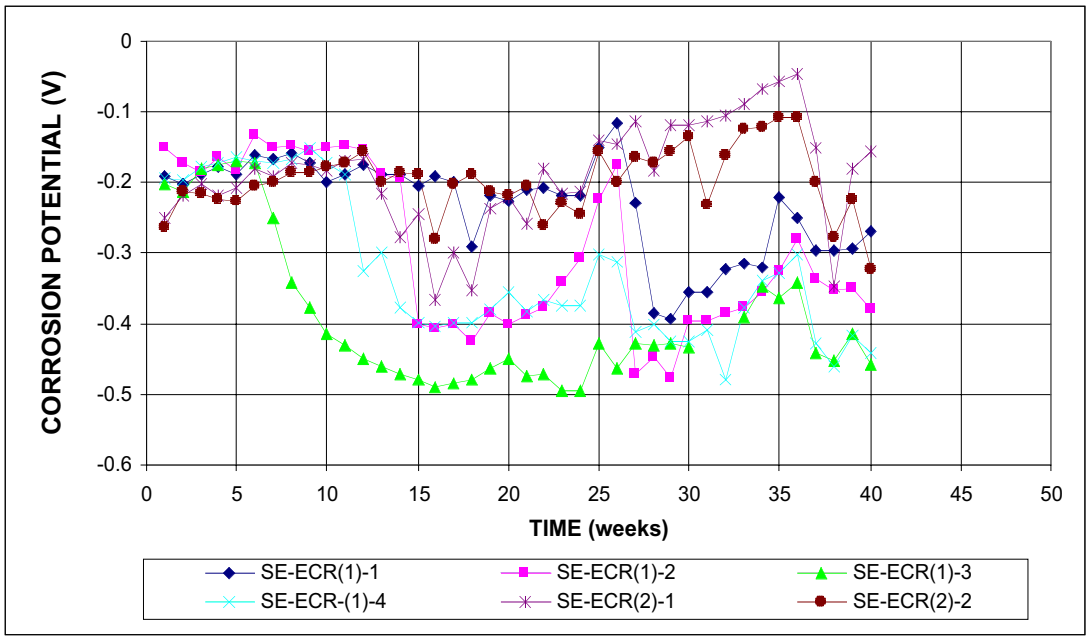

Figure A.48b - Southern Exposure Test. Corrosion potential vs. CSE, bottom mat. Epoxy-coated steel, w/c=0.45, ponded with 15% NaCl solution.

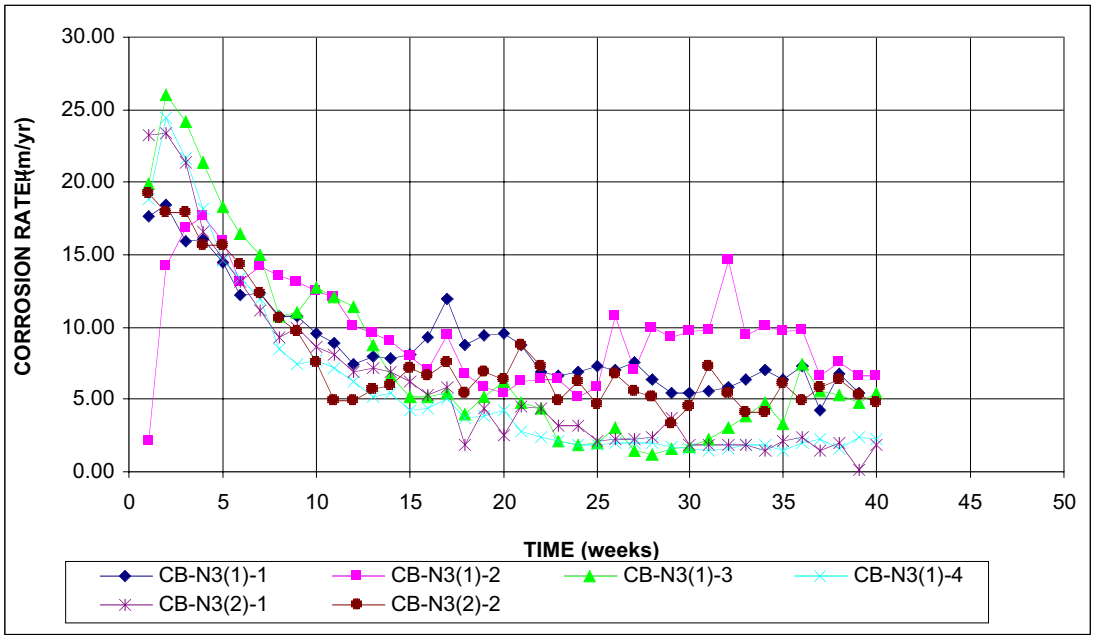

Figure A.49 - Cracked Beam Test. Corrosion rate. Conventional, normalized steel, w/c=0.45, ponded with 15% NaCl solution.

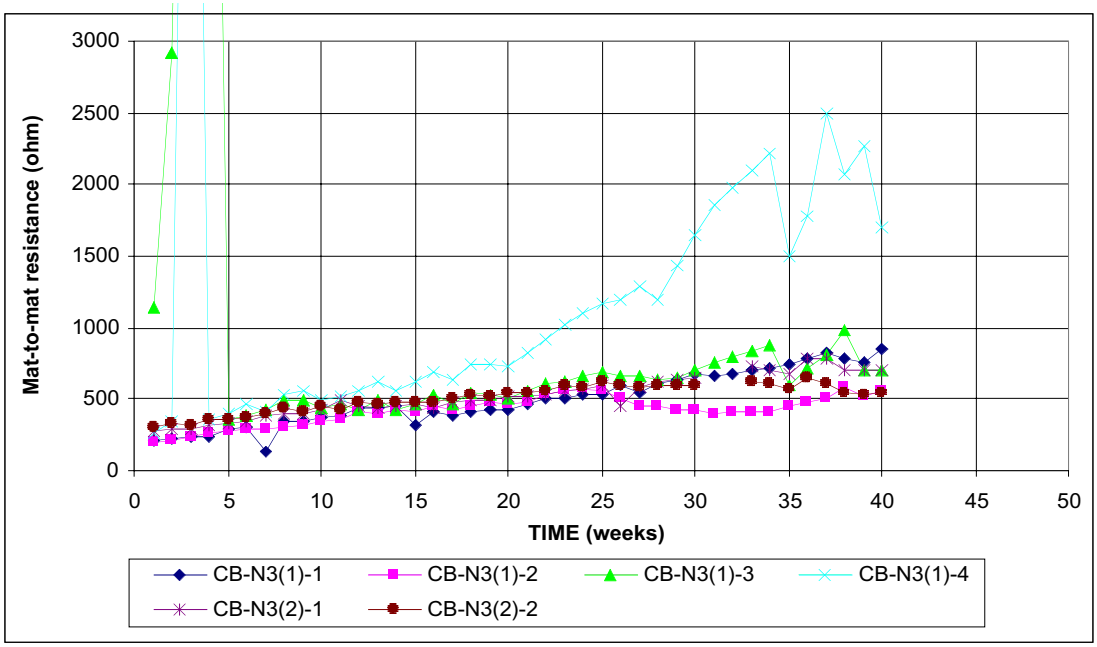

Figure A.50 - Cracked Beam Test. Mat-to-mat resistance. Conventional, normalized steel, w/c=0.45, ponded with 15% NaCl solution.

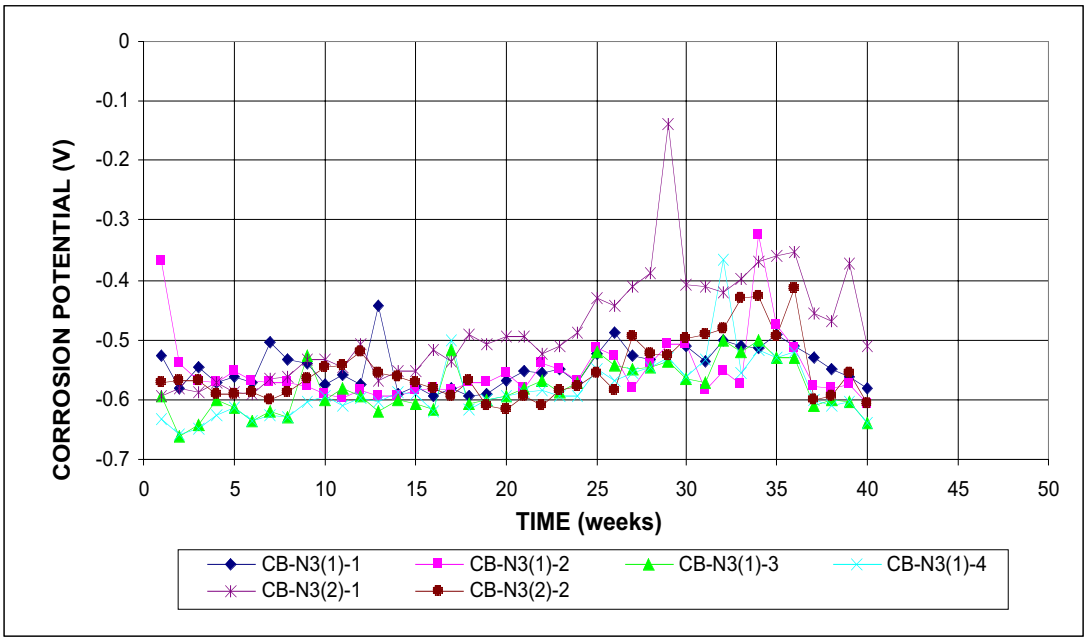

Figure A.51a - Cracked Beam Test. Corrosion potential vs. CSE, top mat. Conventional, normalized steel, w/c=0.45, ponded with 15% NaCl solution.

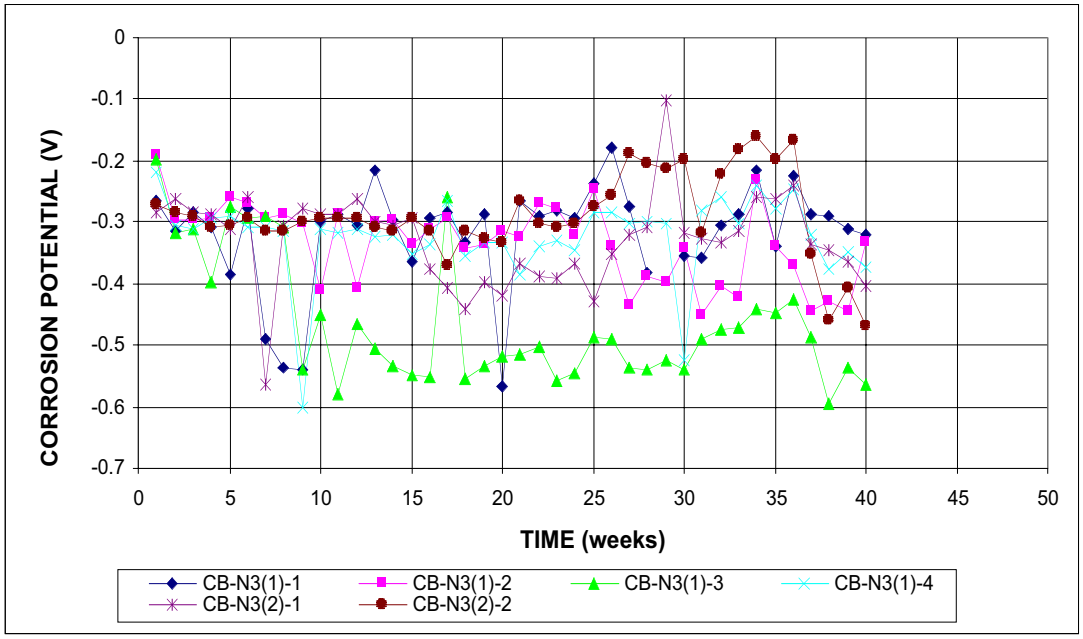

Figure A.51b - Cracked Beam Test. Corrosion potential vs. CSE, top mat. Conventional, normalized steel, w/c=0.45, ponded with 15% NaCl solution.

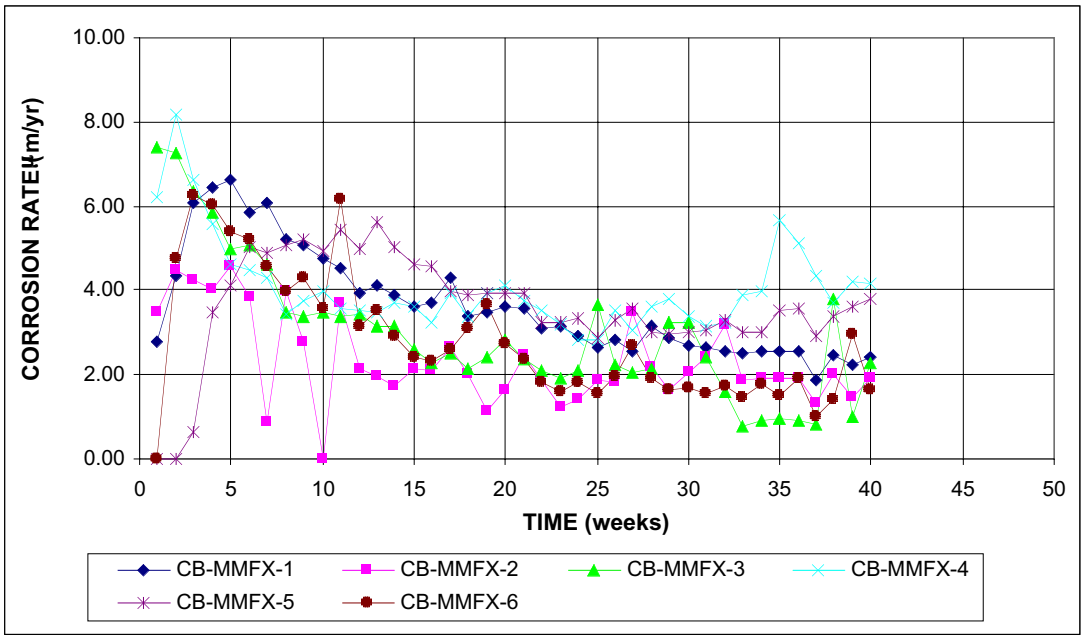

Figure A.52 - Cracked Beam Test. Corrosion rate. MMFX steel, w/c=0.45, ponded with 15% NaCl solution.

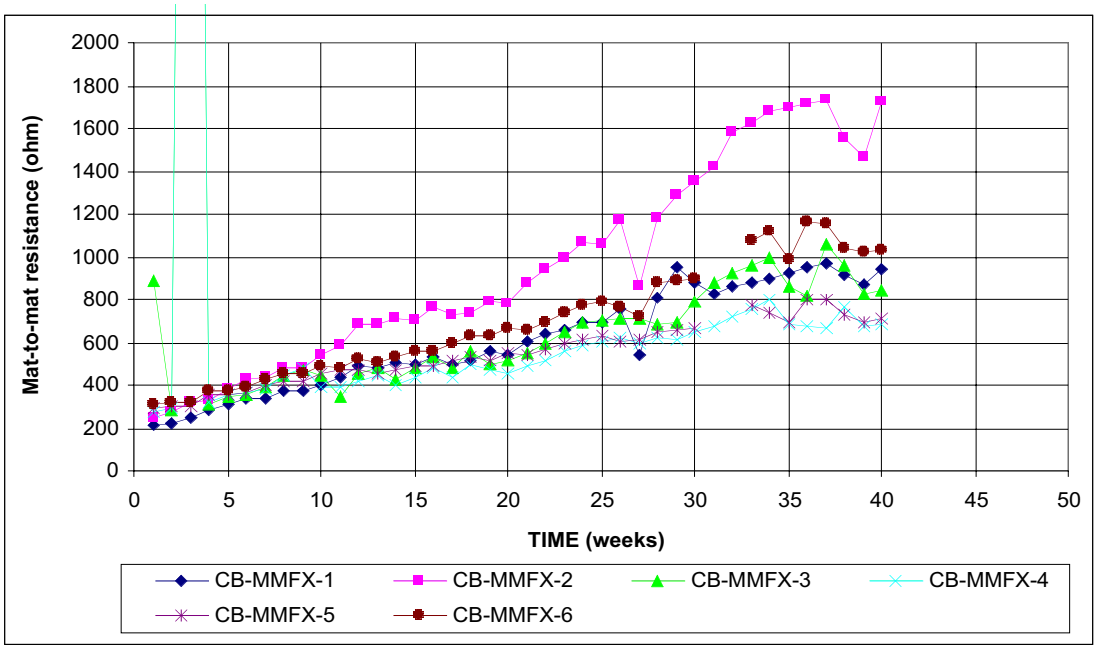

Figure A.53 - Cracked Beam Test. Mat-to-mat resistance. MMFX steel, w/c=0.45, ponded with 15% NaCl solution.

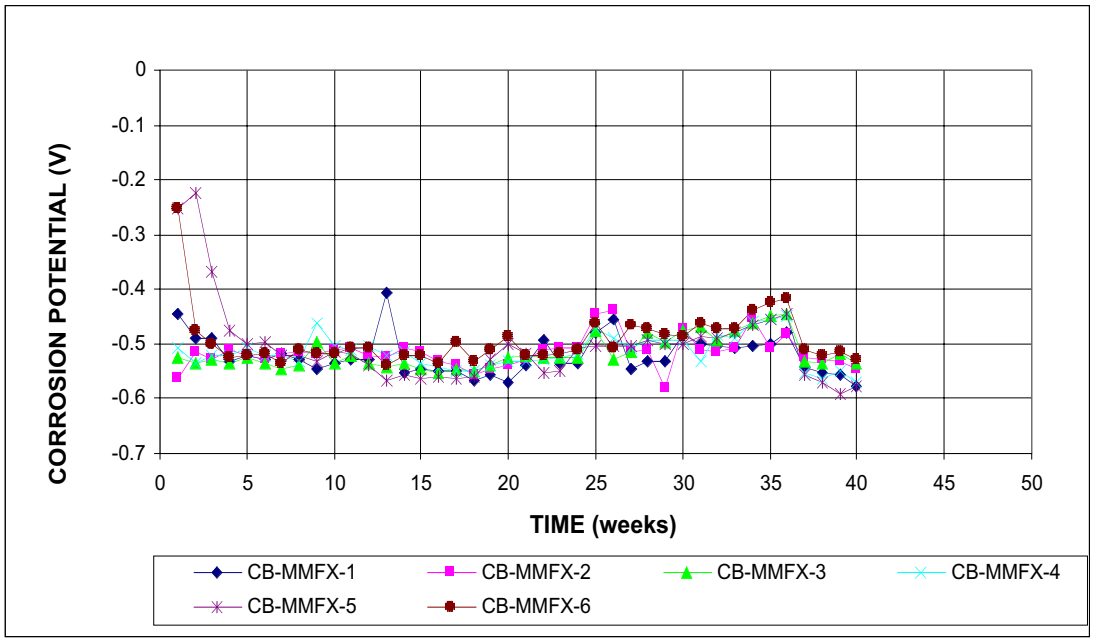

Figure A.54a - Cracked Beam Test. Corrosion potential vs. CSE, top mat. MMFX steel, w/c=0.45, ponded with 15% NaCl solution.

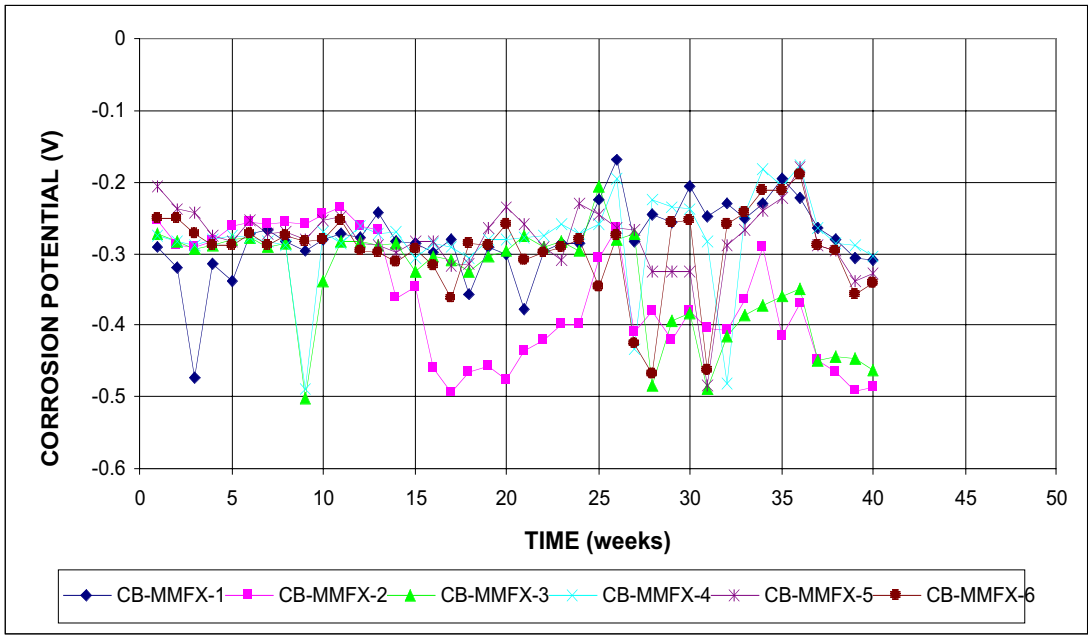

Figure A.54b - Cracked Beam Test. Corrosion potential vs. CSE, bottom mat. MMFX steel, w/c=0.45, ponded with 15% NaCl solution.

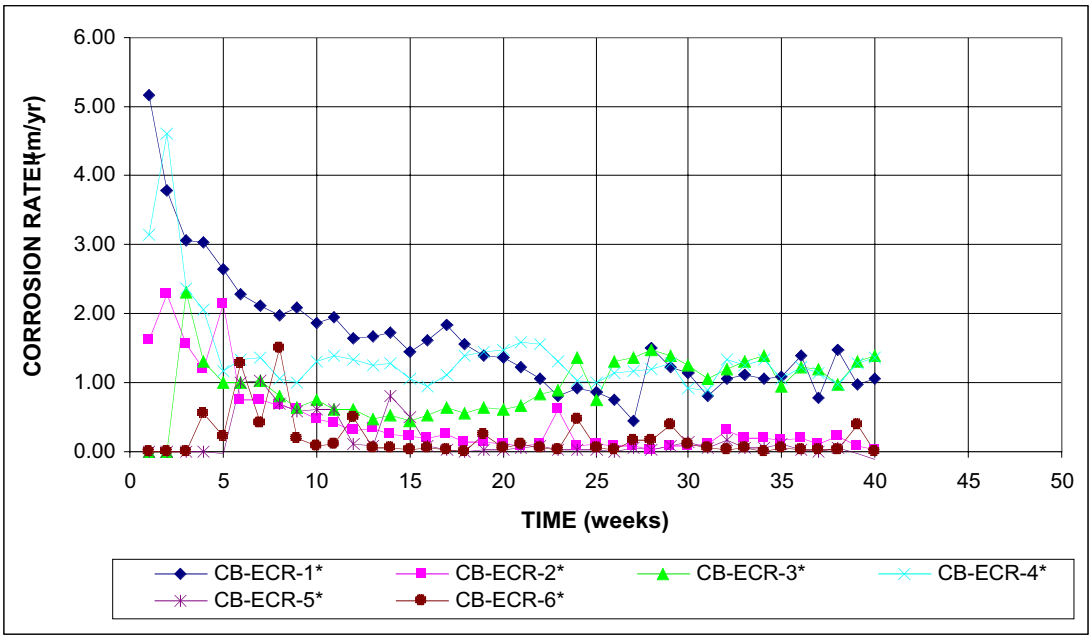

Figure A.55 - Cracked Beam Test. Corrosion rate based on total area of bar exposed to solution. Epoxy-coated steel, w/c=0.45, ponded with 15% NaCl solution.

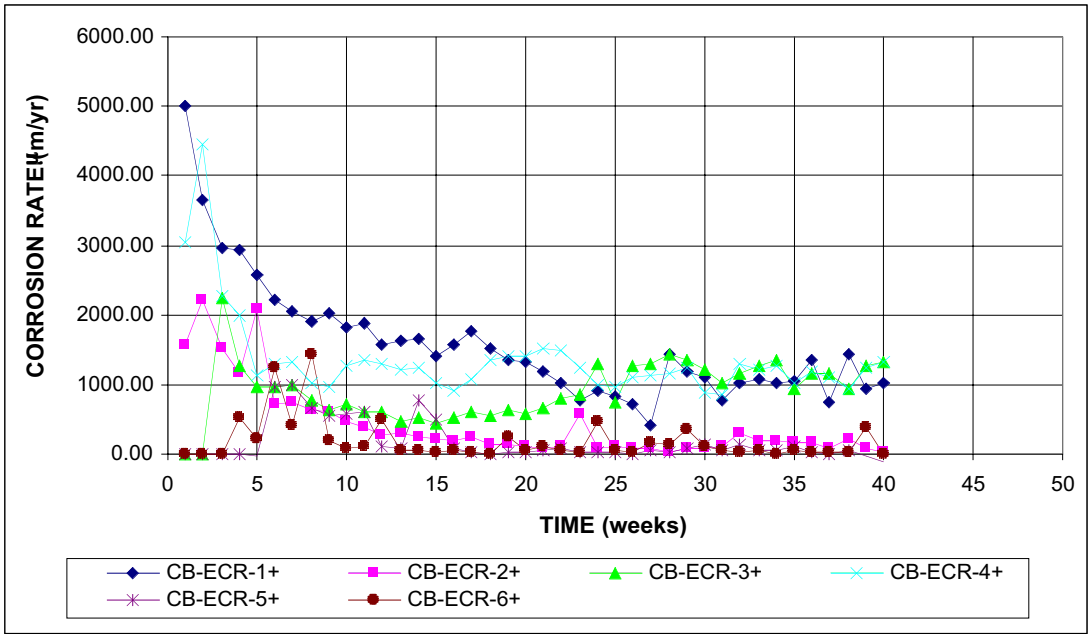

Figure A.56 - Cracked Beam Test. Corrosion rate based on exposed area of steel (four $^{1}/_{8}$-in. diameter holes in epoxy). Epoxy-coated steel, w/c=0.45, ponded with 15% NaCl solution.

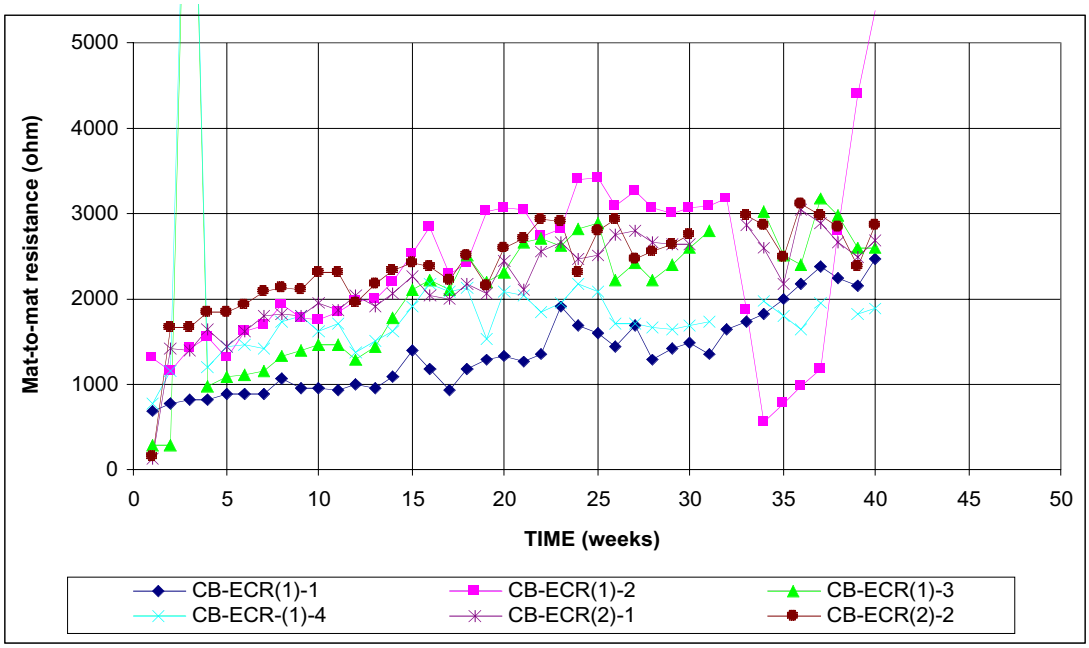

Figure A.57 - Cracked Beam Test. Corrosion rate based on exposed area of steel (four $^{1}/_{8}$-in. diameter holes in epoxy). Epoxy-coated steel, w/c=0.45, ponded with 15% NaCl solution.

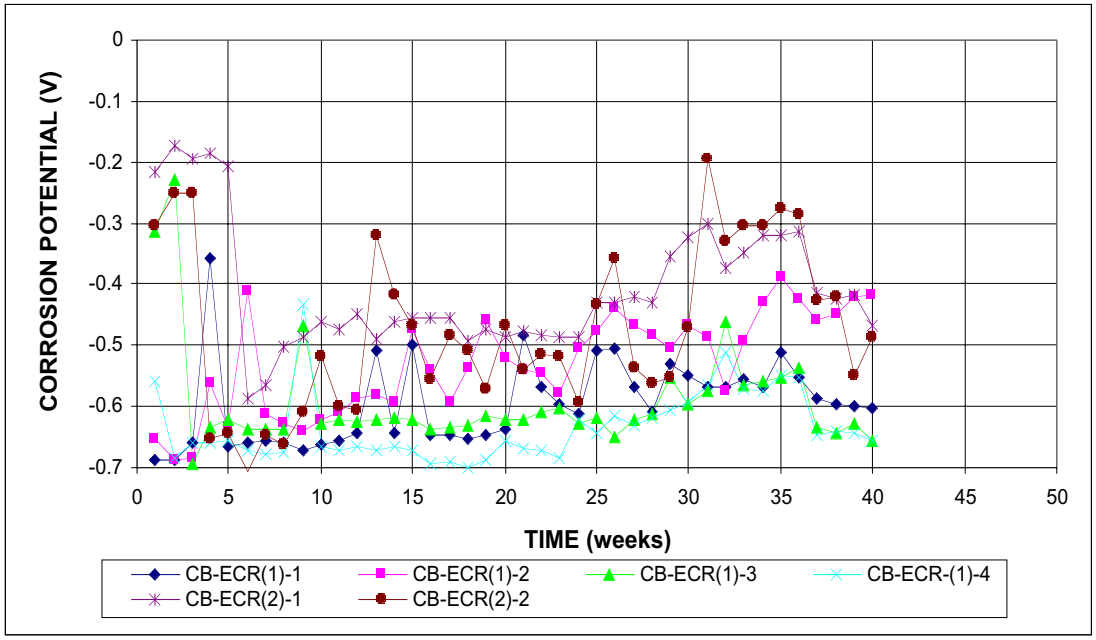

Figure A.58a - Cracked Beam Test. Corrosion potential vs. CSE, top mat. Epoxy-coated steel, w/c=0.45, ponded with 15% NaCl solution.

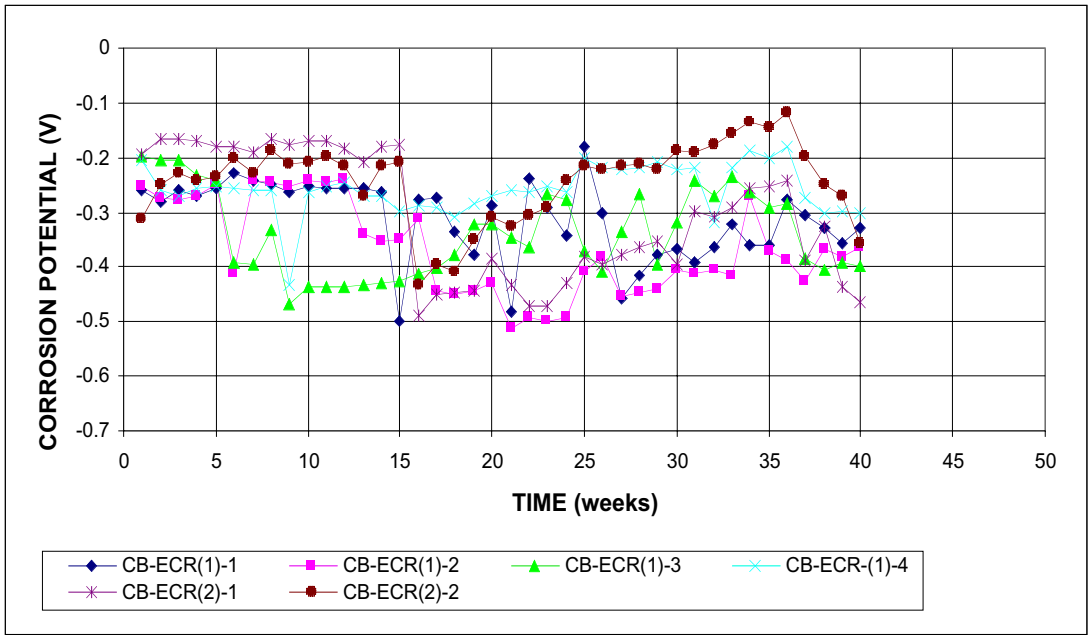

Figure A.58b - Cracked Beam Test. Corrosion potential vs. CSE, bottom mat. Epoxy-coated steel, w/c=0.45, ponded with 15% NaCl solution.